# The Cenozoic Magmatism of East Africa: Part IV – The Terminal Stages of Rifting Preserved in the Northern East African Rift System

Tyrone O. Rooney

*Dept. of Earth and Environmental Sciences, Michigan State University, East Lansing, MI 48823, USA*

**Abstract**

The Afar Depression is a broad region of subdued topography wherein the Red Sea, Gulf of Aden, and East African Rift System converge at a triple junction. This mature sector of the East African Rift System is characterized by attenuated continental lithosphere, with the implication that lavas erupted here can provide insights into the composition of sub-lithospheric magma reservoirs. Magmas in Afar and Yemen largely have geochemical characteristics consistent with a mixture of melts derived from the Afar plume, and from a hybrid endmember comprised of the depleted upper mantle and Pan-African lithosphere. Lavas erupted in the Erta ‘Ale range do not comport with this model and instead appear to have been derived from melting of a lithospheric mantle metasome that is likely related to prior Afar plume-lithosphere interaction. The extant data show no significant change in the reservoirs contributing to magmatism during the development of the rift in this region, however the surface distribution of magmatism reveals a relationship between rift evolution and magmatism. In Yemen, magmatic activity is limited to the regional Mid Miocene Resurgence event at ca. 10 Ma, and small-volume alkaline volcanism along the evolving Gulf of Aden margin from 6 Ma to present. In contrast, a much more extensive magmatic record is preserved in Afar. Coincident with the development of the rift margin, initial magmatism in Afar during this period (20 to 10 Ma) was dominantly in the form of

Figure 1

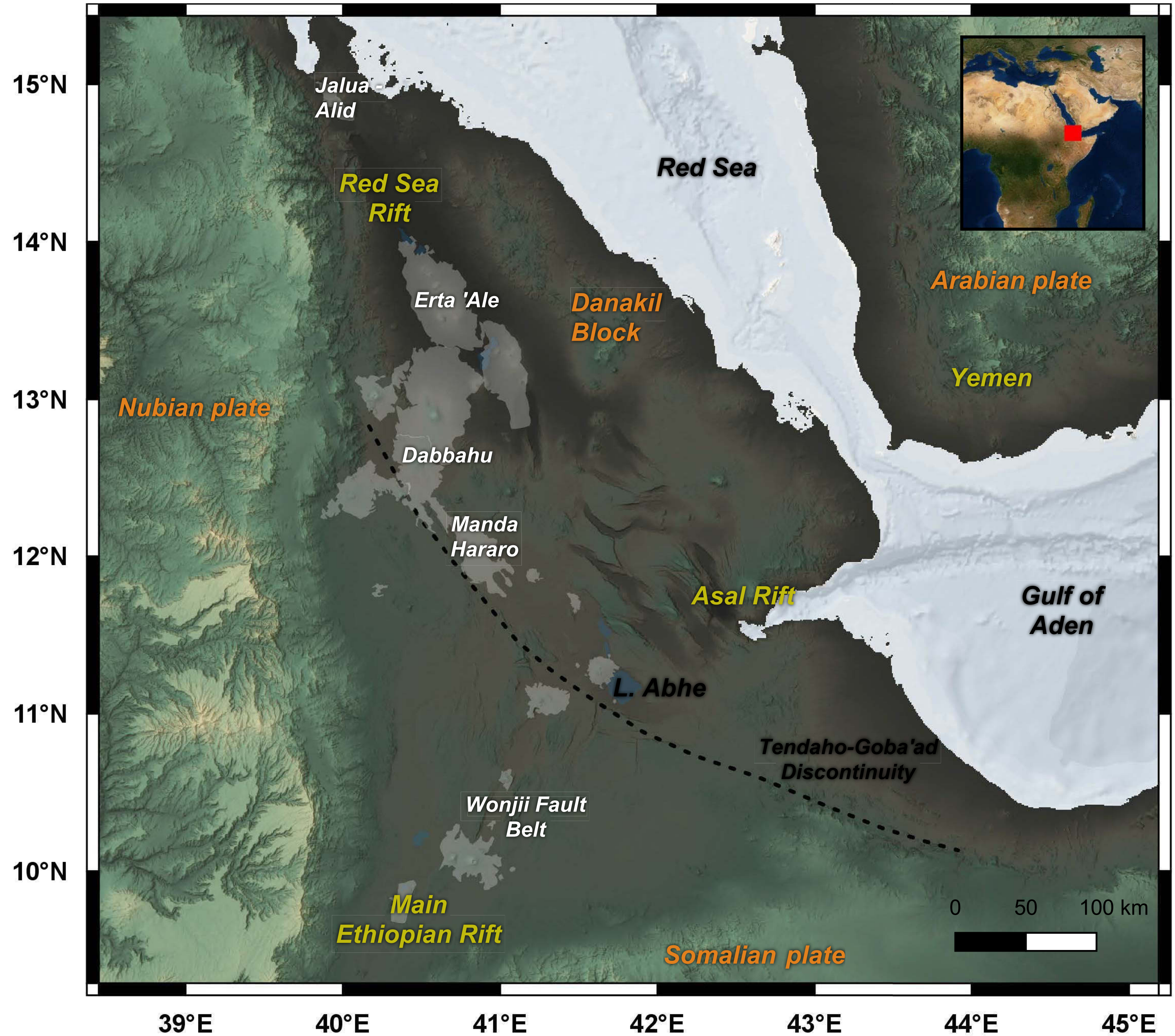

15°N
14°N
13°N
12°N
11°N
10°N
39°E
40°E
41°E
42°E
43°E
44°E
45°E
Jalua - Alid
Red Sea Rift
Red Sea
Erta 'Ale
Danakil Block
Arabian plate
Yemen
Nubian plate
Dabbahu
Manda Hararo
Asal Rift
Gulf of Aden
L. Abhe
Tendaho-Goba'ad Discontinuity
Wonjii Fault Belt
Main Ethiopian Rift
Somalian plate
0
50
100 km

Figure 2

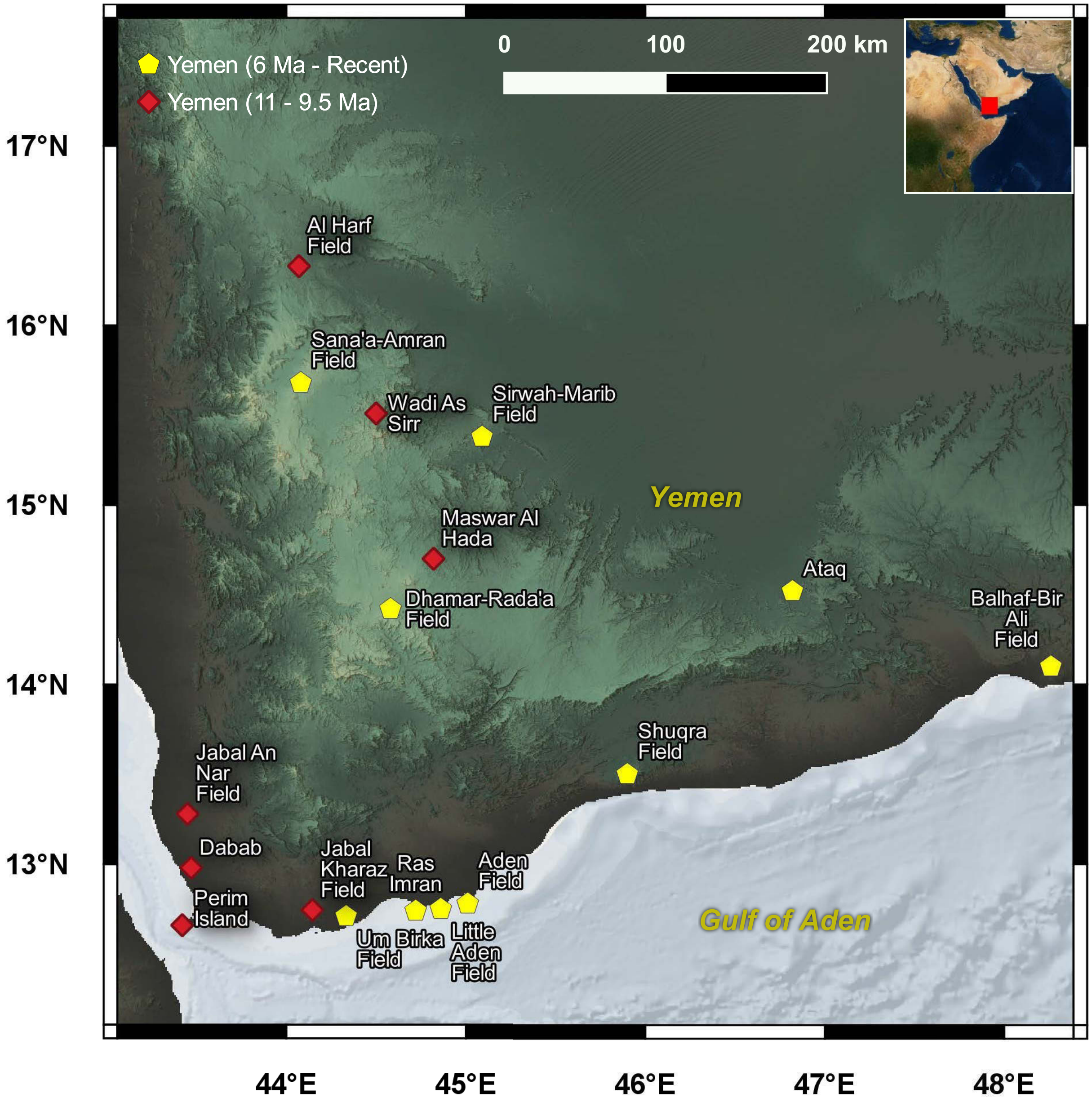
Yemen (6 Ma - Recent)
Yemen (11 - 9.5 Ma)
0
100
200 km
17°N
16°N
15°N
14°N
13°N
44°E
45°E
46°E
47°E
48°E
Al Harf Field
Sana'a-Amran Field
Wadi As Sirr
Sirwah-Marib Field
Yemen
Maswar Al Hada
Dhamar-Rada'a Field
Ataq
Balhaf-Bir Ali Field
Shuqra Field
Jabal An Nar Field
Dabab
Perim Island
Jabal Kharaz Field
Ras Imran
Aden Field
Um Birka Field
Little Aden Field
Gulf of Aden

Figure 3

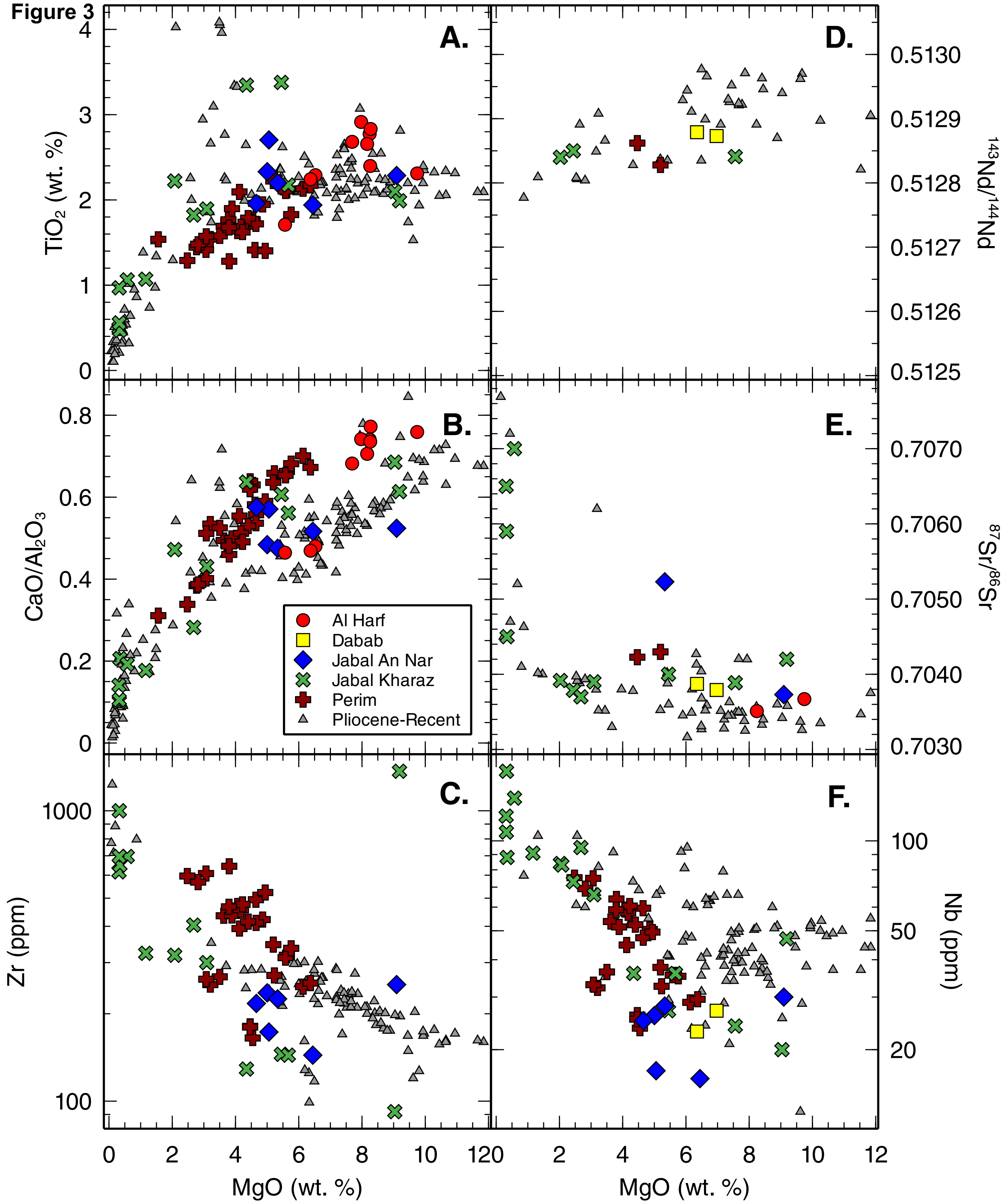

A.
B.
C.
D.
E.
F.
TiO2 (wt. %)
CaO/Al2O3
Zr (ppm)
143Nd/144Nd
87Sr/86Sr
Nb (ppm)
MgO (wt. %)
MgO (wt. %)
Al Harf
Dabab
Jabal An Nar
Jabal Kharaz
Perim
Pliocene-Recent

Figure 4

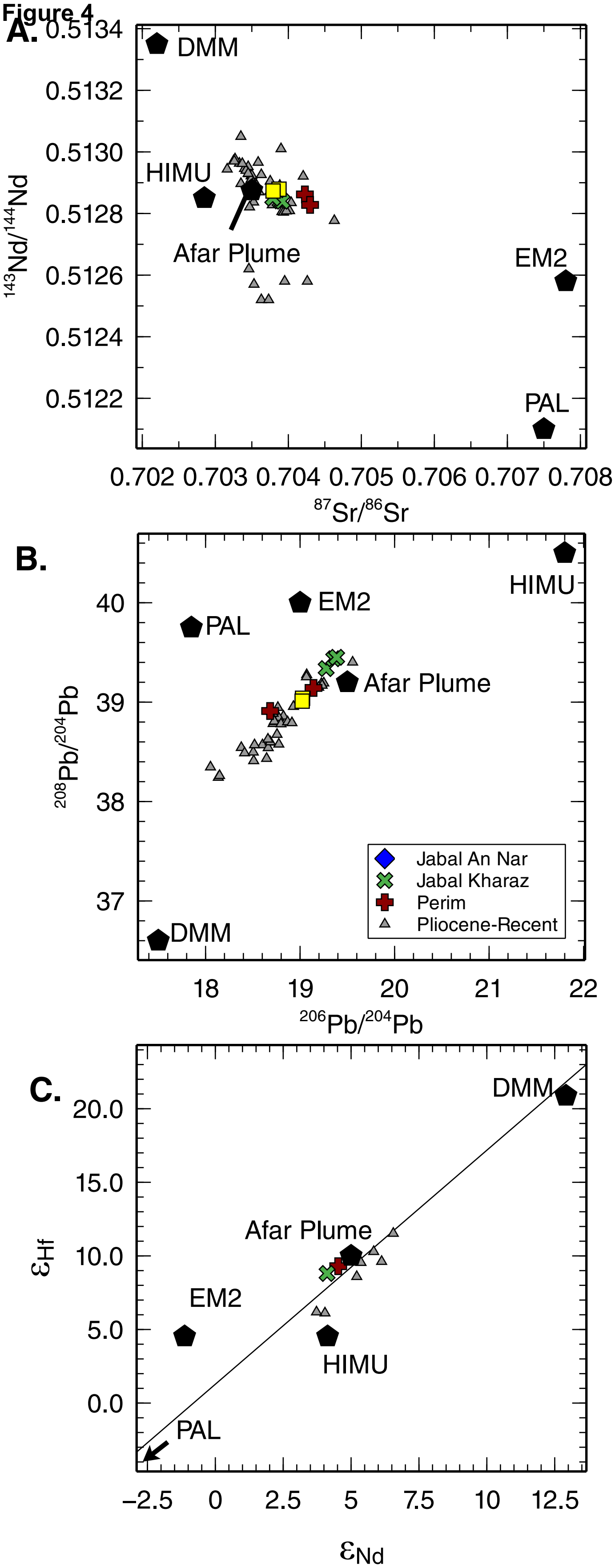

A.
DMM
HIMU
Afar Plume
EM2
PAL
0.5134
0.5132
0.5130
0.5128
0.5126
0.5124
0.5122
143Nd/144Nd
0.702 0.703 0.704 0.705 0.706 0.707 0.708
87Sr/86Sr
B.
HIMU
EM2
PAL
Afar Plume
DMM
40
39
38
37
208Pb/204Pb
18 19 20 21 22
206Pb/204Pb
Jabal An Nar
Jabal Kharaz
Perim
Pliocene-Recent
C.
DMM
Afar Plume
EM2
HIMU
PAL
20.0
15.0
10.0
5.0
0.0
εHf
−2.5 0 2.5 5 7.5 10 12.5
εNd

Figure 5

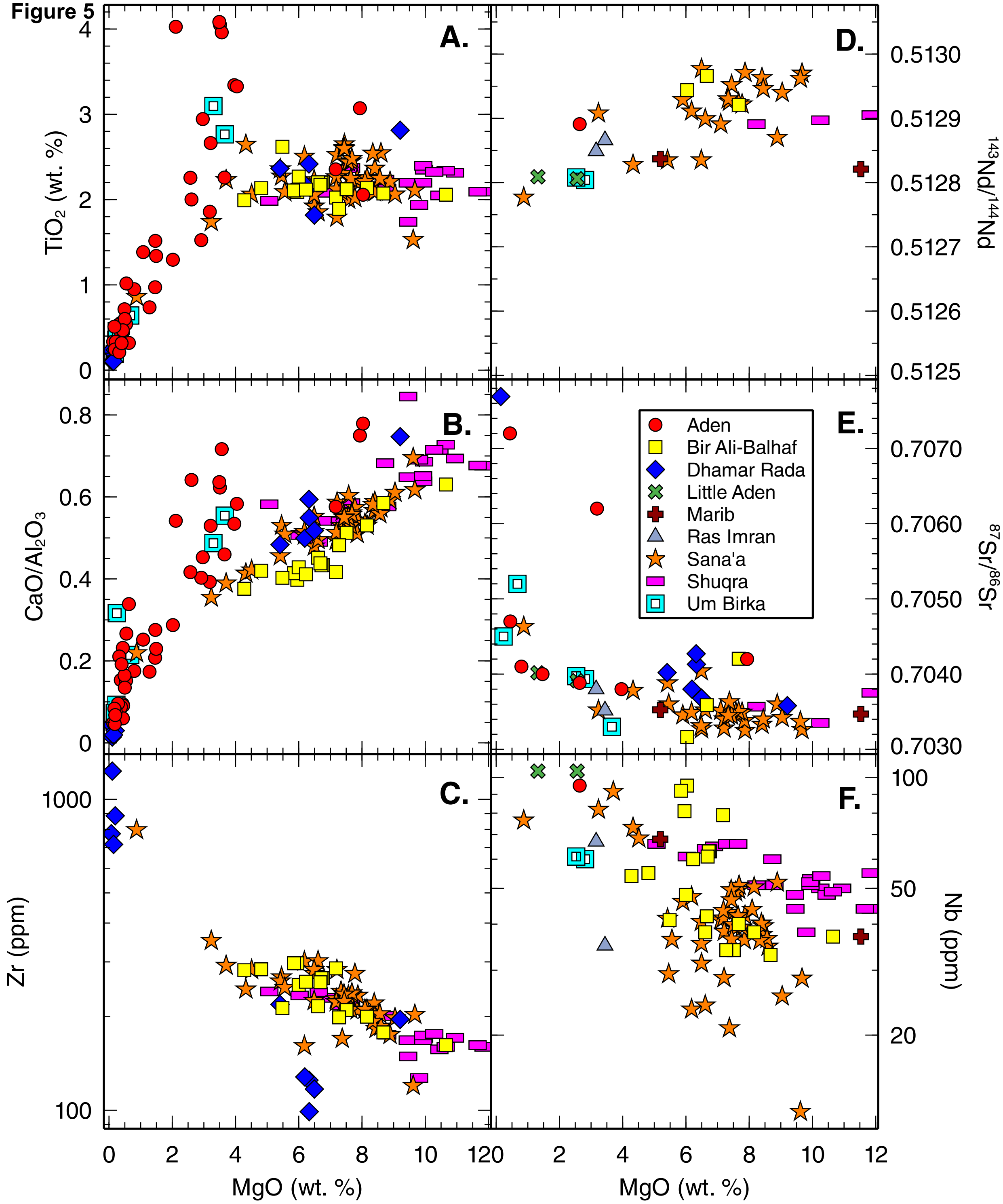

A.
B.
C.
D.
E.
F.
TiO2 (wt. %)
CaO/Al2O3
Zr (ppm)
143Nd/144Nd
87Sr/86Sr
Nb (ppm)
MgO (wt. %)
MgO (wt. %)
Aden
Bir Ali-Balhaf
Dhamar Rada
Little Aden
Marib
Ras Imran
Sana'a
Shuqra
Um Birka

Figure 6

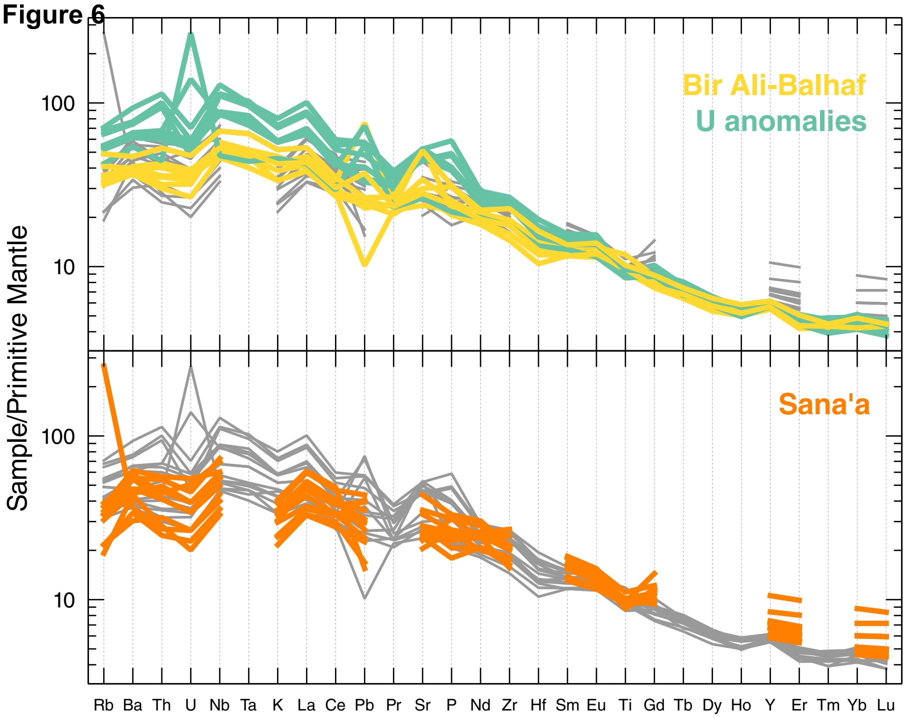
Bir Ali-Balhaf
U anomalies
Sana'a
Sample/Primitive Mantle
100
10
100
10
Rb Ba Th U Nb Ta K La Ce Pb Pr Sr P Nd Zr Hf Sm Eu Ti Gd Tb Dy Ho Y Er Tm Yb Lu

Figure 7

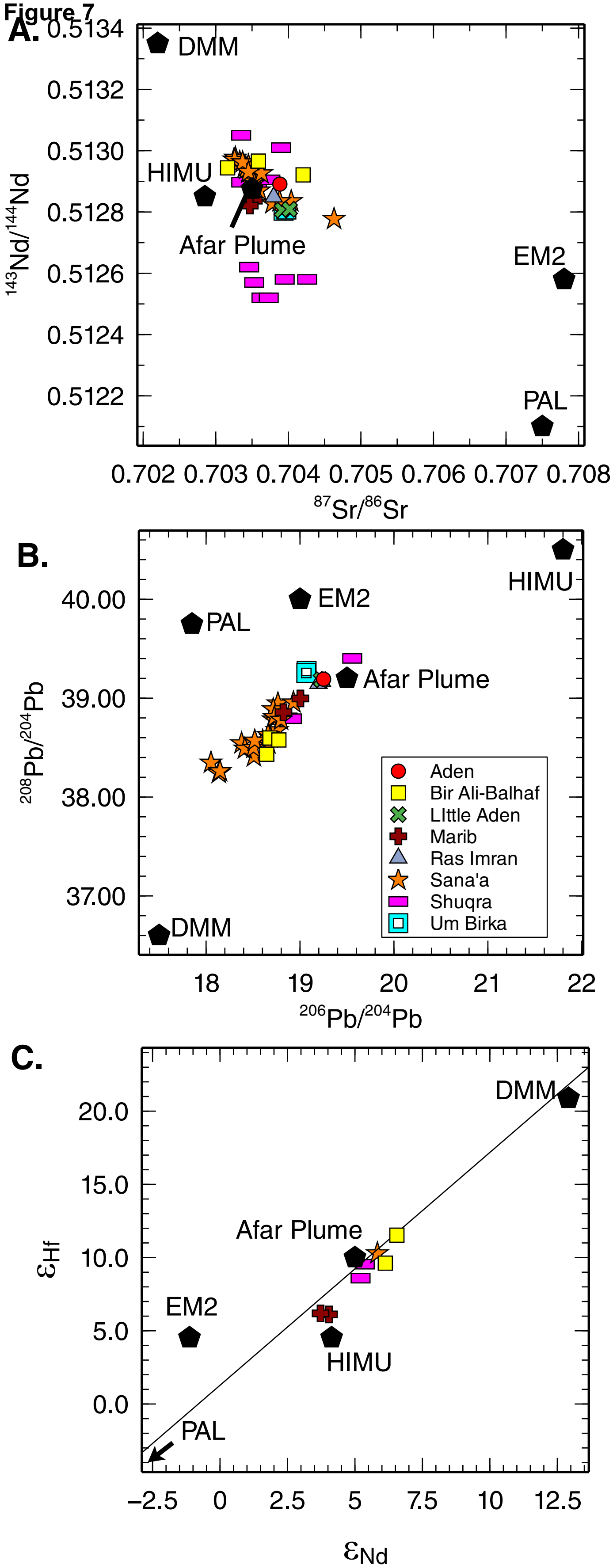
A.
DMM
HIMU
Afar Plume
EM2
PAL
0.5134
0.5132
0.5130
0.5128
0.5126
0.5124
0.5122
143Nd/144Nd
0.702 0.703 0.704 0.705 0.706 0.707 0.708
87Sr/86Sr
B.
HIMU
EM2
PAL
Afar Plume
DMM
40.00
39.00
38.00
37.00
208Pb/204Pb
18 19 20 21 22
206Pb/204Pb
Aden
Bir Ali-Balhaf
LIttle Aden
Marib
Ras Imran
Sana'a
Shuqra
Um Birka
C.
DMM
Afar Plume
EM2
HIMU
PAL
20.0
15.0
10.0
5.0
0.0
εHf
–2.5 0 2.5 5 7.5 10 12.5
εNd

Figure 8

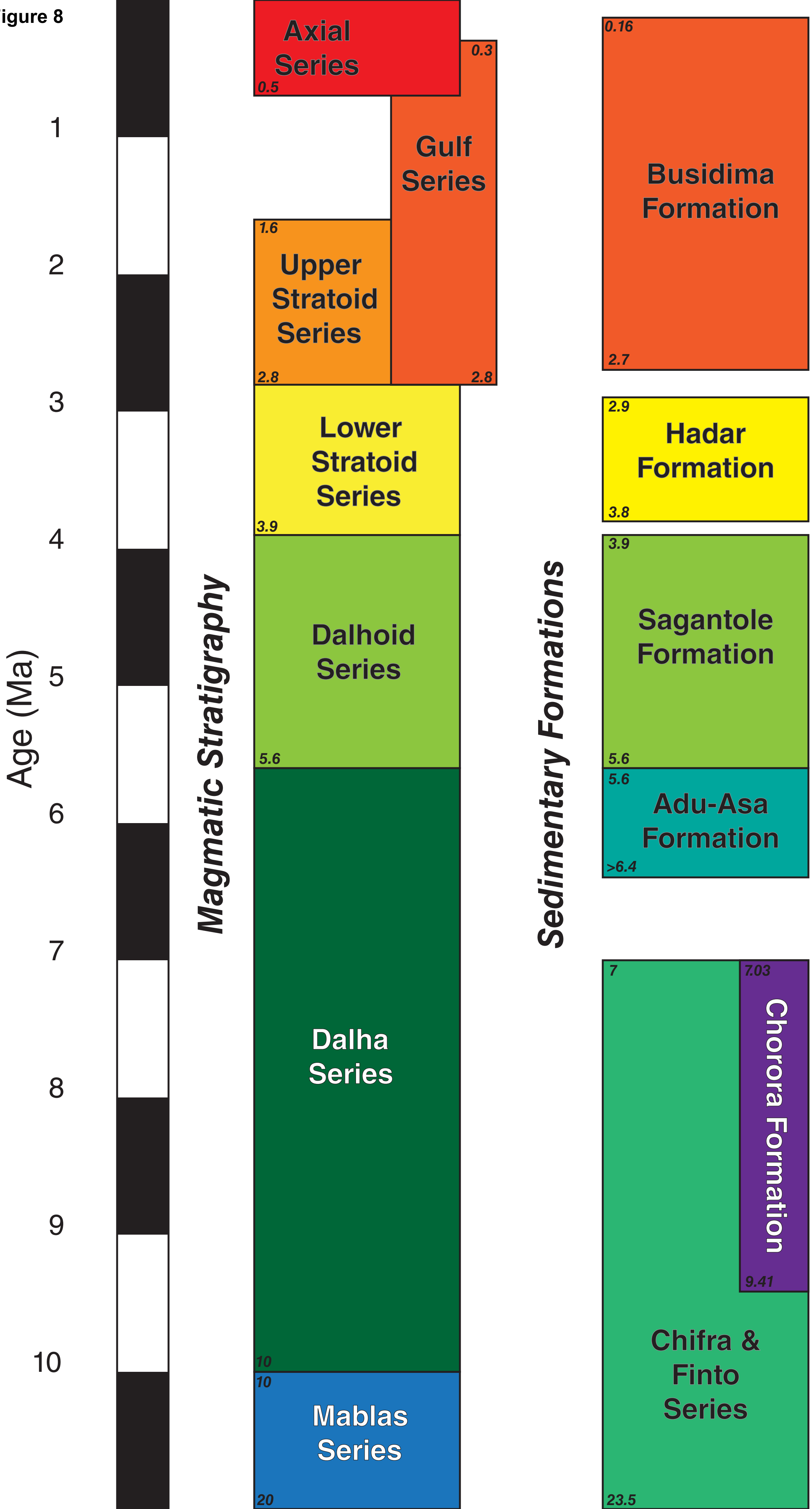

Age (Ma)
1
2
3
4
5
6
7
8
9
10
Magmatic Stratigraphy
Axial Series
0.5
0.3
Gulf Series
1.6
Upper Stratoid Series
2.8
2.8
Lower Stratoid Series
3.9
Dalhoid Series
5.6
Dalha Series
10
10
Mablas Series
20
Sedimentary Formations
0.16
Busidima Formation
2.7
2.9
Hadar Formation
3.8
3.9
Sagantole Formation
5.6
5.6
Adu-Asa Formation
>6.4
7
7.03
Chorora Formation
9.41
Chifra & Finto Series
23.5

Figure 9

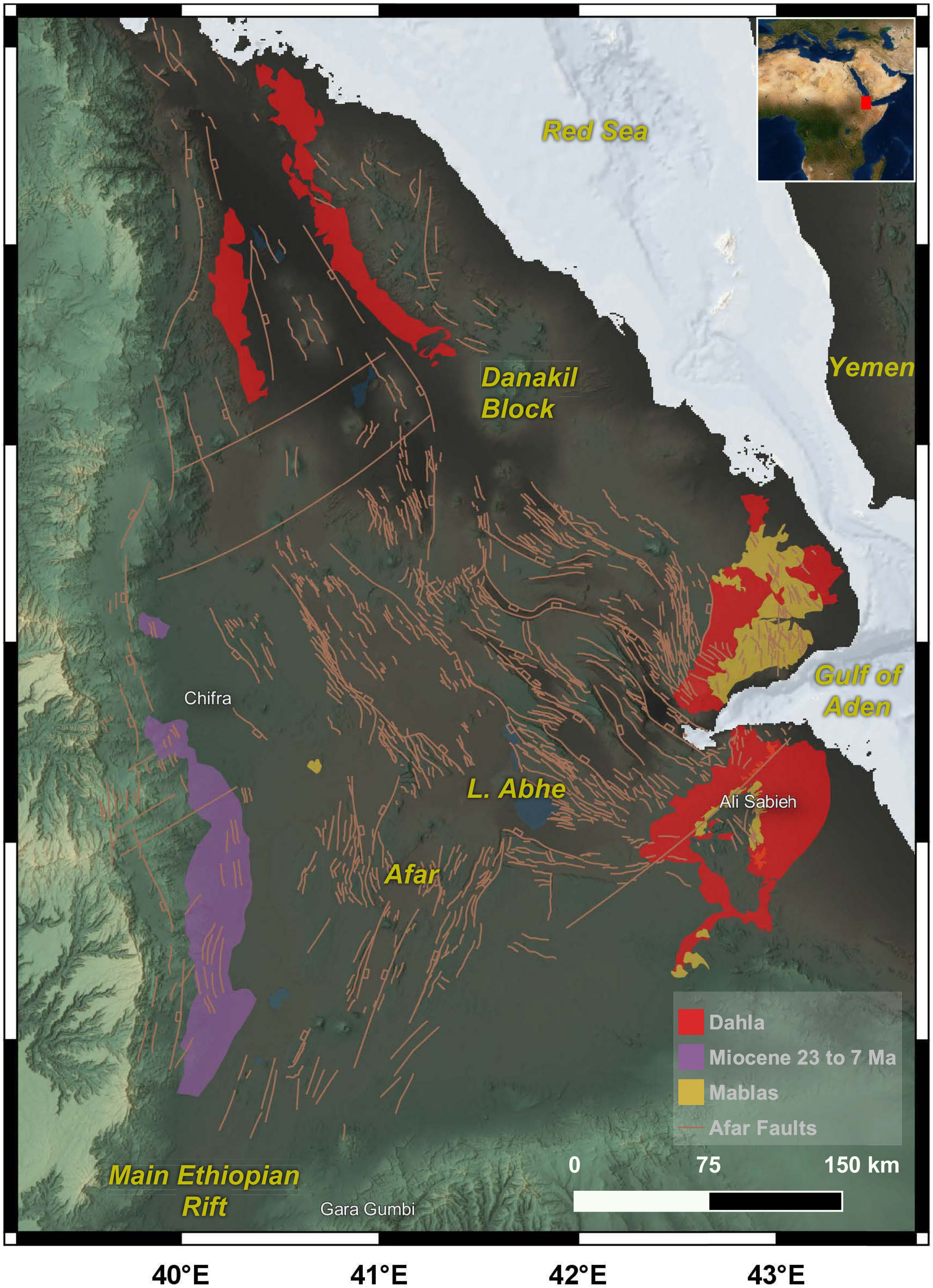

15°N
14°N
13°N
12°N
11°N
10°N
40°E
41°E
42°E
43°E
Red Sea
Yemen
Danakil Block
Gulf of Aden
Chifra
L. Abhe
Ali Sabieh
Afar
Main Ethiopian Rift
Gara Gumbi
Dahla
Miocene 23 to 7 Ma
Mablas
Afar Faults
0
75
150 km

Figure 10

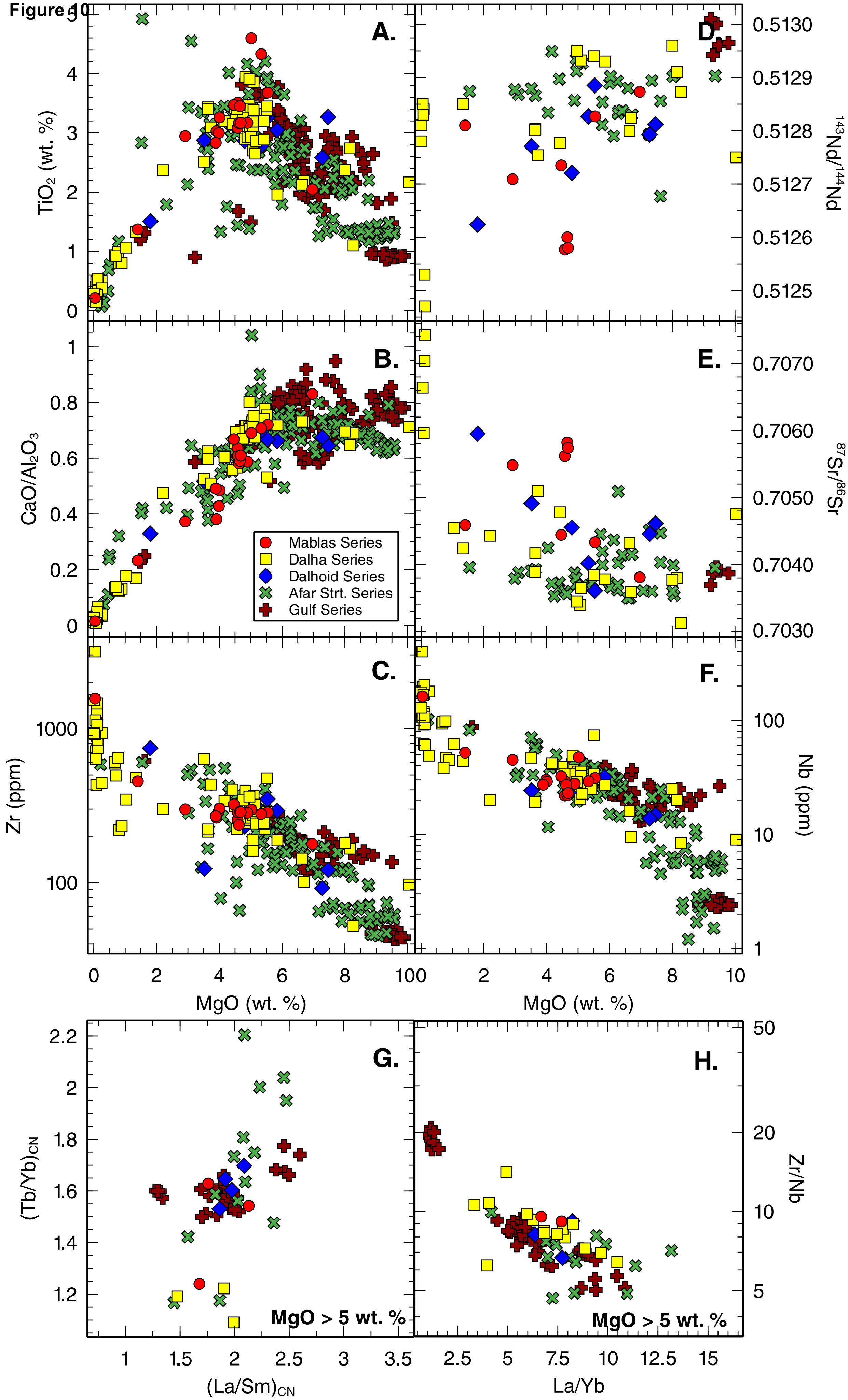

A.
B.
C.
D.
E.
F.
G.
H.
TiO2 (wt. %)
CaO/Al2O3
Zr (ppm)
143Nd/144Nd
87Sr/86Sr
Nb (ppm)
MgO (wt. %)
MgO (wt. %)
(Tb/Yb)CN
(La/Sm)CN
Zr/Nb
La/Yb
MgO > 5 wt. %
MgO > 5 wt. %
Mablas Series
Dalha Series
Dalhoid Series
Afar Strt. Series
Gulf Series

Figure 11

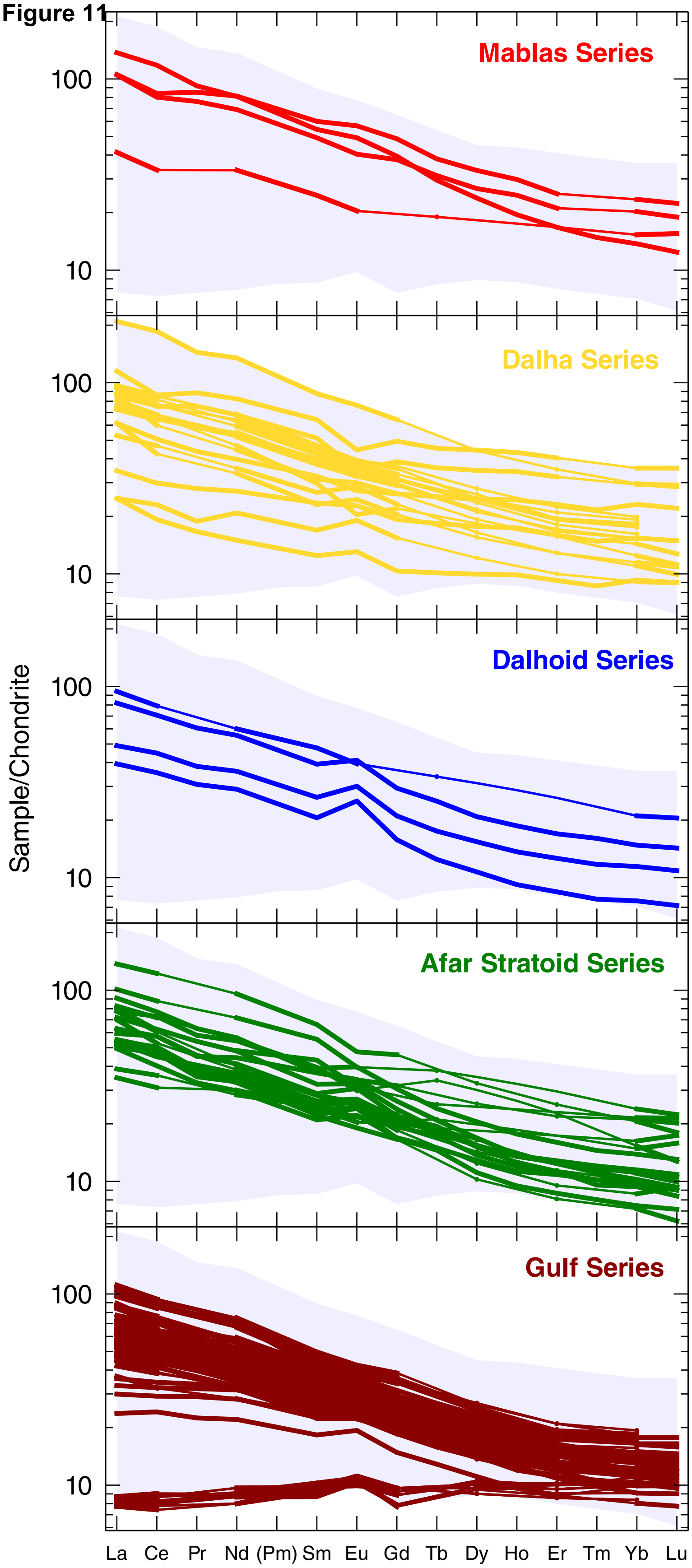
Mablas Series
Dalha Series
Dalhoid Series
Afar Stratoid Series
Gulf Series
Sample/Chondrite
100
10
La Ce Pr Nd (Pm) Sm Eu Gd Tb Dy Ho Er Tm Yb Lu

Figure 12

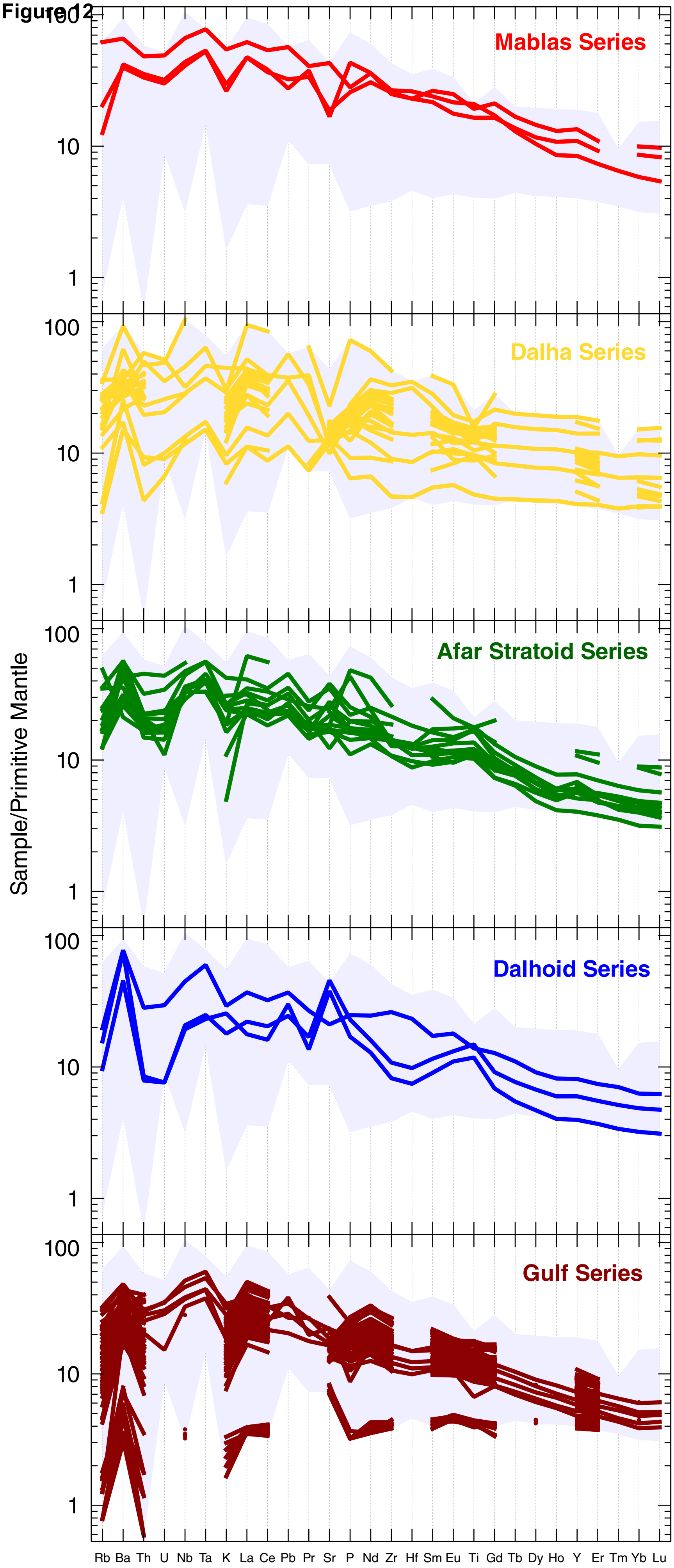

Mablas Series
Dalha Series
Afar Stratoid Series
Dalhoid Series
Gulf Series
Sample/Primitive Mantle
100
10
1
Rb Ba Th U Nb Ta K La Ce Pb Pr Sr P Nd Zr Hf Sm Eu Ti Gd Tb Dy Ho Y Er Tm Yb Lu

Figure 13

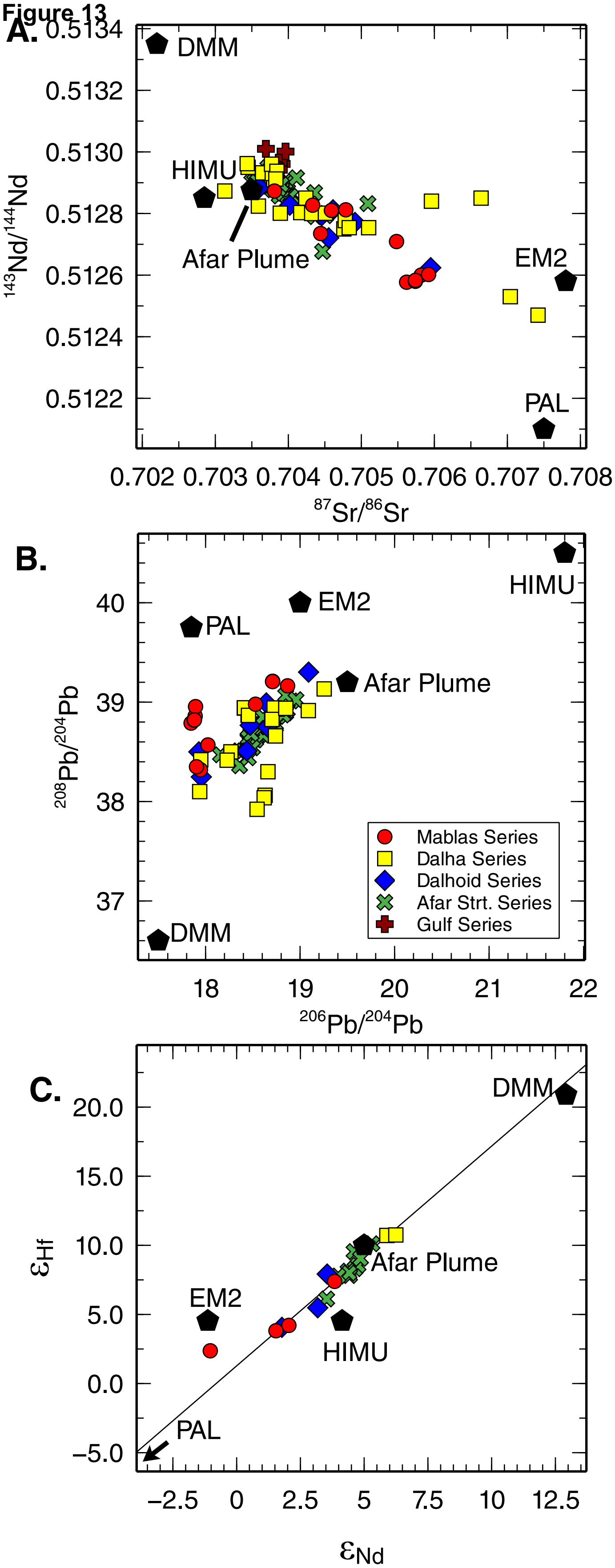
A.
0.5134
0.5132
0.5130
0.5128
0.5126
0.5124
0.5122
DMM
HIMU
Afar Plume
EM2
PAL
0.702 0.703 0.704 0.705 0.706 0.707 0.708
$^{87}Sr/^{86}Sr$
$^{143}Nd/^{144}Nd$
B.
40
39
38
37
PAL
EM2
HIMU
Afar Plume
DMM
Mablas Series
Dalha Series
Dalhoid Series
Afar Strt. Series
Gulf Series
18 19 20 21 22
$^{206}Pb/^{204}Pb$
$^{208}Pb/^{204}Pb$
C.
20.0
15.0
10.0
5.0
0.0
−5.0
DMM
Afar Plume
EM2
HIMU
PAL
−2.5 0 2.5 5 7.5 10 12.5
$\varepsilon_{Nd}$
$\varepsilon_{Hf}$

Figure 14

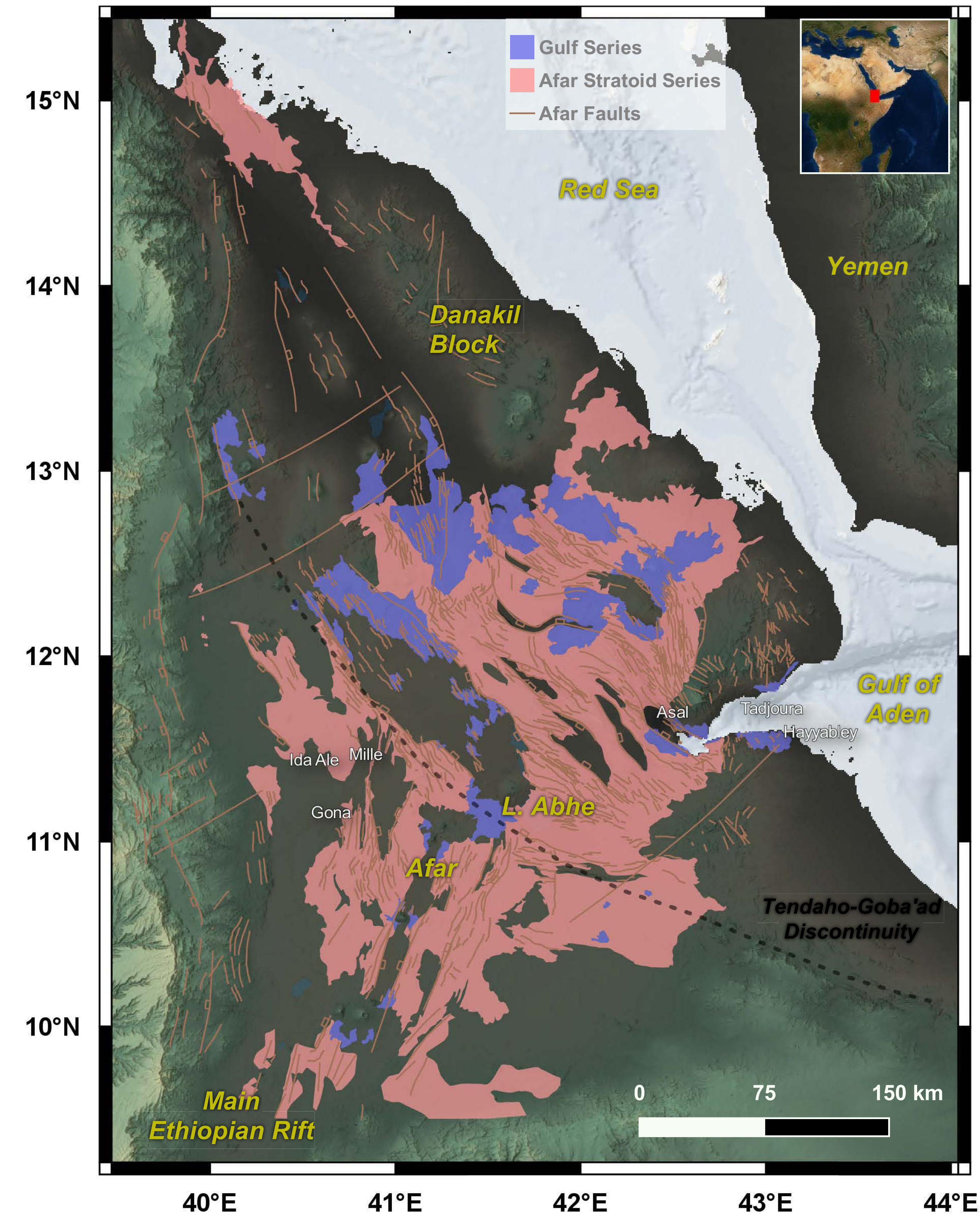

Gulf Series
Afar Stratoid Series
Afar Faults
Red Sea
Yemen
Danakil Block
Gulf of Aden
Asal
Tadjoura
Hayyabley
Ida Ale
Mille
Gona
L. Abhe
Afar
Tendaho-Goba'ad Discontinuity
Main Ethiopian Rift
0
75
150 km
15°N
14°N
13°N
12°N
11°N
10°N
40°E
41°E
42°E
43°E
44°E

**Figure 15**

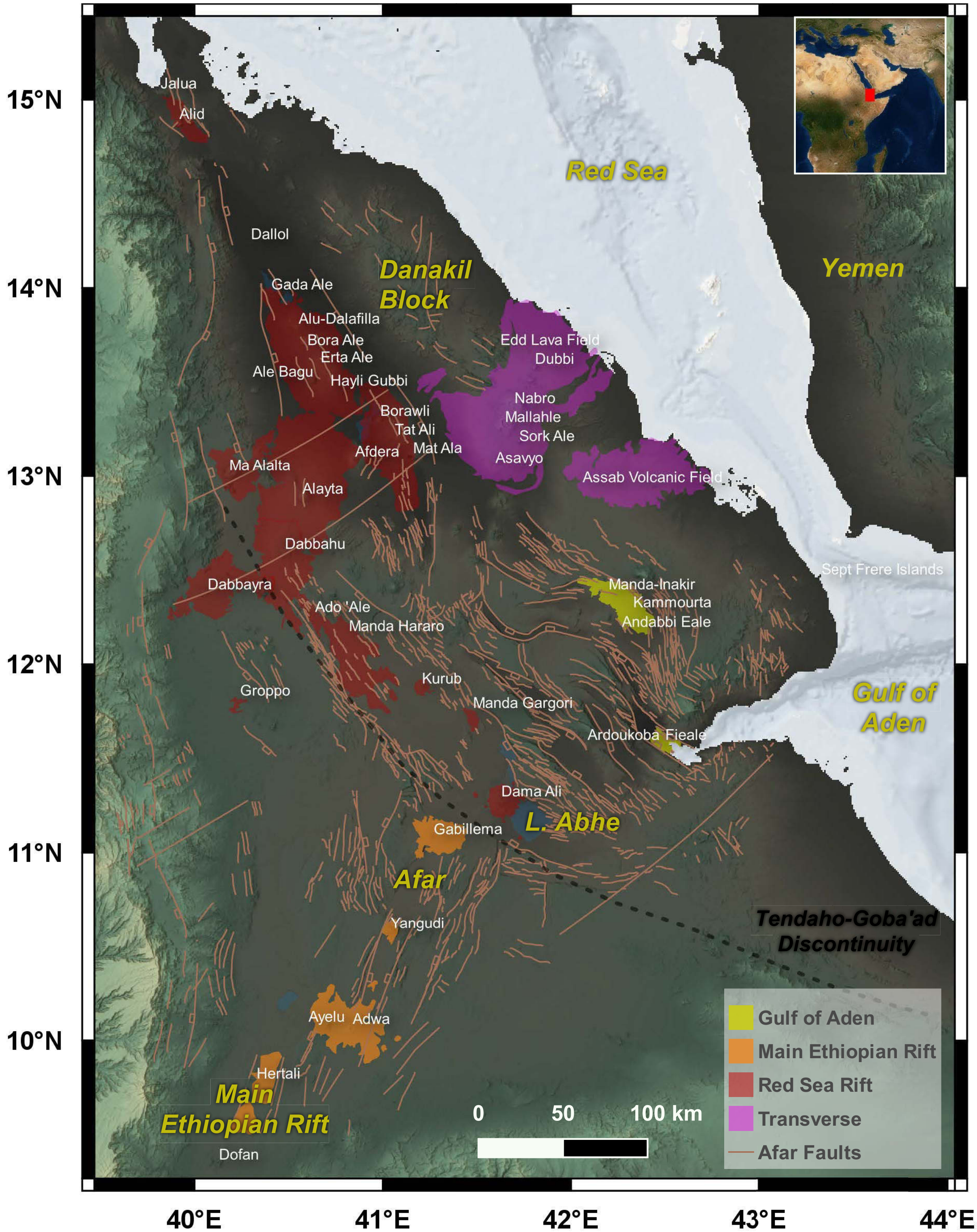

15°N
14°N
13°N
12°N
11°N
10°N
40°E
41°E
42°E
43°E
44°E
Jalua
Alid
Red Sea
Dallol
Gada Ale
Danakil Block
Yemen
Alu-Dalafilla
Bora Ale
Erta Ale
Ale Bagu
Hayli Gubbi
Edd Lava Field
Dubbi
Nabro
Mallahle
Sork Ale
Borawli
Tat Ali
Afdera
Mat Ala
Asavyo
Ma Alalta
Alayta
Assab Volcanic Field
Dabbahu
Sept Frere Islands
Dabbayra
Manda-Inakir
Kammourta
Andabbi Eale
Ado 'Ale
Manda Hararo
Kurub
Groppo
Manda Gargori
Gulf of Aden
Ardoukoba
Fieale
Dama Ali
L. Abhe
Gabillema
Afar
Yangudi
Tendaho-Goba'ad Discontinuity
Ayelu
Adwa
Hertali
Main Ethiopian Rift
Dofan
0
50
100 km
Gulf of Aden
Main Ethiopian Rift
Red Sea Rift
Transverse
Afar Faults

Figure 16

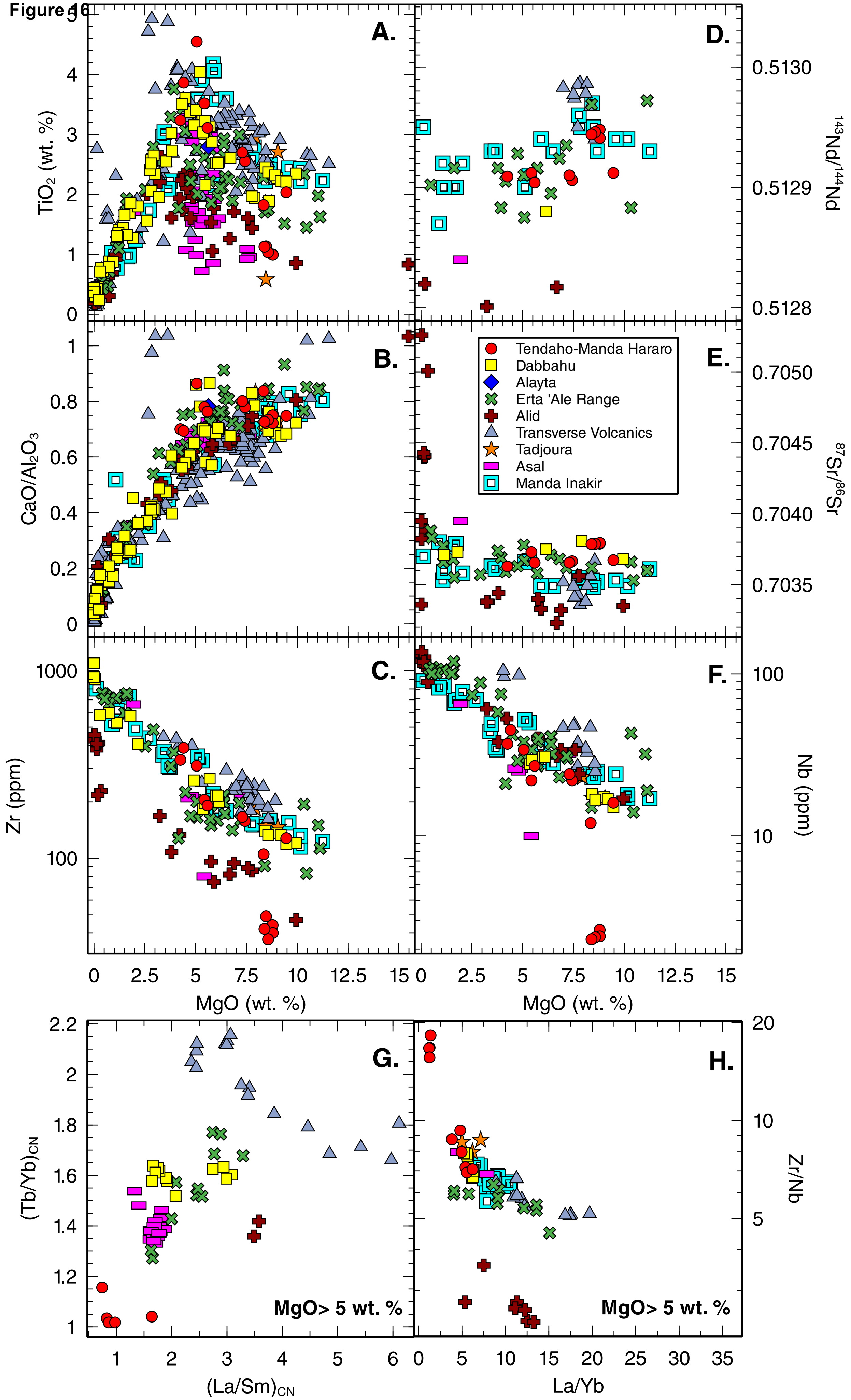
A.
B.
C.
D.
E.
F.
G.
H.
TiO2 (wt. %)
CaO/Al2O3
Zr (ppm)
143Nd/144Nd
87Sr/86Sr
Nb (ppm)
MgO (wt. %)
MgO (wt. %)
(Tb/Yb)CN
(La/Sm)CN
La/Yb
Zr/Nb
MgO> 5 wt. %
MgO> 5 wt. %
Tendaho-Manda Hararo
Dabbahu
Alayta
Erta 'Ale Range
Alid
Transverse Volcanics
Tadjoura
Asal
Manda Inakir

**Figure 17**

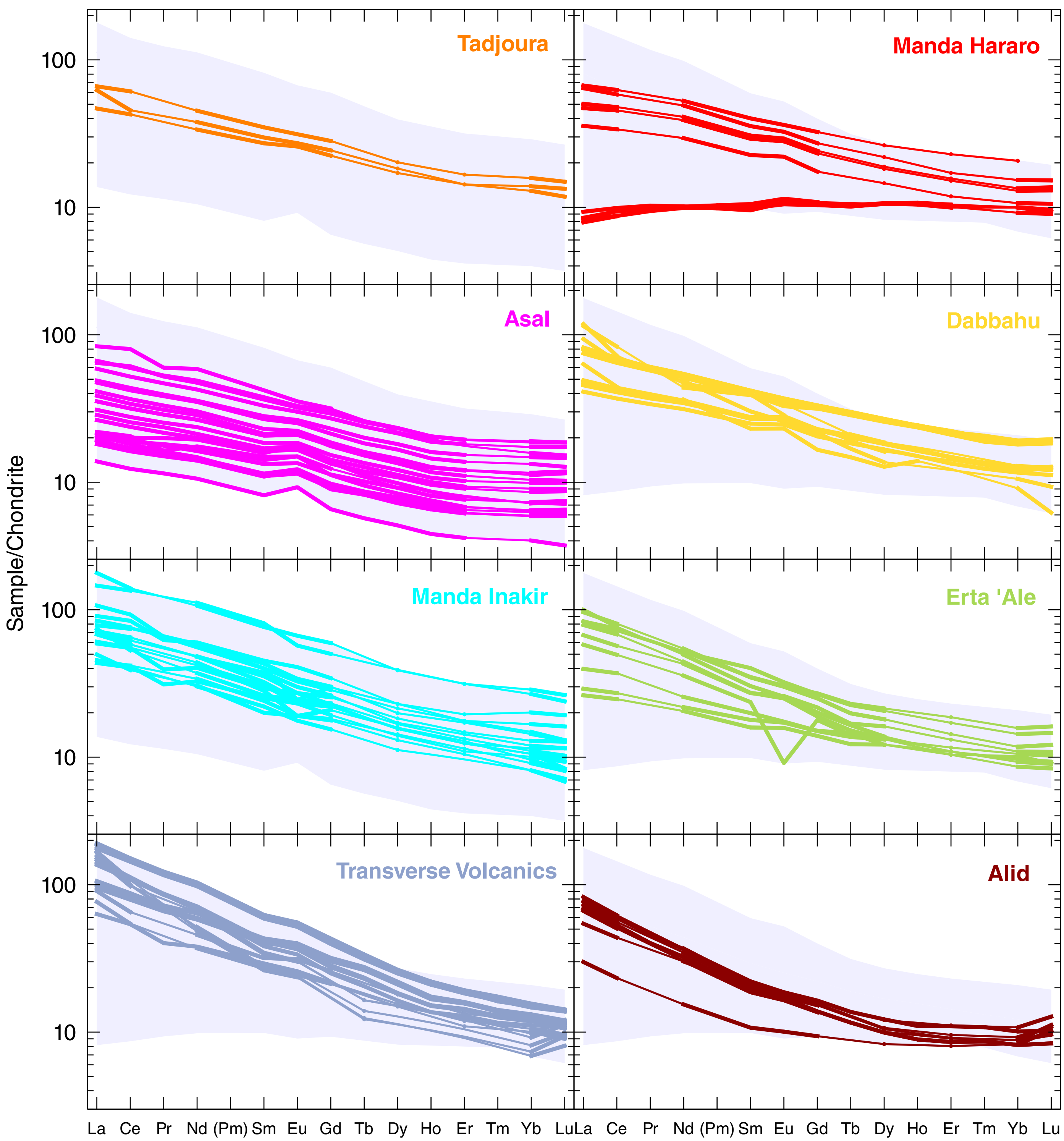

Tadjoura
Manda Hararo
Asal
Dabbahu
Manda Inakir
Erta 'Ale
Transverse Volcanics
Alid
Sample/Chondrite
100
10
La Ce Pr Nd (Pm) Sm Eu Gd Tb Dy Ho Er Tm Yb Lu

Figure 18

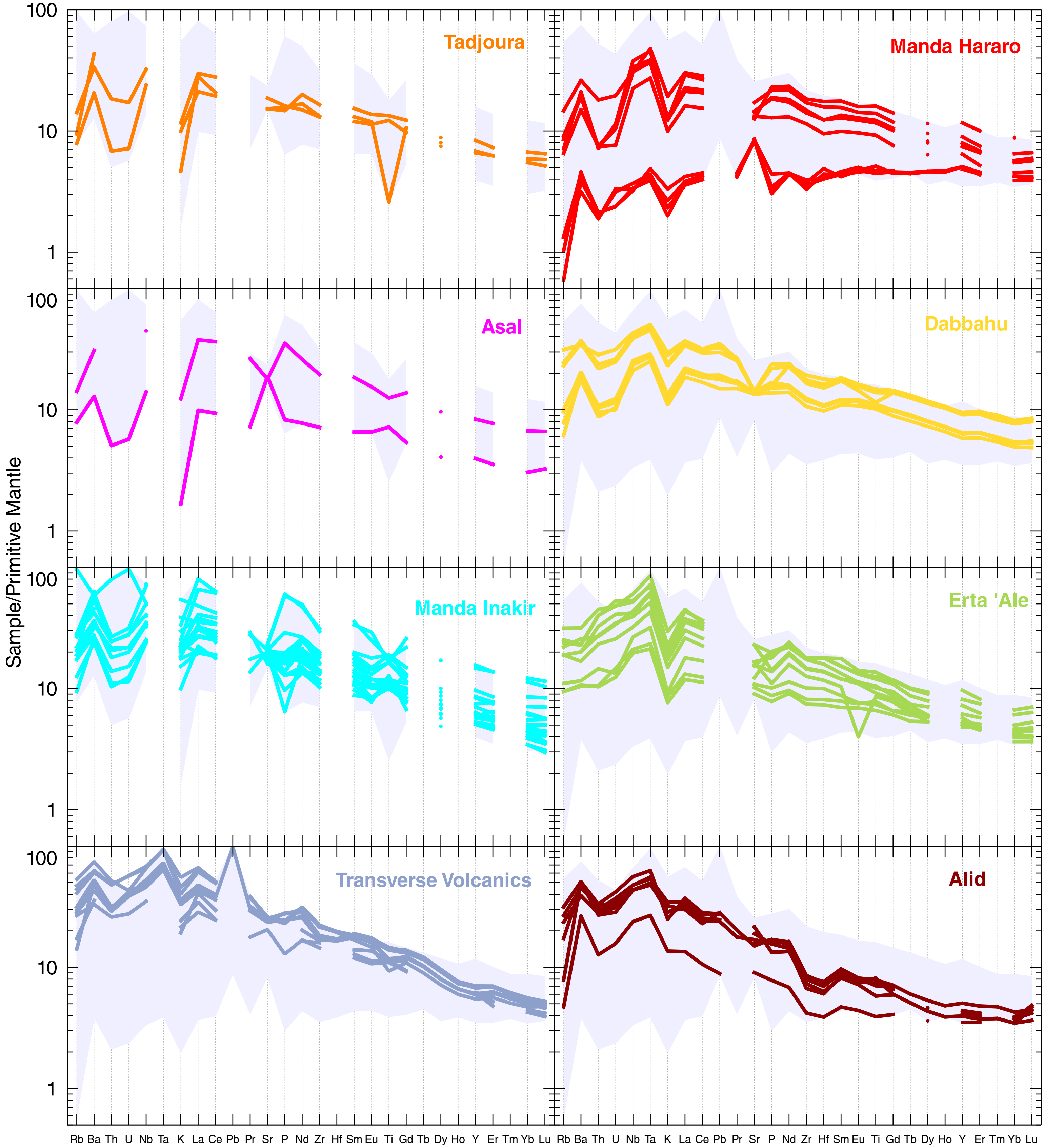
Tadjoura
Manda Hararo
Asal
Dabbahu
Manda Inakir
Erta 'Ale
Transverse Volcanics
Alid
Sample/Primitive Mantle
100
10
1
Rb Ba Th U Nb Ta K La Ce Pb Pr Sr P Nd Zr Hf Sm Eu Ti Gd Tb Dy Ho Y Er Tm Yb Lu

Figure 19

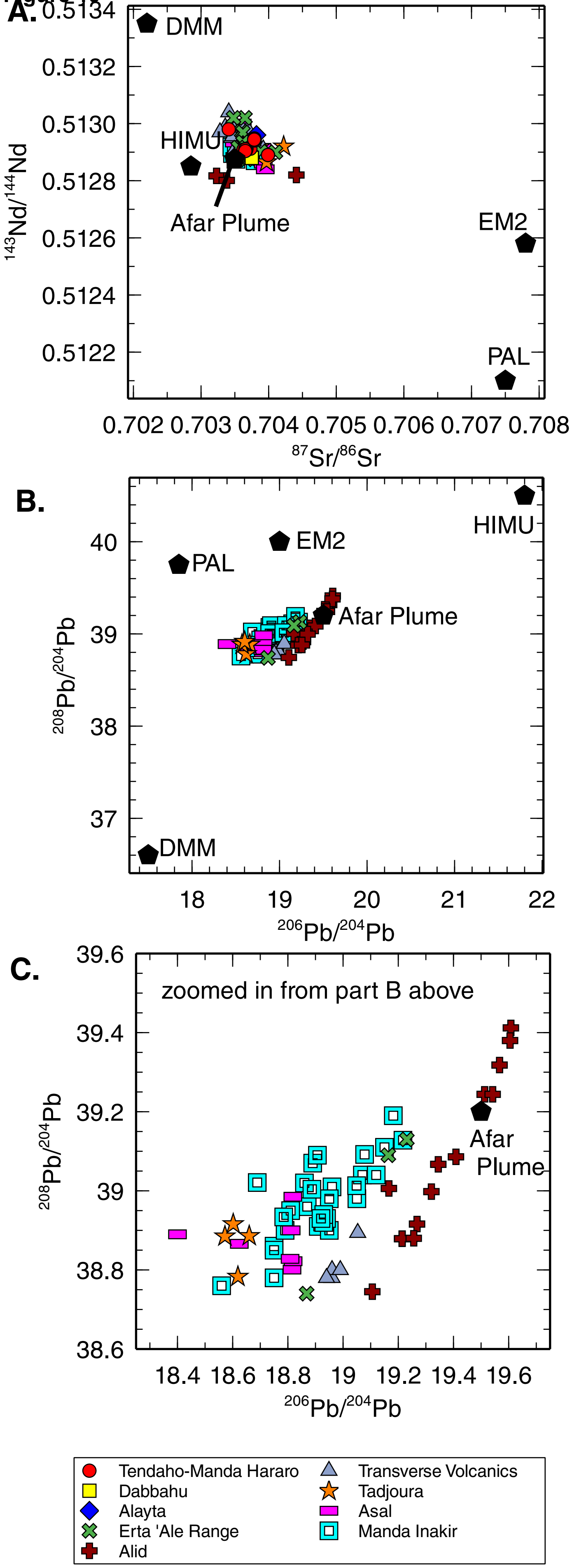

A.
DMM
HIMU
Afar Plume
EM2
PAL
0.5134
0.5132
0.5130
0.5128
0.5126
0.5124
0.5122
$^{143}Nd/^{144}Nd$
0.702 0.703 0.704 0.705 0.706 0.707 0.708
$^{87}Sr/^{86}Sr$
B.
HIMU
EM2
PAL
Afar Plume
DMM
40
39
38
37
$^{208}Pb/^{204}Pb$
18 19 20 21 22
$^{206}Pb/^{204}Pb$
C.
zoomed in from part B above
Afar Plume
39.6
39.4
39.2
39
38.8
38.6
$^{208}Pb/^{204}Pb$
18.4 18.6 18.8 19 19.2 19.4 19.6
$^{206}Pb/^{204}Pb$
Tendaho-Manda Hararo
Dabbahu
Alayta
Erta 'Ale Range
Alid
Transverse Volcanics
Tadjoura
Asal
Manda Inakir

**Table 1**

| Magma Type | Characteristics | Origin |
|---|---|---|
| I – Incompatible element depleted family of magmas | Extreme depletions in most elements forming a relatively flat incompatible trace element normalized pattern. Subtype Ia exhibits positive anomalies in LILE (e.g. Ba). | Associated with Eocene and Oligocene Flood basalts and remains of uncertain origin. |
| II – OIB Family of magmas | Exhibits a typical OIB-like pattern in a primitive mantle normalized diagram. Type IIa extend to MgO-rich compositions and are less silica undersaturated. Type IIb have lower SiO2 and elevated CaO and incompatible trace elements | Origin of Type IIa is controversial and may be associated with material within the Afar plume, lithospheric material metasomatized by the plume, or delaminated. Type IIb are likely derived from melting of lithospheric mantle metasomses. |
| III – The Moderate Family of Magmas | Typified by a distinctive Ba peak, a U-Th trough, and a Nb-Ta peak. The slope of the REE are controlled by the depth and degree of melting. | The most common magma type within the East African Rift and is interpreted to be a melt of a plume-influenced upper mantle. |
| IV – Intermediate Composition | Typified by a pattern that is a simple mix of Type II and Type III magma | Contamination of a Type III magma as it passes through the lithosphere and either assimilates a metasome or mixes with a Type II melt. |
| V – Potassic Metasomes | Typified by a relatively flat pattern in the most incompatible trace elements within the primitive mantle normalized figure, with small negative anomalies in U and K, and a mild depletion in Zr-Hf. | Melts derived from a phlogopite-bearing lithospheric mantle metasome. Well-developed within the Virunga Province in the Western Branch. |
| VI – Depleted Source | Typified by extreme depletion in the most incompatible trace elements that resemble MORB, but with unusual positive anomalies in LILE | Uncertain – may be a plume component but more work needed. |

Table 1: Classification of magma types erupting in the East African Rift. This classification adds to that presented in Rooney (2017) and is presented in more detail in Part V of the synthesis series. These magma types are predominantly identified on the basis of commonalities in patterns in primitive mantle normalized incompatible trace element diagrams. Other magma groups may emerge as further work is undertaken in the region and this list should therefore be viewed as preliminary and subject to addition in the future.

large silicic eruptions, with lesser volumes of crustally contaminated Mablas basalts. The development of rift-marginal basins at ca. 7 Ma was coincident with the widespread eruption of fissural basalt of the Dalha Series. The Dalhoid Series represents a pulse of magmatism from ca. 5.6 to 3.9 Ma, which correlates with the initiation of sedimentation within the Sagantole Formation. The initiation of the lower member of the Afar Stratoid Series at ca. 3.9 is broadly contemporaneous with sedimentation within the Hadar Formation, while the upper member (2.6 Ma) correlates with the Busidima Formation. The Gulf Basalt Series (2.8 to 0.3 Ma) temporally overlaps the upper member of the Afar Stratoid Series, but represents the first manifestations of the coincidence of strain localization and magmatism within rift axial grabens. The subsequent Axial Series (ca. 0.7 Ma to present), manifests as basaltic cones and central silicic volcanoes within three zones aligned with the Main Ethiopian Rift, Red Sea Rift, and Gulf of Aden. The evolution in Afar from initial large-scale silicic volcanic events to basin-wide fissural basaltic flows, to modern zones of focused magmatism, broadly parallels the localization of strain during the same period. This intimate relationship between the mechanism of strain accommodation and surface manifestation of magmatism in Afar has the implication that the modern zones of focused magmatism and strain are the pre-cursors of oceanic spreading centers. While Afar is clearly at an advanced stage in the rifting process, whether these modern zones are the *direct* precursors to oceanic spreading centers remains unresolved.

## 1. Introduction

The northern termination of the East African Rift, preserved in Afar and Yemen, is referenced in many introductory text books as a type locality of a triple junction. Within the geoscientific literature this region is also recognized as representing the transition between continental rifting and sea floor spreading (e.g., Makris and Ginzburg, 1987; Bastow and Keir, 2011; Bastow et al., 2018). As the home of 'Lucy' and other early hominids, this region is equally notable within the paleoanthropology community (Johanson and Taieb, 1976; Kimbel and Delezene, 2009; White et al., 2009; Haile-Selassie et al., 2015; Villmoare et al., 2015; Kappelman et al., 2016). Thus, while Afar represents the manifestation of different concepts and processes to each community that may study it, when interpreted collectively, the results emanating from these disparate fields can provide insights that no one study can hope to attain. In this contribution I explore the magmatic history of Afar (and Yemen), its relationship to the broad tectonic events underway in East Africa, and place these magmatic events into the stratigraphic framework developing within the region. The narrative generated by this geoscientifically regimented approach, while necessary to provide insight into the magmatic evolution of the region, should also be infused with imagination from the reader. The parallel evolution of the rift and early hominids makes the study of magmatism in Afar the study of our own development. Thus, “whilst this planet has gone cycling on according to the fixed law of gravity, from so simple a beginning endless forms most beautiful and most wonderful have been, and are being, evolved.” – Charles Darwin.

The Afar Depression is a broad region of subdued topography wherein the Red Sea, Gulf of Aden, and East African Rift System converge as a R-R-R triple junction at Lake Abhe (Tesfaye et al., 2003) (Fig 1X). As with many triple junctions, the precise geometry of the intersection is complex and megascale accommodation zones are necessary for interlinking the different rift systems (Tesfaye et al., 2003). Northern Afar is dominated by the N25°W orientation of the Red Sea system, southern Afar shows a N25°E orientation resulting from the Main Ethiopian Rift, whilst eastern Afar exhibits E-W trending structures associated with the Gulf of Aden (Tesfaye et al., 2003) (Fig 1X). The influence of these currently narrow zones of focused strain are superimposed upon a more broadly thinned crust (Bastow and Keir, 2011; Bastow et al., 2018), and presumably lithospheric mantle (e.g., Lavayssière et al., 2018). This somewhat elementary description of the tectonic conditions in Afar is, however, complicated by the presence of the Danakil Block (Fig 1X). Notably, the NNW oriented Erta Ale-Alid-Julua axial volcanic sectors in northern Afar are aligned with the Red Sea Rift, but are not strictly part of any southward progression of the Red Sea rift into Afar, which terminated at ~15°N (Eagles et al., 2002) (Fig 1X). Instead, these volcanic structures are related to motion of the adjacent Danakil microplate and the propagation of rifting northward from the Lake Abhe/ Tendaho-Goba'ad discontinuity (Eagles et al., 2002; McClusky et al., 2010; Sani et al., 2017) (Fig 1X). Such observations show that while Afar is an important locale in terms of representing a mature endmember for continental rifting, the tectonic conditions within this region remain complex and the interested reader is referred to the rich extant structural geology and geodetic literature for further information.

Modern zones of focused strain within Afar represent the closest relative to oceanic spreading centers and have thus attracted a significant amount of attention in constraining the transition from continental rifting to oceanic spreading. The initial recognition of the Wonji Fault Belt as a volcano-tectonic lineament traversing the northern Main Ethiopian Rift and Afar (Fig 1X) prompted discussion about the potential of this lineament representing a proto oceanic trough (Mohr, 1967). These early interpretations have been expanded by Hayward and Ebinger (1996), who showed that the zones of focused strain within the northern MER and Afar were 'segmented' in a manner that was similar to oceanic ridges. Moreover, these authors noted a progressive change in rift segmentation from the MER into Afar as the crust thinned and magma supply increased. These discrete rift sectors were later termed 'segments' and further constraints were placed upon their morphology noting that fault lengths decreased from south to north (Ebinger and Casey, 2001; Casey et al., 2006). Such insights prompted comparison between slow spreading oceanic ridges and the zones of focused volcano-tectonic activity within the MER, though it has also been recognized that the 'segments' lack the 'hard linkage zones of transform faults' (Casey et al., 2006). These models are supported by the organization of the upper mantle in the region, which has also been labelled as 'segmented' (Hammond et al., 2013). However, given the acknowledged role crustal thickness continues to play in controlling the structure and division of the modern zones of focused strain within the MER and Afar (Beutel et al., 2010; Bastow and Keir, 2011; Bastow et al., 2018), I adopt the term 'sector' to describe what has been termed 'segment' by others, as I judge that potential confusion may arise between the process of segmentation within oceanic and continental lithosphere where 'segment' is utilized. There remains a robust debate within the scientific community as to how these zones of focused strain may act as the precursors to oceanic ridges.

A consequence of the intersection of three extensional systems in Afar is the presence of a significantly attenuated continental plate. Prior constraints have recognized that the mechanisms by which extension is accommodated (and the plate thins) in Afar ranges from faulting and stretching to magma intrusion, each of which plays different roles during the breakup process (Beutel et al., 2010; Bastow and Keir, 2011; Daniels et al., 2014; Bastow et al., 2018). Seismic evidence shows thinned crust of about 25 km in southern Afar (Maguire et al., 2006) and < 20km in northern Afar (Bastow and Keir, 2011; Reed et al., 2014). Such attenuation of the continental crust is likely accompanied by a sympathetic thinning of the lithospheric mantle; it should be noted though that constraining the precise depth of the lithosphere – asthenosphere boundary in a region with evidence of diking and pervasive melt-lithosphere interaction (Gao et al., 2010; Desissa et al., 2013) using seismic methods alone can result in ambiguous outcomes (Rychert et al., 2012; Lavayssière et al., 2018). Afar thus affords an important window into the composition of sub-lithosphere reservoirs contributing to magmatism within the East African Rift. Elsewhere within the Rift, the complex metasomatic history of the Proterozoic, and in particular Archean lithospheric mantle, presents challenges in interpreting the isotopic composition of rift lavas (see part III of the synthesis series: Rooney (2020a)). In principle, the thinned plate should reduce potential contributions from ancient lithospheric mantle metasomes, and thus allow for a clearer understanding of how the Afar plume may influence rifting through magma generation.

Petrologic constraints have shown that the temperature of the sub-lithospheric mantle in Afar is elevated beyond that of typical ambient mantle (Rooney et al., 2012b; Ferguson et al., 2013a). Furthermore, the Sr-Nd-Pb-Hf-He isotope systems point to compositions consistent with a plume reservoir contributing to magmatism in Afar (e.g., Schilling et al., 1992; Deniel et al., 1994; Pik et al., 2006; Montagner et al., 2007; Rooney et al., 2012a). These constraints are consistent with seismic evidence of anomalous upper mantle conditions (Bastow et al., 2005, 2008, 2010), suggestive of compositionally and thermally heterogeneous material rising through the transition zone from the lower mantle African LLSVP (Benoit et al., 2006; Chang and Van der Lee, 2011; Cornwell et al., 2011; Hansen and Nyblade, 2013; Thompson et al., 2015). In aggregate, these data paint a compelling picture of an upper mantle beneath Afar that is profoundly impacted by the Afar plume. The data I present within this contribution show that Type III magmas (Rooney, 2017) dominate the modern volcanic record, consistent with the interpretation that such lavas are derived from a mix of three components: The Afar Plume, depleted upper mantle, and the Pan-African lithosphere (Rooney et al., 2012a). The ubiquitous presence of this magma type in a region that exhibits unambiguous plume-influence such as Afar, strengthens interpretations as to the origin of this magma type in other parts of the East African Rift. While much of the current scientific focus in Afar is on the modern impact of rifting on the regional crust and mantle, insights as to how the Afar depression has evolved can come from stratigraphic studies within the rift basins.

Work on the older basins along the rift margins has dominantly focused on the tectonic context of these units and the localization of strain (Wolfenden et al., 2005; Stab et al., 2016). Starting at formations dated to ca. 10 Ma and younger, focus on vertebrate fossils (Suwa et al., 2015), and in particular early hominins (Haile-Selassie et al., 2015; Villmoare et al., 2015) has resulted in abundant high-quality argon dating, magnetostratigraphy, and detailed tephra-stratigraphy (Walter and Aronson, 1982; Campisano and Feibel, 2008b, 2008a; Dupont-Nivet et al., 2008; Quade et al., 2008; Roman et al., 2008; Deino et al., 2010; DiMaggio et al., 2015a, 2015b; Saylor et al., 2016). The resulting stratigraphic understanding of basins in Afar are among the most well constrained for any rift globally (WoldeGabriel et al., 2001; Campisano and Feibel, 2008b; Quade et al., 2008; Campisano, 2012). Within this contribution I examine the stratigraphic record in Afar and neighboring Yemen in order to constrain the temporal evolution of magmatism and leverage modern constraints on the conditions of the East African upper mantle to probe what may have occurred in the past. I show that there is remarkable coherence between the identified magmatic units in Afar and tectonic events recorded in basin evolution. These results firmly link the magmatic events in Afar over the past 20 Ma with the evolving rift basin.

## 2. Yemen

### *2.1 General Background*

Following the eruption of flood basalts and the subsequent Early Miocene shield building phase, it has been thought that the extrusive magmatic activity in Yemen may have ceased following the same temporal cues as East Africa. Widespread intraplate magmatism on the Arabian Peninsula during this period may reflect a larger-scale destabilization of the Arabian lithosphere, with potential implications for magmatic events in Yemen from 20 Ma to present. Here I describe evidence of a continued linkage between magmatic events in Yemen and East Africa during this period.

Examining the distribution of existing K-Ar ages in Yemen, it is apparent that there are distinct events at ca. 10 Ma, 6 Ma, and from 3 Ma to Recent. More granular divisions are possible in the period from 6 Ma to Recent, but it is unclear what widespread continuity such divisions may possess (Orihashi et al., 1998). I have chosen to divide the magmatic periods in Yemen that post-date the Early Miocene shield building phase (see Rooney, 2017) into two events: A Mid Miocene Resurgence (ca. 11 to 9.5 Ma), and Pliocene to Recent volcanic fields (ca. 6 Ma to Recent). This approach differs from that in the existing literature. For example, Baker et al., (1997) group ca. 10 and 6 Ma volcanic fields and create a second division encompassing the Recent inland volcanic fields. Mattash et al. (2014) instead combine all this magmatic activity into a "Late Miocene to Recent volcanic Series" that they termed YMR. While "YMR" is a useful umbrella term that is currently the accepted stratigraphic name used for such rocks in Yemen (Beydoun et al., 1998), it is inadequate to describe the magmatic events from a mechanistic perspective. My rationale for creating two subdivisions of YMR are that there are two discrete magmatic events. The first (Mid Miocene Resurgence) has a short temporal duration, and the widely distributed magmatic centers associated with this event do not seem to have a later reactivation. The second event (Late Pliocene to Recent) has a much more extensive temporal duration, and critically, magmatic activity has continued in many Pliocene to Recent magmatic fields from 6 Ma to present. The spatial and temporal characteristics of magmatism thus warrant this two-fold division (Fig. 2).

### *2.2 Mid Miocene Resurgence (~11-9.5 Ma)*

This magmatic event is restricted in spatial extent to individual volcanic centers. The volcanic centers of Wadi As Sirr, Maswar Al Hada, Jabal An Nar, Al Harf, Perim Island, and Jabal Kharaz yield ages that range from 9.5 Ma (± 0.3) to 11.5 Ma (± 0.3), but generally cluster around 10-10.5 Ma (Gass and Mallick, 1968; Capaldi et al., 1983, 1987; Mallick et al., 1990; Manetti et al., 1991). This observation has the implication that there is a remarkable temporal consistency in a resurgence in magmatic activity from Yemen, through Afar and into the Northern Main Ethiopian Rift at ca. 10.5 Ma (See discussion in Part II of this synthesis series; Rooney (2020b)). These magmatic events took the form of basaltic plateaus, and central volcanoes exhibiting a wide range of magmatic products (Capaldi et al., 1983, 1987; Mallick et al., 1990). Magmatism during this period is typically transitional to tholeiitic in composition.

### *2.3 Ca. 6 Ma to Recent*

This volcanic period manifests as the Sana'a Amran, Dhamar-Rada'a, Sirwah-Marib, Shuqra, and Bir Ali/Balhaf volcanic fields (Cox et al., 1977; Baker et al., 1997; Heikal et al., 2014), and activity at little Aden, Aden Volcano, Um Birka, and Ras Imran (Gass and Mallick, 1968; Dickinson et al., 1969). Recent activity is also recorded on the volcanic islands of Jabel at-Tair (eruption 2007), the Zubair Group, Zuqar, and the Hunaish Islands (Volker et al., 1993; Mattash et al., 2014), and within the Red Sea and Gulf of Aden spreading axes, however these oceanic regions are beyond the scope of this review. Basaltic volcanism during this period commenced ca. 6.18 Ma (± 0.33) and continued until recent times (Orihashi et al., 1998; Mattash et al., 2014). More detailed geochronological analyses have suggested four phases during which basaltic volcanism within these fields was active (ca. 5-6 Ma), 3.6-2.9 Ma, 2.2-1.7 Ma, and <1.3 Ma (Orihashi et al., 1998). I have not divided data into these temporal groupings as the spatial overlap in these pulses makes it difficult to assign lavas to the individual pulses without accompanying geochronology on each sample. The modern volcanic episode dominantly takes the form of cinder cones and associated flows that extend over a wide area but have a limited thickness, and are thus volumetrically less significant than the Oligocene events (Baker et al., 1997). A significant shift towards more alkaline compositions is evident during this period in comparison to the prior Late Miocene events (Manetti et al., 1991; Cox et al., 1993). This shift in alkalinity has been explained by melting of a lithospheric mantle previously metasomatized by the Afar mantle plume that has been subsequently destabilized by extension (Baker et al., 1997).

*2.4 Geochemical Variation of Lavas from Yemen*

For lavas representing the Mid Miocene resurgence, there is a wide array of compositions erupted, resulting in some scatter in the variation of elements versus MgO (Fig. 3). There may be tentative evidence of two parallel trends in Nb and Zr, with much of the Mid Miocene dataset above 5 wt.% MgO trending to much lower values than the subsequent Pliocene-Recent activity (Fig. 3). There is no evidence of crustal assimilation within the MgO versus $^{87}Sr/^{86}Sr$ and $^{143}Nd/^{144}Nd$ plots (Fig. 3), consistent with multi-isotope plots showing a composition close to the Afar plume, but with mixing towards the depleted mantle and lithosphere endmembers (Fig. 4). No extended trace element data are available for rocks from this time period and we thus do not know what lava type (i.e. three fold division established by Rooney 2017) these magmas may exhibit.

Lavas from the Pliocene-Recent volcanic period display a coherency in their patterns that is typified by overlapping vectors of magma evolution (Fig. 5). Exceptions to this are lavas from the Aden and Um Birka fields (both coastal volcanic fields near the triple junction region), where $TiO_2$ and $CaO/Al_2O_3$ extend to much higher values in comparison to the other fields (Fig. 5), suggesting heterogeneity in the mode of magmatic evolution. Most magma series in East Africa exhibit an increase in $TiO_2$ until the stabilization of Fe-Ti oxides at about 5% MgO during a fractional crystallization sequence. The Aden and perhaps Um Birka fields appear to follow such a sequence, however the Shuqra, Bir Ali-Balhaf, Sana'a fields exhibit virtually no change in $TiO_2$ content from 12 to 4 wt.% MgO (Fig. 5). There is no clear evidence of crustal assimilation in these lavas in terms of co-variation of $^{87}Sr/^{86}Sr$ and $^{143}Nd/^{144}Nd$ with MgO (Fig. 5), suggesting that this variation is caused either by the fractionation of a Ti-rich phase, or by mixing between a primitive and evolved magma. Titanian-augite has been noted as a phenocryst phase in some of these lavas (Heikal et al., 2014), and the fractionation of this phase would be consistent with the lack of $TiO_2$ enrichment and steeper $CaO/Al_2O_3$ trend and present in these lavas (Fig. 5). High-pressure fractionation, which has been previously proposed, is thus favored for these lava Series (Heikal et al., 2014), with the exception of lavas that may have developed on attenuated lithosphere near the triple junction.

Primitive mantle normalized trace element patterns have proven useful in establishing distinct magma types throughout East Africa (Rooney, 2017). Within this series of synthesis papers, six such magma types have thus-far been identified; all magma types are amalgamated in the final contribution (Part V: Rooney (2020c)) (Table 1). Despite the utility of such primitive mantle normalized figures, it is difficult to apply them in Yemen as there is a profound lack of modern geochemical data on post Traps Series magmas. Sufficient incompatible trace element information needed to construct a primitive mantle normalized diagram is available from only two studies (Baker et al., 1997; Heikal et al., 2014), and provide thus only limited constraints on the Sana'a field and Bir Ali-Balhaf fields. These datasets appear to show that at Sana'a, a Type III magma pattern (Rooney, 2017) may be evident, though Th is more enriched than is typically observed (Fig. 6). Some samples from the Bir Ali-Balhaf field show an identical pattern to those of Sana'a, but with a consistent depletion in the more compatible trace elements (Fig. 6). A subset of these rocks displays a curious U depletion that manifests as a fractionation of U/Th, an enrichment in most of the other more incompatible trace elements, and a notably high P content (Fig. 6). These samples also appear to have depletions in CaO and FeO*. The origin of this variation is unknown and may represent source variability or assimilation - further geochemical studies of this region are required to address this issue. A compilation of rocks from the Red Sea and Gulf of Aden are not part of this review, however it is notable that recent eruptions on volcanic islands in the Red Sea off the coast of Yemen have yielded Type II magmas (Mattash et al., 2014), similar to that in the Erta 'Ale field in Afar.

Crustal assimilation has been recognized as an important process in earlier magmatic episodes in Yemen (Baker et al., 1996). This process likely impacts the more recent rocks at the more evolved end of the spectrum (e.g., Sana'a), though there is little co-variance of MgO with $^{87}Sr/^{86}Sr$ and $^{143}Nd/^{144}Nd$ in the more mafic compositions (Fig. 5). The isotopic variation of lavas from Yemen is, however, complicated by metasomatic processes that have impacted the continental lithospheric mantle (Menzies and Murthy, 1980; Baker et al., 1997; Sgualdo et al., 2015). Close to the triple junction, the lithosphere is thought to have undergone significant melt-rock reaction with plume-related lavas (Baker et al., 1997). More distant from this region, the array of compositions recorded in xenoliths spans the range of mantle derived rocks, indicating a long metasomatic history (Sgualdo et al., 2015). Caution should be exercised, however, as xenoliths rarely sample the metasomes that contribute to melt generation (e.g., Shaw et al., 2007), and the precise composition of the metasomes that contribute to melt generation in this region remains ambiguous. Metasomatic processes enriching the lithospheric mantle are consistent with the unusual placement (Fig. 7) of some lavas in multi-isotope space such as the low $^{143}Nd/^{144}Nd$ samples from the Ataq diatreme that are interpreted a partially derived from the melt of a lithospheric metasome (Menzies and Murthy, 1980). The two samples from Marib (Bertrand et al., 2003), which are the most inland of the samples analyzed, are deflected below the mantle array in $\varepsilon_{Nd}$-$\varepsilon_{Hf}$, plotting significantly away from the Afar Plume in comparison to samples from Shuqra, Sana'a, and Bir Ali-Balhaf (Fig. 7). Such samples, and others from the Arabian plate distant from the triple junction have similar isotopic characteristics, indicating the contribution of another endmember to melt generation – a HIMU-like lithospheric metasome (Bertrand et al., 2003), which is widespread within the regional lithospheric mantle away from the influence of the Afar plume, and has evolved as a result of enrichment associated with the Pan-African assembly of the continent (Rooney et al., 2014).

### *2.5 Summary of Magmatism in Yemen*

The post-traps magmatic episodes in Yemen exhibit some commonalities with contemporaneous activity in the northern MER and Afar. Notably, the Mid Miocene Resurgence event at ca. 10 Ma appears to have had a significant impact on eruptions within the Yemen region, expanding the spatial extent of this event, which has been previously defined on the basis of activity in the Northern Kenya Rift, Turkana, the MER, and the Afar margin.

## 3. Afar

The current division of magmatic series in Afar results from broad observations about the deformation of units and the extensive K-Ar dating campaigns that took place dominantly during the 1970s. This approach, in combination with the largely similar eruptive style and composition of magma in Afar during this period, has led to significant ambiguity with respect to the definition specific magmatic units. In this section I use a combined approach of time and process to re-define existing magmatic units. Specifically, extensional events in Afar provide the clearest rationale for the division of the magmatic units. I therefore utilize the growing detailed sedimentary record of basin development in Afar and link the temporal window for a magmatic unit to such formations (Fig. 8). Where processes may be heterogeneous across the region, I note the temporal overlap in magma formation names.

### *3.1 Development of the Rift Margin (20 to 10 Ma)*

#### 3.1.1 Timing of magmatic activity

Following the eruption of the Adolei basalts (part of the Early Miocene Resurgence Phase – see Part I of the synthesis Series: Rooney (2017)) there was a period that is relatively quiescence in terms of basaltic magmatic activity, and is instead dominated by largely rhyolitic eruptions (and subordinate basalts) termed the Mablas Series (Fig. 8). This magmatic unit is extensive around the Ali Sabieh region and north of the Gulf of Tadjoura in Djibouti (Le Gall et al., 2018), forming a broadly N-S alignment parallel to the shoreline (Fig. 9). These volcanic units are typically alkaline or peralkaline with some crustal involvement in their evolution (Deniel et al., 1994). Where exposed, thicknesses have been measured to 600m (Varet, 2017). The timing of this unit was thought by Audin et al. (2004) to extend from 25.2 to 12.4 Ma, though this range is larger than that of the recent geologic map of Djibouti, which has the Series (basalt and rhyolite combined) extending from 18.8 to 9.5 Ma. Vellutini (1990) note that the early dates attributed to the Mablas Series may relate to an earlier rhyolite episode from 25 to 19 Ma. This time period is coincident with the Early Miocene resurgent phase, and are correlative with the Kemise rhyolites (25.9 Ma ± 0.16 $^{40}Ar/^{39}Ar$), Ataye rhyolite (25.3 Ma ± 0.13 $^{40}Ar/^{39}Ar$), and Senbete Ignimbrites (24.8 Ma ± 0.13 $^{40}Ar/^{39}Ar$) from the Western Afar Margin (Ukstins et al., 2002; Wolfenden et al., 2005). I thus prefer a more constrained time frame for the Mablas Series that is provided by the $^{40}Ar/^{39}Ar$ analyses of the bottom and top flows within the Mablas rhyolites, which yield a range from 15.4 Ma (± 0.3 $^{40}Ar/^{39}Ar$) to 11.8 Ma (± 0.6 $^{40}Ar/^{39}Ar$) (Zumbo et al., 1995). This period thus broadly correlates with the ca. 300m thick rhyolitic ignimbrites of the 'Main Silicic Phase' along the SE Afar margin that is dated from 13.3 Ma (± 0.25) to 11.05 Ma (± 0.25) (Kunz et al., 1975; Juch, 1978). Along the Western Afar margin, the Shewa Robit Ignimbrite Formation ranges from 19.76 Ma (± 0.07 $^{40}Ar/^{39}Ar$) to 14.90 Ma (± 0.06) (Wolfenden et al., 2005), and could be correlated with the Mablas Series.

A curiosity along this margin is the Aneno Formation - defined as massive fissural basalts at least 300m thick whose base are constrained to 15.9 Ma ± 0.5 (Wolfenden et al., 2005). Little is known about this unit and its relationship with the evolving margin or the basaltic component within the Mablas Series. The basaltic component of the Mablas, which is considered to have started later than the rhyolites, might be correlative with the ca. 10 Ma basaltic event discussed previously given the K-Ar ages that extend from 9.7 to 11 Ma (Barberi et al., 1975b)(note though that the recent map of Djibouti provides an age range from 13.5 to 9.5). At this time, it is unclear if the Mablas Basalts are related to the regional ca. 10 Ma event that is recorded in Afar along the SE and NW margin (See Part II of the synthesis: Rooney (2020b)). It is notable, however, that this time period in Afar is not one where typically large volumes of basalts are evident, and has been described by some authors as a time where the rift margin is ‘starved’ of volcanism (Stab et al., 2016). This stands in stark contrast to the regions surrounding the Afar Depression. In Yemen and Central Ethiopia, the Mid-Miocene resurgence sees the eruption of massive platforms of basalts – an event notably absent from Afar. Further examination of lavas from this period are necessary to resolve these curious observations.

Magmatic activity during this phase is synchronous with the development of the rift margin in Afar. Beginning at ca. 25 Ma, extension along the western Afar margin dominated the tectonic environment (Wolfenden et al., 2005; Stab et al., 2016). The subsequent localization of strain along this margin remains controversial. Wolfenden et al. (2005) suggest a progressive localization of strain into a series of rift marginal basins, which eventually migrated towards the modern rift axis. In contrast, Stab et al. (2016) present evidence that strain along the western Afar margin was diffuse until ca. 4 Ma. The data presented herein cannot address these disparate models, however the critical shared observation from both is that this period from ca. 20 to 10 Ma is one of rift development in Afar. Thus, the correlation of significant silicic magmatic activity with the evolution of the rift margin remains a robust observation, and is consistent with parallel rift evolution-silicic volcanism inferences further south within the Main Ethiopian and Kenya Rifts (see part II of the synthesis series: Rooney (2020b)).

#### 3.1.2 Geochemical Composition of Magmatism during the Rift Margin Phase

The origin of primitive magmas during this time period is not well-constrained as few data points exist with sufficiently high MgO values (Fig. 10) to effectively probe the mantle source conditions. The Mablas Series follows the same magma differentiation trends as other magma series in Afar (Fig. 8). The only notable distinction of the Mablas Series in comparison to other units is a tendency toward elevated Zr/Nb in comparison to other magma series (Fig. 10). While the volume of this data is modest, the Mablas data presented here are from three different studies suggesting this observation is a shared feature of the Series. It should be noted that Zr values do not differ, requiring slight relative depletions in Nb to account for the Zr/Nb variance, and is suggestive of potential crustal assimilation.

Chondrite-normalized patterns for the Mablas Series track closely with that of the later Afar Stratoid Series but differ from the flatter HREE patterns evident in some of the Dalha Series (Fig. 11). Primitive mantle normalized patterns indicate a Type III magma (see Rooney, 2017 for a listing of magma types), with characteristic Ba, Nb and Ta peaks combined with a Th-U trough, but these peaks and troughs have limited amplitude in comparison to the regional dataset (Fig. 12). Type III magmas have been described as a mixture of Afar Plume, the Depleted Mantle, and a Pan African lithosphere component (Rooney et al., 2012), and it is likely the case that this describes the origin of the Mablas Series rocks. In many magma suites throughout the region it can be difficult to distinguish between lithospheric contamination that is associated with assimilation of the crust, and the mixing/dripping of lower lithospheric materials into the upper mantle (e.g., Furman et al., 2016). However, the Mablas Series shows clear indications of crustal assimilation (Fig. 10). Notably, the strong correlation between MgO and $^{87}Sr/^{86}Sr$, in addition to $^{143}Nd/^{144}Nd$ (Fig. 10), reflects a crustal assimilation fingerprint in the evolution of this magma series. The lithospheric signal evident within the Mablas Series results in a deviation away from the Afar Plume and depleted mantle components (Fig. 13). The precise composition of the assimilant is unclear but is comprised of radiogenic $^{87}Sr/^{86}Sr$, and unradiogenic $^{143}Nd/^{144}Nd$, $^{176}Hf/^{177}Hf$, and Pb isotopes that occupies a space similar to that of the previously modelled Pan-African Lithosphere endmember (Fig. 13).

### 3.2 The Dalha Series and the Development of Rift Marginal Basins (10 to 3.9 Ma)

This time period in Afar benefits from detailed stratigraphic work undertaken pursuant to paleoanthropological studies. While such stratigraphic works have focused on basins where sediment has accumulated, parallel studies have identified a synchronous magmatic event that has been broadly termed the "Dalha Series" that may be comprised of different members (e.g., Dalha Basalts, Somali Basalts). Here I examine the Dalha Series in the context of the evolving stratigraphic framework for Afar and create a new magmatic subdivision – the Dalhoid Series (Fig. 8).

#### *3.2.1 Dalha Series*

This fissural basaltic episode was initially thought to have been between 8 and 4 Ma (Barberi et al., 1975b; Varet et al., 1975), occurring dominantly in the marginal portions of the basin near the Red Sea (Barberi and Varet, 1978). The thickness of the Series varies widely, for example along the Red Sea margin it varies from 10 to 1000 meters (Varet, 2017), and along the Western Afar margin from 50 to 200m (Wolfenden et al., 2005). The Dalha Series was distinct from the underlying units due to the angular unconformity evident at their contact. A compilation of ages from Audin et al. (2004) showed dates ranging from 3.9 Ma to 8.3 Ma, though the new ages obtained by Audin range from 4.77 Ma (± 0.08) to 7.69 Ma (± 0.13). Since its original inception, the Dalha Series has been sub-divided to form the 'Somali Basalts', a remarkably undeformed group that occurs only along the Djibouti-Somali border and is dated to between 7.2 and 3.6 Ma (Daoud et al., 2011). We incorporate the Somali Basalts into the greater Dalha

Series (Fig. 8). It can be challenging to distinguish between the Dalha Series and the later Afar Stratoid Series as they are structurally and compositionally alike. This problem is particularly acute along the western Afar margin, though this difficulty also occurs in the well-mapped Djibouti region, where rocks originally mapped as Somali Basalts were more precisely dated to be much younger (Audin et al., 2004). This issue has been recognized previously, where both the Dalha and Stratoid Series are, in many places, in a continuous and conformable contact (Varet, 2017). Such difficulties are discussed below, with the proposed introduction of a new magma series to resolve some of the existing ambiguities.

Unlike the earlier Mablas Series, the rocks that comprise the Dalha Series extend to much more magnesian values (Fig. 10). Similar to older the Mablas Series, lavas of the Dalha Series plot at slightly depleted values of Nb, which can result in elevated Zr/Nb (Fig. 10), though not to the same degree as the Mablas Series. A critical distinction between the Dalha Series and all others in the region is the relatively flat HREE profile evident from Gd to Lu (Fig. 11; 12). This results in a somewhat low value for Tb/Yb in comparison to the other magma series (Fig. 8). The observation of relatively flat HREE patterns is derived from multiple studies, and is thus a potential tool for distinguishing lavas of this type. Dalha Series magmas exhibit typical Type III characteristics (Ba-Nb-Ta peaks, combined with Th-U troughs) (Fig. 13). Lavas of the Dalha Series exhibit clear indications of crustal assimilation, with $^{87}Sr/^{86}Sr$ and $^{143}Nd/^{144}Nd$ trending towards lithospheric compositions with decreasing MgO (Fig. 10). This observation is consistent with multi-isotope plots showing the Dalha Series lavas extending from a largely plume-like composition towards the same lithospheric contamination space as the earlier Mablas Series (Fig. 13).

#### *3.2.2 Dalha Series and Basin Development*

Following the major fissural basaltic event and trachytic shield volcanic episode discussed above, magmatic activity within the Afar region localized into rift marginal basins (e.g., Chernet et al., 1998). These basins have proven exceptionally important repositories of fossils, resulting in well-constrained stratigraphy at specific fossiliferous locations. The formations within these basins are described from south to north along each margin:

*Chorora Formation*: This Formation occurs for ca. 115 km along the SE Afar Margin and lies above the ca. 10 Ma Anchar basalts (also termed the Upper Trap Series), which are part of the Mid Miocene Resurgence event (See part II of the synthesis series: Rooney (2020b)). This Formation consists of dominantly lacustrine and riverine sediments with intercalations of tephra (Katoh et al., 2016). Extensive mapping of the Formation and detailed geochronology has constrained the Formation to between 9.41 and 7.03 Ma (mean values of K-Ar and $^{40}Ar/^{39}Ar$ by Katoh et al., 2016) (Fig. 8). The unit is capped in places by basaltic flows dated at 6.72 Ma ± 0.16 and 6.94 Ma ± 0.17 (Katoh et al., 2016). The Formation is fractured and tilted by subsequent faulting associated with the development of the Afar Margin. Silicic activity is also recorded during this time period as a trachyte from Gara Gumbi at 6.85 Ma ± 0.10 (Chernet et al., 1998). Subsequent magmatic activity (5.60 Ma ± 0.09 to 4.68 Ma ± 0.10) (Chernet et al., 1998) migrated to the northwest and took the form of relatively undeformed silicic centers and fissural basalts that have been assigned to the Afar Stratoid Series. Note that on the country-scale map of Ethiopia, sediments of the Chorora Formation are considered to occur within the ‘Danakil Group’, which is mapped along the margins of the Erta ‘Ale range. Given the occurrence of basalts within the Danakil Group we assign this unit to the Dalha series at present (flanking the Erta ‘Ale range). Further geochronological work is required to confirm or refute this tentative assignation.

*Kessem Formation:* I have previously described the Kessem Formation with rocks from the Ethiopian Rift, however it is important to summarize here that the Formation has a lower portion that consists of the same basaltic event that also occurs at base of the Chorora Formation, and has an upper portion that is comprised of volcanoclastics that terminate at 6.6 Ma (Wolfenden et al., 2005). The unit has been tilted and deformed as the rift margin developed.

*Bercha Formation:* Defined by Wolfenden as a series of basaltic to intermediate lavas that total 400 m in thickness. The uppermost portion of the Formation is dated at 7.12 Ma (± 0.04 $^{40}Ar/^{39}Ar$) Wolfenden et al. (2005).

*Burka Formation:* Defined by Wolfenden et al. (2005) as a package of intercalated basalts and rhyolites that is not itself dated, but is constrained to have an age between the Oligocene Flood Basalts at ca. 30 Ma and the subsequent undeformed basaltic activity that is dated elsewhere along the margin at 6.64 Ma ± 0.04 and attributed to the 'Dalha Series' (Wolfenden et al., 2005).

*Chifra and Finto "Series":* These Series occur from 11.5 to 12°N and consist of basalts, rhyolites and tuffs. The Series are tilted and deformed up to 35° (Stab et al., 2016). These Series are different to the others described above as they include the underlying Early Miocene Resurgent phase activity that is dated in this area from 22.9 Ma (± 0.3) to 23.5 Ma (± 1.2) (Stab et al., 2016) (Fig. 8). Subsequent basaltic activity is dated at 7.69 Ma (± 0.50), with no apparent deposits dated between the Early and Late Miocene (Stab et al., 2016). This observation is notable as it provides a northern termination in the rift of the ca. 10 Ma fissural basaltic event that forms the base of most other contemporaneous formations in Afar. The upper portion of the Series are rhyolites and volcanoclastics that are as young as 7.00 Ma (± 0.35) (Stab et al., 2016). This is consistent with an age peak for xenocrystic feldspars of 7.27 Ma in the adjacent basin (Deino et al., 2010). Stab et al. (2016) indicate that accumulation of the Chifra and Finto Series terminated at ca. 7 Ma. Overlying these volcanoclastic deposits are flat-lying "Stratoid Series" basalts (5.39 Ma ± 0.28 to 3.97 Ma ± 0.10) and rhyolites (undated) (Stab et al., 2016) that resemble the units overlying the Chorora Formation from the SE Afar margin. These units are shown as the mixed Miocene symbol in the accompanying map.

These data show distinct similarities in the marginal grabens developing in the region during this period. Following the widespread ca. 10 Ma fissural basalt event (Mid Miocene Resurgence – see Part II of the synthesis: Rooney (2020b)), the development of the rift margin and associated grabens facilitated more localized silicic activity and sediment accumulation from 9 to 12 °N along the NW and SE rift margin. This period of accumulation is abruptly terminated by the migration of magmatic activity basinward at ca. 7 Ma. This resulted in profound deformation and tilting of these formations, which are then onlapped by a subsequent phase of magmatism that is bimodal with large silicic centers and fissural basalts that date from 6.94 to 3.97 Ma. However, significant complexity occurs during this period, which may be subdivided into a Dalha and Stratoid Series.

### 3.2.3 Distinguishing Dalha from Stratoid – the genesis of the Dalhoid Series (5.6 to 3.9 Ma)

Between ca. 6.85 and 3.9 Ma there exists some degree of ambiguity as to the proper assignment of basaltic units to a specific magmatic series. This period reflects the widespread commencement of a new phase of magmatic activity throughout Afar, with an accompanying range of approaches to nomenclature. Wolfenden et al. (2005) use the term ‘Dalha Series’ to describe 50-200m thick fissural basalts occurring along the northwestern rift margin that date from ca. 6.64 Ma to about 5.3 Ma (commencement of the Sagantole Formation – see Renne et al., 1999) (Fig. 8). This Series is broadly equivalent with the dominantly basaltic Adu-Asa Formation along the same margin (Kleinsasser et al., 2008). The Adu-Asa Formation consists of at least 185m of dominantly basaltic flows dated from >6.4 Ma to 5.2 Ma (Kleinsasser et al., 2008) (Fig. 8). The Dalha Series dips towards the basin and is separated from the underlying units by ‘a regionally extensive tectonic unconformity’. The basalts from the NE rift margin have a similar age range to the unnamed basalts (6.72-6.94 Ma) capping the Chorora Formation along the SE margin and we thus correlate them given basalts from both margins cap a ca. 10-7 volcanocalstic sequence.

Following the stratigraphic arrangement of Wolfenden et al. (2005), the Dalha Series basalts terminate with the Sagantole Formation (Fig. 8) – an important hominid-bearing sedimentary sequence with volcanic intervals dated extensively to occur between ca. 5.6 and 3.9 Ma (Renne et al., 1999; WoldeGabriel et al., 2001, 2009; Quade et al., 2008). The Sagantole Formation includes a basalt dated to 5.18 Ma (± 0.07 $^{40}Ar/^{39}Ar$), indicating that basaltic flows were contemporaneous with this dominantly sedimentary formation (Renne et al., 1999). Importantly, the basalt within the Sagantole Formation is not the only basaltic flow recorded in Afar during this interval. Further north at Chifra, basalts extend from 5.39 Ma (± 0.28) to 3.97 Ma (± 0.10), with a peak in xenocrystic feldspars from the adjacent basin at 4.60 Ma suggesting contemporaneous silicic activity (Deino et al., 2010; Stab et al., 2016). Along the SE rift margin, basalts in the rift basin adjacent to the Chorora Formation date from 5.59 Ma (± 0.10) to 4.68 Ma (± 0.10) and are contemporaneous with the development of several large silicic centers as noted above (5.14 Ma ± 0.08 to 5.60 Ma ± 0.09) (Chernet et al., 1998). The period from ca. 5.6 Ma to 3.9 Ma thus has a significant basaltic episode that seems focused along the rift margins, yet its assignment to specific stratigraphic groups is ambiguous. These rocks might fall under a more permissive classification of the Dalha Series of 8.6 to 3.6 Ma as noted in the recent geologic map of Djibouti (Le Gall et al., 2015). Equally, rocks of this age have also been correlated with the Afar Stratoid Series by others (Chernet et al., 1998; Stab et al., 2016). The extensive work on rift marginal basins undertaken since the original classification of the Dalha Series in the 1970s suggests that a distinct period of sediment accumulation is contemporaneous with a pulse of magmatic activity from ca. 5.6 to 3.9 Ma, and that it may now be useful to form a new magmatic series recognizing this distinct event. I thus propose the use of an intermediate name for such rocks - the 'Dalhoid Series', which represent the basaltic and silicic volcanism that accumulated during this interval from 5.6 to 3.9 Ma across the Afar Depression (Fig. 8).

There exist relatively few geochemical datapoints for lavas that have been clearly stratigraphically constrained to within the strata we have defined as Dalhoid (Fig. 10). Despite the limited sample suite, the existing samples are particularly well-characterized. These samples follow trends similar to both the Dalha and Afar Stratoid Series (Fig. 10). The Dalhoid Series follow the same crustal assimilation pathways as the Dalha Series, exhibiting strong correlation between $^{87}Sr/^{86}Sr$ and $^{143}Nd/^{144}Nd$ with MgO (Fig. 10). This similarity with the Dalha Series must be interpreted within the context of the REE patterns for the Dalhoid Series, which shows much steeper HREE trends (Fig. 11), with Tb/Yb fractionation consistent with the Afar Stratoid Series (Fig. 10). The Dalhoid Series exhibits a Type III pattern in terms of primitive mantle normalized incompatible element concentrations (Fig. 12); it is somewhat different from the Dalha and Mablas Series patterns in having a typically clearer trough in Th-U and peak in Nb-Ta. These tentative observations require further exploration with a much larger dataset. The behavior of the Dalhoid Series in multi-isotope space parallels the Dalha and Mablas Series whereby significant crustal contamination results in arrays towards lithospheric endmembers (Fig. 13). Broadly, the similarity between the Dalhoid and Afar Stratoid Series in terms of primitive mantle and chondrite normalized patterns (Fig. 11; 12) suggests a similar shared parental magma, which is distinct from the earlier Dalha Series. It is likely that the Dalhoid Series is an initial pulse of magmatism associated with the Afar Stratoid Series event, but this pulse experienced crustal assimilation that is similar to the earlier Dahla and Mablas magma Series. Assuming such an origin for the Dalhoid Series, there is little geochemical necessity for a division between this Series and the Afar Stratoid Series. However, the current ambiguity in relation to the regional stratigraphy in this region requires the creation of this new unit.

### *3.3 The Afar Stratoid Series and Hadar/Busidima Formations (3.9 to 1.6 Ma)*

This time period in Afar is synonymous with the most extensive magmatic event within the Afar Depression, while simultaneously hosting some of the most important hominin fossil sites within the rift. As with the previous period I explore this interval in the magmatic context of the Afar Stratoid Series and the stratigraphic context provided by paleoanthropology studies.

#### 3.3.1 The Afar Stratoid Series

Much like the Dalha (and Dalhoid) Series which came before, the Afar Stratoid Series is a fissural magmatic event typified by vast volumes of basalt that erupted over a 55,000 $km^2$ region in the Afar Depression (Fig. 14) (Varet et al., 1975; Lahitte et al., 2003b). The volcanic pile is thought to reach at least 1000m in thickness (Barberi and Santacroce, 1980; Varet, 2017). The majority of the Afar Stratoid Series is comprised of basalt, though rhyolite intercalations are observed, becoming more common towards the upper part of the sequence (clustered at 1.3 to 1.5 Ma), where about 20 central volcanoes are also evident (Barberi and Santacroce, 1980; Lahitte et al., 2003b). The central volcanoes are built through effusive activity (e.g. domes etc) and pyroclastic events are unusual (Barberi and Santacroce, 1980; Lahitte et al., 2003b). As discussed above, the precise timing of the Afar Stratoid Series has been a matter of some debate. Compilations of existing data and new K-Ar work provided a clear time window from 3.27 Ma (± 0.06) to 1.36 Ma (± 0.11) as the period over which the Stratoid Series was erupted (Kidane et al., 2003; Lahitte et al., 2003b). However, another compilation and additional work on the Stratoid Series revealed a range of dates older than the 3.27 Ma upper bound previously suggested (Stab et al., 2016). Closer to the rift margin, ages are notably older, extending from 3.30 Ma (± 0.05) to 3.97 Ma (± 0.10), with a peak in xenocrystic feldspar near the western Afar margin at 3.91 Ma (Deino et al., 2010; Stab et al., 2016). On the basis of the array of older dates I assign an upper limit of 3.9 Ma to the initiation of the Afar Stratoid Series, correlating with the end of the Sagantole Formation (discussed above) (Fig. 8). Lavas erupted prior to this period are grouped with the Dalhoid Series (3.9 to 5.6 Ma). Previous work on mapping the distribution of the Afar Stratoid Series on the basis of field expression and aerial photographs, resulted in a subdivision of the Series into an Upper and Lower Stratoid Series (Kidane et al., 2003). The Lower Stratoid Series was considered older than 2.6 Ma and had a tabular expression with flat topography (Kidane et al., 2003). The Upper Stratoid Series (younger than 2.6 Ma) were also tabular and laterally continuous with scoria sometimes separating flows and are well exposed along faults (Kidane et al., 2003). As with the division between the Dalha and Stratoid Series, the transition to the subsequent Gulf Series can be problematic. Kidane et al. (2003) note a sequence of basalts that date from 0.59 Ma (± 0.16) to 1.11 Ma (± 0.09) that were previously mapped as Stratoid Series, though the revised dating and morphology more correctly place them with the later Gulf Basalts (Fig. 8). Such difficulties are to be expected where continuous basaltic volcanism makes distinct temporal breaks ambiguous.

While the extent of the Afar Stratoid Series has generally been bounded by the topographic limits of the Afar Depression (Fig. 14), the southern extent of the Afar Stratoid Series has typically been difficult to constrain due to the rapid sedimentation within the Main Ethiopian Rift covering older sequences. However, along the western Afar margin at 9.5°N, the base of a 200m thick sequence of trachytes yields a date of 3.50 Ma (± 0.11 $^{40}Ar/^{39}Ar$) that has been correlated with the Afar Stratoid Series (Wolfenden et al., 2005). While compositionally distinct from the dominantly basaltic Afar Stratoid Series, this trachytic sequence may reveal a transitional continuity between the Stratoid magmatic event and contemporaneous silicic pyroclastic activity within the MER. Notably, after a ca. 3 Ma unconformity, magmatism is again recorded in the MER from 3.555 Ma in the form of the pyroclastic Balchi Formation (Wolfenden et al., 2004). These data thus show that the eruption of the Lower Stratoid Series was broadly contemporaneous with a flare up in magmatism more broadly than has been previously recognized. Indeed it now seems likely that the magmatic event that resulted in the eruption of the Afar Stratoid Series in Afar, manifested as more evolved magmatism in the MER during what is termed there as 'The Stratoid Phase: 3.9 to 0.5 Ma' – see part II of the synthesis series (Rooney, 2020b).

There exists a significant volume of data on the Afar Stratoid Series, from mafic endmembers through to more evolved compositions (Fig. 10). The Stratoid lavas form evolutionary trends that parallel earlier magma series (Fig. 10). A significant distinction between the Afar Stratoid Series and the earlier Dalha Series lavas is the slope of the HREE, which is more pronounced in the Afar Stratoid Series (Fig. 11), resulting in elevated values of Tb/Yb (Fig. 8). The Afar Stratoid Series exhibit a Type III primitive mantle lava pattern (Fig. 12), similar to the earlier Mablas, Dalha, and Dalhoid Series. A notable distinction between the Afar Stratoid Series and the earlier lava series is a lack of obvious crustal contamination (Fig. 10). The Afar Stratoid Series lavas do not follow the same contamination vectors in terms of $^{87}Sr/^{86}Sr$ and $^{143}Nd/^{144}Nd$ versus MgO (Fig. 10), and instead occur within the mixing space defined between the Afar Plume, Depleted Mantle, and Pan-African Lithosphere components (Fig. 13).

There exists a subset of the Afar Stratoid Series that erupted along the Afar margin within the Woranso-Mille paleoanthropology region that have a distinctly depleted character in terms of the most incompatible trace elements in comparison to the other Stratoid Series lavas (Fig. 10). These incompatible element depleted lavas resemble a subset of the Gulf Series erupted in Djibouti (Hayyabley Volcano: Daoud et al., 2010). These unusual Afar Stratoid Series lavas are high in MgO and exhibit exceedingly low concentrations of Nb, consistent with other low concentrations in incompatible trace elements that were measured (e.g., Rb, Ba, Zr). While a full trace element suite has not yet been presented for these samples (Alene et al., 2017), they exhibit characteristics of Type VI lavas – a lava type restricted to the Afar Depression and requires the contribution of a significantly depleted source to their petrogenesis. Such lavas are thought to derive from a depleted component within the Afar plume (Barrat et al., 2003; Daoud et al., 2010). Further analysis of these samples will be necessary to determine whether these lavas are Type VI or constitute another lava type.

### 3.3.2 Hadar and Busidima Formations

The eruption of the Lower Stratoid Series is contemporaneous with the initial development of the Hadar Formation, a roughly coeval unnamed sedimentary formation around Mile (Deino et al., 2010), and the As Aela deposits in the Gona area (Quade et al., 2008). The Hadar Formation is typically characterized by sands, muds, and tuffaceous intervals (Campisano and Feibel, 2008b). The date for the initiation of sedimentation within the Hadar Formation was discussed by Wynn et al. (2008) as being close to 3.80 Ma. The Hadar Formation rocks in that region overlie what was termed by the authors as 'Dalha Series Basalts' – renamed herein to Dalhoid Series, upon which a paleosol has developed. To the north, Deino et al. (2010) date a basalt at the base of the Formation at 3.82 Ma (± 0.18 $^{40}Ar/^{39}Ar$), however it is argued by the authors that the sequence at this locality is not precisely correlated with the Hadar Formation proper. Here I use the ca. 3.8 Ma date for the initiation of sedimentation in the Hadar Formation and adopt ca. 2.9 Ma as the upper limit, consistent with the recently determined upper-most tephra in the Formation of 2.931 Ma ± 0.017 (DiMaggio et al., 2015b) (Fig. 8). While most stratigraphic sections describing the Hadar Formation do not exhibit significant intercalated basalts, work by Alene et al. (2017) has placed contemporaneous flows from the Lower Stratoid Series in context of the existing sedimentary stratigraphy. Alene et al., (2017) shows that at least 6 discrete basaltic flows occur during the interval from 3.82 Ma (± 0.18 $^{40}Ar/^{39}Ar$) (Deino et al., 2010) to roughly 3 Ma. Moreover, significant volcanic events occur during this time period away from the sedimentary basins – e.g., Ida Ale complex (Hall et al., 1984; Walter et al., 1987).

The eruption of the Upper Stratoid Series Basalts (commencing at 2.6 Ma: Kidane et al., 2003; Lahitte et al., 2003b) is contemporaneous with the initial development of the Busidima Formation at ca. 2.7 Ma (Fig. 8). The boundary between the Hadar and subsequent Busidima Formation (2.7 Ma to 0.16 Ma) is represented by an angular unconformity  (Quade et al., 2004). Critically, the abundant conglomerates present in the Busidima Formation differ from the finer grained sediments of the preceding Hadar Formation. These observation have been used to suggest a major tectonic reorganization event in Afar at ca. 2.7 Ma (Quade et al., 2004, 2008; Wynn et al., 2008; Campisano, 2012). Given the synchronicity between a magmatic pulse in the form of the Upper Stratoid Basalts and clear evidence of extension on the basis of stratigraphic constraints, it is apparent that the Afar Stratoid Series magmas are controlled by extensional processes. Pulses in extension correlate with increases in magma flux. Evidence as to the cause of this new tectonic event is preserved within the Gulf Series lavas.

### *3.4 The Gulf Series, a New Umbrella Term (2.8 to 0.3 Ma)*

Here I define a new term – the Gulf Series as a necessary addition to the literature given advances in distinguishing different lava types within what had previously been termed ‘the Gulf Basalts’, with the consequent increase in contemporaneous named stratigraphic units. It is not possible to use the prior ‘Gulf Basalts’ nomenclature for this umbrella term, as this name has been used as a discrete mapped unit on the modern geological map of Djibouti (LeGall et al., 2016). I thus propose the use of ‘Gulf Series’ as an umbrella term incorporating lavas that previously fell under the definition of the Gulf Basalts – i.e., the first lavas in Afar to have become associated with faults during the localization of strain, representing a transitional phase between the widespread Stratoid Series and the localized magmatic activity associated with the development of discrete grabens (Lahitte et al., 2003a). This definition is deliberately broad and results in the amalgamation of different magmas erupted over a wide time interval (Fig. 8). For example, in Djibouti where detailed mapping has occurred (Le Gall et al., 2015), broadly contemporaneous units are recognized as being geochemically distinct from the Gulf Basalts (i.e. Goumarre and Hayyabley Basalts: Daoud et al., 2010). In the case of the Goumarre basalts, which are more enriched in incompatible trace elements in comparison to the Gulf Basalts, these lavas are interpreted as being erupted more distant from the evolving rift axis (Daoud et al., 2011). Such geochemical heterogeneity, is however, to be expected where differences in the degree of melting or source lithology may yield different magma types.

The Gulf Series lavas are not as volumetrically significant in comparison to the previous Dalha and Stratoid Series. Lavas of the Gulf Series are found dominantly around the Gulf of Tadjoura (Daoud et al., 2010), and along the margins of the modern rift grabens (Fig. 14) (Lahitte et al., 2003b; Stab et al., 2016). Members of the Gulf Series were incorporated in early work as being part of the Upper Stratoid Series, and are also termed the Tadjoura Series by some authors (Deniel et al., 1994). It is important to note that my definition of the Gulf Series can create ambiguities with respect to the age range for this unit given that it relies upon strain localization – a process which is not synchronous throughout Afar. The existing temporal constraints suggest a time interval that could extend from 2.8 Ma (Le Gall et al., 2015) to 0.332 Ma (Lahitte et al., 2003b), however this large range results from a spatial heterogeneity in when strain localization began. The older initiation of the Gulf Series (2.8 Ma) noted by Le Gall et al. (2015) results from the impact of the Tadjoura Rift in Djibouti over the past 3 Ma (Daoud et al., 2011). In contrast, the much younger interval of between 1.11Ma (± 0.09) to 0.332 Ma (± 0.4) noted for the rift sectors in other parts of Afar (Kidane et al., 2003; Lahitte et al., 2003b) is consistent with the relative young age of these features.

The temporal range over which the Gulf Series was active provides important constraints in understanding the evolution of Afar. The process-based definition for the Gulf Series results in an intentional temporal overlap between the Afar Stratoid Series and the Gulf Series. The implication of this, is that while broad flows associated with the Afar Stratoid Series dominated much of Afar during the Pliocene, the earliest dated Gulf Series lava from Djibouti were recording the propagation of the Tadjoura Rift, resulting the coincidence of lava and strain localization in this region at ca. 2.8 Ma. When combined with the evidence of an unconformity between the Hadar and Budisima Formations, and the initiation of the Upper Stratoid Series, the period from 2.6 to 2.8 Ma is a time of significant change in Afar.

The Gulf Series lavas exhibit geochemical patterns consistent with the earlier magmatic units in Afar and are not clearly distinct from these groups. Indeed on the basis of geochemical characteristics alone, these magmas are indistinguishable from the Afar Stratoid Series. The Gulf Series are typically Type III magmas, however Type VI magmas have been observed in Djibouti at Hayyabley Volcano (Daoud et al., 2010). Similar to the Afar Stratoid Series lavas that share the same characteristics, these Type VI lavas are typically depleted in the most incompatible trace elements (Fig. 11; 12). Isotopic analyses of the Gulf Series is limited to Type VI lavas, which have been interpreted as a distinct depleted component of the Afar plume (and not the plume endmember used on isotopic plots within this synthesis). This depleted component as exemplified by Type VI lavas of the Gulf Series plots at relatively unradiogenic values of Pb isotopes, but relatively radiogenic $^{143}Nd/^{144}Nd$ and unradiogenic $^{87}Sr/^{86}Sr$ and (Fig. 13). Further study is needed to constrain the origin of this depleted component, which is also evident in some Quaternary Axial lavas from Manda Hararo (Barrat et al., 2003) – see Axial lavas section below.

### *3.5 The Axial Series (Ca. 0.7 Ma to present)*

The focusing of magmatic activity that commenced during the eruption of the Gulf Series has continued to the present day. Modern volcanism is limited to discrete regions in Afar coincident with graben formation (Fig. 15). The existence of the Afar Triple Junction and the migration of extensional strain from the Gulf of Aden and Red Sea systems has resulted in potentially overlapping extensional systems (Manighetti et al., 2001). Here we term volcanic rocks that form along the axis of these new graben structures the 'Axial Series'.

I divide the geochemical variation diagrams into the rifts extending from the triple junction region northwards towards the Red Sea (Tendaho Graben, Manda Hararo, Dabbahu, Alayta, Erta 'Ale Range, and Alid), and from the Gulf of Aden in Djibouti south towards the MER (Tadjoura, Asal, Manda Inakir). Note that the continuation of the Axial Series into the MER as the Gabillema & Adda'do, Hertali-Angele, Fantale-Dofan sectors is described in Part II of the synthesis (Rooney, 2020b). The Transverse Volcanics, which are found along the margin of Red Sea system, are discussed with this group.

#### 3.5.1 Erta 'Ale & Tat 'Ale

The Erta 'Ale range is considered part of the southern propagation of the Red Sea Rift, exhibiting linear characteristics of the fissural eruptions, and potential ridge continuity via a transfer zone with the Red Sea rift. However, the direction of rift propagation is not from north to south. The Erta 'Ale range represents the rifting of the Danakil block from Afar, whose tip is currently at Alid, and has propagated northward (Fig. 15). Thus, the Erta 'Ale range is not a sector of the relatively mature Red Sea Rift system in a strict sense. While modern magmatism in Afar has typically taken the form of rift-constrained flows, which young progressively inward toward the core of a graben and are punctuated by central silicic volcanoes (Lahitte et al., 2003a; Ferguson et al., 2010, 2013a), the Erta ‘Ale rift sector exhibits activity dominantly associated with basaltic shield volcanoes. The relief of these shields is perhaps not always evident when considering elevation alone - the topography within the Danakil Depression extends below sea level (-126m), but the lava lake of Erta ‘Ale volcano sits at ca. 570m (Oppenheimer and Francis, 1998; Varet, 2017), consistent with the construction of a significant, dominantly basaltic edifice (Hagos et al., 2016). Rhyolites are also present in the Erta ‘Ale range, exhibiting similar composition and mode of origin to rocks from other rift sectors in Afar (Barberi and Varet, 1970; Barberi et al., 1974b; Bizouard et al., 1980; Barrat et al., 1998).

The axis of the Danakil Depression is largely comprised of a series of very active shield volcanoes erupted through fissural vents that have continued to erupt into historical times (Field et al., 2012, 2013; Pagli et al., 2012; Yirgu et al., 2014). Modern activity is typically precipitated by diking events, destabilizing shallow magma chambers (e.g., Pagli et al., 2012). However, this activity is punctuated, as no significant deformation was recorded along the range during long periods (e.g., 1993 to 1997: Amelung et al., 2000). From south to north these edifices are comprised of: Tat ‘Ali, Hayli Gubi, Ale Bagu, Erta ‘Ale, Borale ‘Ale, Dalafilla, Alu, Gada ‘Ale, and Alid (Duffield et al., 1997; Lowenstern et al., 1999; Hagos et al., 2016). Alid lies across a salt plain from the rest of the range, and might be considered its own sector, and indeed is unusual in that the core of Alid ‘volcano’ is actually a domed intrusive core draped with volcanic products (Duffield et al., 1997). The edifice of Alu volcano is also not constructed by lava accumulation and has been interpreted as a forced fold over a sill (Magee et al., 2017). The initial stage of volcanism in the Erta ‘Ale rift sector is typically described as ‘Stratoid Basalts’, which remain poorly dated within this region and should not be confused with the Afar Stratoid Series. The earliest dates for activity within the Erta ‘Ale range consist of a 1.2 Ma (± 0.5) (Barberi et al., 1972) from Alu, and 1.129 Ma (± 0.012 $^{40}Ar/^{39}Ar$) (Duffield et al., 1997) from Alid. We assign these to the ‘Gulf Series’ eschewing the catchall ‘Stratoid’ term frequently used in describing this initial stage of activity in the Erta ‘Ale rift sector. Magmatism has continued since this initial time centered on the different edifices but also forming flows on the rift floor (e.g., Alid: Duffield et al., 1997).

Volcanism within the Erta ‘Ale range shows a transitional concentration of $TiO_2$, when considered in the context of other groups from along the Red Sea trend within Afar (Fig. 16). In a general sense, the concentration of $TiO_2$ in primitive lavas divides into three initial types: (A) Low $TiO_2$ for Alid, (B) Intermediate $TiO_2$ for the Erta ‘Ale range, Dabbahu, and Tendaho-Manda Hararo, and (C) High $TiO_2$ for the Transverse Volcanics (Fig. 16). This same pattern is replicated in Zr, but not Nb. The origin of this variation likely relates to both variations in the degree of melting (see discussion on the Transverse Volcanics), and differences in the lithology of the mantle source (see discussion on Alid later). Broadly, Erta ‘Ale range lavas are similar to Dabbahu in terms of the slope of the REEs (Fig. 16; 11). However, this similarity is not reflected in the primitive mantle normalized diagram, where Erta ‘Ale lavas display a distinct Type II magma signature (Fig. 17). This signature is particularly evident in the lack of discrete Ba and Nb-Ta peaks, and the Th-U trough. Where sufficient data is available, the Type II magma signature is shared among all the samples from the Erta ‘Ale range. In contrast to lavas from the Pre-Axial Phase (e.g., Dalha Series), there is no correlation between MgO and $^{143}Nd/^{144}Nd$ and $^{87}Sr/^{86}Sr$ isotopes (Fig. 16). This lack of a crustal assimilation signature is reflected in a clustering of data close to the Afar Plume composition (Fig. 18).

Alid volcano, which is separated from the rest of the Erta ‘Ale range by a plain, is very distinctive geochemically (Fig. 16). The magmatic products of Alid typically plot in the more depleted field of REEs from the region, but overlap other groups (Fig. 11). Alid lavas display a Type III magma pattern but with some unusual concentration variations (Fig. 17). Notably, Alid lavas are among the most enriched in the more incompatible trace elements, but this enrichment falls progressively from La to Lu (Fig. 17). A pronounced negative Zr-Hf anomaly is also evident for the Alid lavas, also manifesting as low Zr/Nb (Fig. 16). Little evidence of any correlation between MgO and $^{143}Nd/^{144}Nd$ and $^{87}Sr/^{86}Sr$ is evident (though more evolved samples have a spike in $^{87}Sr/^{86}Sr$ towards more radiogenic values) (Fig. 16). In multi-isotope space, Alid lavas plot at unusually unradiogenic $^{143}Nd/^{144}Nd$ when considering their $^{87}Sr/^{86}Sr$, with some evidence of a deflection towards the HIMU field (Fig. 18). Pb isotopes form a linear array that may indicate mixing between the Afar plume (or a more radiogenic endmember than the plume) and the depleted upper mantle component. However, given the trace element evidence noted above, a different and yet unconstrained endmember may equally contribute to these lavas. The negative Zr-Hf anomaly hints at apatite in the source of these lavas and might reflect a metasomatic signature distinct from Erta ‘Ale. Further work is required to resolve this issue.

### 3.5.2 Manda Hararo - Dabbahu - Alayta Rift

Three distinct rift sectors are described herein that connect the Main Ethiopian Rift to the South and Erta ‘Ale range in the north. From a magmatic perspective, these rift sectors are dominantly comprised of the Gulf Basalts and the Afar Stratoid Series along the rift margins, and recent basalts and silicic central volcanoes along their axes. The major silicic centers along this rift sector include Dame ‘Ale, Manda Gargori, Kurub, Ado ‘Ale, and Dabbahu. Some confusion occurs with the name of Dabbahu, which is used to denote the entire edifice, however the upper reaches of the edifice are termed Boina (fumerole), and this term has been used in previous publications (Barberi et al., 1974b, 1975a; Bizouard et al., 1980; Lahitte et al., 2003a). Dabbahu, which is the best studied magmatic center in the region, was built upon 0.072 to 0.058 Ma high MgO fissural lavas that appear continuous with the Alayta shield to the north (Barberi et al., 1974b; Medynski et al., 2013). It has been suggested that this event represents the transfer of magma from deep magma chambers towards chambers shallower in the crust (Medynski et al., 2013). Over these initial basalts are intermediate composition lavas (0.058 – 0.045 Ma), which began forming the steeper slopes of Dabbahu (Medynski et al., 2013), which are followed by silicic domes, flows, and pyroclasts until the present day (Barberi et al., 1974b; Medynski et al., 2013). Given the wide array of lava compositions present at Dabbahu, Barberi et al. (1974b) was able to show that the pantellerites (peralkaline rhyolites) of Dabbahu were formed entirely through shallow fractional crystallization of a basaltic parent magma with no obvious signs of crustal assimilation, though the data included lavas derived from two distinct magmatic cycles (Medynski et al., 2013). Field et al. (2013) further showed that mixing between less- and more-evolved lava compositions occurred within closely spaced dikes (or sills) shortly before eruption.

Away from the central volcanoes, basaltic magmatism in this rift has a distinct topographic expression. The most recent basalts occur at the lowest elevations within the axial graben, consistent with extension through magma intrusion (Ferguson et al., 2013a). Within the rift at Dabbahu, across axis analysis of the basalts reveals a decreasing age from 0.196 Ma (± 0.016 $^{40}Ar/^{39}Ar$) to < 2 ka in the axial graben (Ferguson et al., 2013a), and symmetrical magnetic lineations that are similar to that observed in oceanic basins (Bridges et al., 2012). This rift sector intersects with the Main Ethiopian rift in the vicinity of the Tendaho Graben (Acocella et al., 2008) and continues northwards in the Alayta rift to intersect with the Erta ‘Ale range (Lahitte et al., 2003b). The Alayta Range is a significant volcanic rift sector that includes the 1400m high Alayta shield volcano. Surrounding the volcano is an extensive basaltic lava field and in all has a surface area equivalent to the Erta ‘Ale range. Barberi et al. (1970) describe Alayta as still in the ‘shield phase’ and is growing through fissural lava flows emanating from NNW orientated fissures. Barberi et al. (1970) suggests a 1907 eruptive event might be attributed to Alayta. Afdera volcano, which occupies the transitional region between the Alayta and Erta ‘Ale rift sectors is a basaltic shield upon which rhyolitic lava domes have been constructed (Barberi et al., 1970).

Since the volcanic crisis in Afar in 2005 (Wright et al., 2006), the Dabbahu - Manda Hararo – Alayta sector of Afar has been the focus of intensive scientific investigation. This research has resulted in a new understanding of the mechanisms of dike emplacement (and magma eruption) in mature continental rift settings. The current interest in this rift sector relates to the 14 dike intrusion events, related earthquakes and associated rhyolite ash eruption of Dabbahu in 2005 (Ayele et al., 2009; Belachew et al., 2011, 2012; Grandin et al., 2011; Field et al., 2012). Remote sensing records show additional eruptions August 2007, and June 2009, and in May 2010 in the form of basaltic fissural lava flows emanating from where a dike intersected the surface of the axial graben (Ferguson et al., 2010; Barnie et al., 2016). This event was used to probe the episodic nature of extensional events in this region, which have now been constrained to be at approximately century-scale intervals (Ebinger et al., 2010). Further outcomes from this research include a recognition that as the diking event proceeds (and accumulated strain is progressively accommodated), eruption is more a probable outcome as dikes are less likely to travel outwards from the centrally-fed magma source in shallow crust beneath the middle of the rift sector (Barnie et al., 2016). Importantly, this research has also shown that these diking events can be sourced from multiple magma chambers that may be horizontally separated in the crust (Wright et al., 2012).

The majority of samples from Tendaho-Manda Hararo, Dabbahu, and Alayta sectors of these linked rifts exhibits similar geochemical characteristics with exceptions as noted below. With only a single sample from Alayta we are unable to comment further on this sector and significantly more work is required. Linear evolution trends between incompatible trace elements and MgO (e.g., Zr, Nb; Fig. 16) demonstrate a similar evolutionary pathways during magma differentiation for Tendaho-Manda Hararo and Dabbahu (Fig. 16). However, some variability is evident in terms of REE fractionation where Manda Hararo samples have a slightly less enrichment in La, coupled with less depletion in the HREE (Fig. 17). This heterogeneity is most evident in terms of the fractionation of Tb/Yb, where Tendaho-Manda Hararo samples have markedly lower values in comparison to Dabbahu (Fig. 16). Such variance is likely related to the depth of melt extraction and may reflect either differences in the lithospheric thickness between the two sectors, or mantle potential temperature (Ferguson et al., 2013b). Within the Dabbahu sector, two distinct primitive mantle normalized patterns are evident – both somewhat parallel to each other with the exception of Sr (Fig. 18). This separation is likely an artifact of incomplete sampling as these data cluster at MgO values of 5-6% and 8.5-10% and reflect normal magma differentiation processes (Fig. 16).

The majority of samples from these sectors exhibit a Type III magma pattern, consistent with a derivation from a mixture of sources comprised of the Afar plume, depleted upper mantle, and Pan-African lithosphere (Fig. 19). No clear evidence of crustal assimilation is evident given the lack of any clear variation of $^{87}Sr/^{86}Sr$ and $^{143}Nd/^{144}Nd$ with MgO (14). While $^{87}Sr/^{86}Sr$ data is available for a large dataset from Dabbahu (Barberi and Santacroce, 1980), only a single $^{143}Nd/^{144}Nd$ datapoint and no Pb isotopes exist, creating much uncertainty in the interpretation of the origin and crustal assimilation of these rocks. Tendaho-Manda Hararo similarly exhibits a lack of multi-isotope data but in general these sectors cluster around the Afar plume composition (Fig. 19). A significant plume contribution to these lavas is consistent with petrologic modelling suggesting elevated mantle potential temperature in this region (Rooney et al., 2012b; Ferguson et al., 2013b).

The most significant deviation from the consistent Type III magmas erupted along these sectors of the rift are a subset of rocks erupted in the Manda Hararo rift. These lavas, which are similar to rocks from Hayyabley volcano (Daoud et al., 2010) and some Afar Stratoid Series (Alene et al., 2017), exhibit a Type VI lava pattern (Fig. 17; 18). These rare primitive basalts may represent melts derived from a depleted component of the Afar plume, distinct from the composition noted on the multi-isotope plots (Barrat et al., 2003; Daoud et al., 2010).

### *3.5.3 Manda-Inakir, Asal, and Tadjoura Rifts*

These rift sectors are associated with the propagation of extensional strain from the Gulf of Aden (Manighetti et al., 1998; Lahitte et al., 2003b, 2003a). The Asal rift in Djibouti represents the most evolved of these sectors, from which a number of splays emanate, trending to the northwest (Manighetti et al., 1998; Lahitte et al., 2003b). Lahitte et al. (2003a) noticed that there was a correlation between silicic centers and rift propagation within this system and suggested the silicic centers helped guide the propagation of rifting. For this reason, there are abundant (poorly studied) <1 Ma silicic magmatic centers to the northwest of the Asal rift (Lahitte et al., 2003a).

The Tadjoura rift is currently submerged within the Gulf of Tadjoura – part of the Gulf of Aden Rift System. Despite the primary axis of this rift currently being below water, the edges of the rift are still subaerial and preserve lava sequences that extend from ca. 2.8 to 1.0 Ma (see compilation in Daoud et al., 2011). The rift preserves the oldest lavas of the Gulf Basalt Series in the region at 2.8 Ma (Daoud et al., 2011; Le Gall et al., 2015). Consistent with other exposures of the Gulf Series in Afar (e.g., Barrat et al., 2003), a wide range of compositions is also observed within this region (Daoud et al., 2010, 2011). Modern volcanism, which has been probed through dredging of the rift axis, overall shows less geochemical variation - an observation consistent with a more mature system and similar to the most recent axial lavas erupted in the Asal Rift (Schilling et al., 1992; Rooney et al., 2012a).

The Asal Rift represents the on-land portion of the Gulf of Aden system and can also be termed the Asal-Ghoubbet Rift (Manighetti et al., 1998). The Asal Rift is dominated by Fieale volcano and magmatic activity along the rift axis, including the 1978 eruption of Ardoukoba cinder cone. This modern eruption has also prompted multiple U series isotopic studies in attempts to control magmatic timescales. These results show that basalts have spent a protracted period in the crust, interacting with a cumulate pile and degassing over a 900-2000 year timescale (Vigier et al., 1999; Turner et al., 2012). Rocks from the modern Asal Rift are entirely basaltic, however the marginal zones record some rhyolitic products that mark the initiation of the rift at ca. 1 Ma (Audin et al., 1990; Pinzuti et al., 2013; Le Gall et al., 2015). The Gulf Basalts, which are evident along the margin of the Asal rift have been dated to 0.835 Ma (± 0.035) to 0.315 Ma (± 0.053), while lavas in the modern rift axis (sometimes termed the Asal Volcanic Series) have dates of less than 0.320 Ma (Manighetti et al., 1998). Barrat et al., (1993) noted unusual oxygen isotope values in recent rocks from the Asal rift that were interpreted in terms of the assimilation of hydrothermally altered rock. Subsequent work showed a significant control of plagioclase accumulation in the composition of recent rocks erupted in this region (Pinzuti et al., 2013). Consistent with progressive thinning of the lithosphere and consequent adiabatic melting, the depth of melt extraction decreases towards the rift axis (Pinzuti et al., 2013). When these data are combined with evidence of a thin ca. 5-10 km crust in this region, there is discussion as to if the transition from continental rifting to oceanic spreading is complete within the Asal Rift, though the presence of older continental crust still found in drill holes, might suggest a more proto-oceanic model (Vellutini, 1990; De Chabalier and Avouac, 1994).

The Manda and Inakir rifts are two parallel, en-echelon rift sectors in the northwest portion of Djibouti along the Ethiopian border (Audin et al., 1990), and are connected with the Asal rift through the Makarassou fault system (Manighetti et al., 1998; Le Gall et al., 2011). The Inakir rift is older and contains some of older rocks upon which more recent flows are draped

(Audin et al., 1990). This occurrence is similar to Alid volcano in the Erta ‘Ale range (Duffield et al., 1997). The most significant structure in this rift is the 0.872 Ma (± 0.015) Andabbi Eale Volcano (Manighetti et al., 1998). The active Manda Rift is dominated by the Manda shield, but also contains a young 1928 cinder cone (Kammourta) that is considered equivalent to the 1978 Asal rift eruption of Ardoukoba (Audin et al., 1990). Most of the floor of this rift is covered with basalts that date to ca. 0.140 Ma (Manighetti et al., 1998).

Moussa Ali is a large volcanic edifice that lies to the northeast of the Manda-Inakir rift, but lies within the splayed region of broad extension. Moussa Ali consists of a sequence of rocks that extends from basaltic to trachytic in composition. Volcanism at this edifice is thought to have continued from 0.9 Ma (± 0.3) to at least 0.25 Ma (± 0.02 $^{40}Ar/^{39}Ar$) (Chessex et al., 1980; Zumbo et al., 1995)

The three Gulf of Aden related rift systems exhibit distinctive behaviors in terms of the major and trace elements, most likely related to the impact of plagioclase cumulates within the magmas of the region, and in particular within the most evolved Asal sector. Pinzuti et al. (2013) describe in detail how such processes dominate the magma chemistry of magmas erupted in this region, consistent with earlier interpretations that suggest interaction between the magma pile and a cumulate mass within the crust (see above). For that reason, Asal sector lavas do not follow the same evolutionary trends as other lavas in the region (Fig. 16). The Asal sector lavas exhibit an almost vertical array in $TiO_2$ at a constant value of MgO, a feature shared by other incompatible trace elements (Fig. 16). In contrast, the Manda Inakir and Tadjoura lavas follow the same magma differentiation pathways as other axial lavas in Afar (Fig. 16). Chondrite-normalized plots for these sectors show similarities between Manda Inakir and Tadjoura, with equivalent slopes of the HREE (Fig. 17). In contrast, Asal lavas have a much shallower slope, consistent with interpretations from Pinzuti et al. (2013) of a melting source within the rift axis that was somewhat shallow. More complete REE datasets are needed for Tadjoura and Manda

Inakir as the existing plots interpolate from Gd to Yb (Fig. 17), and it is therefore difficult to constrain the precise slope of these lines. The limited trace element data available for these three sectors yields primitive mantle normalized figures with significant omissions (Fig. 18), but despite this it is probable that lavas from the three sectors exhibits a Type III lava pattern.

Limited evidence for crustal assimilation (Fig. 16) is consistent with the data from multi-isotope space that clusters around the Afar plume composition (Fig. 19). In comparison to the Erta ‘Ale range, Alid, and the Transverse volcanics, samples from the three sectors associated with the Gulf of Aden are deflected towards lower $^{206}Pb/^{204}Pb$ at equivalent values of $^{208}Pb/^{204}Pb$ suggesting heterogeneity in the source components of these lavas (Fig. 19). The origin of the difference in Pb isotope characteristics between the Gulf of Aden rifts and the Red Sea-related rifts/volcanics may relate to variably contaminated upper mantle whereby the Gulf of Aden lavas are derived from a source with a more significant contribution from the Pan-African lithosphere (Rooney et al., 2012a). In contrast, lavas from the Red Sea Rift system may simply reflect a less contaminated mantle (Fig. 19). Further investigation of these lavas is necessary as it is also possible that a fourth component (a HIMU-like component) is present within the Red Sea lavas on the basis of the Type II magma pattern and generally more radiogenic $^{206}Pb/^{204}Pb$ values in some lavas. The presence of such a component would be consistent with HIMU-like signatures seen in lavas on the adjacent Arabian plate (Bertrand et al., 2003).

#### *3.5.4 Other modern fields – Transverse Structures*

Barberi et al. (1974a) and Varet (2017) discuss modern volcanic episodes that do not occur along axial portions of the evolving rift sectors as ‘transverse’ structures. The model presented was that older pre-rift structures were re-activated during rifting and suggested a role in axial offsets. The transverse aspect of these regions has been supported by recent fault mechanism constraints as noted below for the Nabro Volcanic Range.

*Nabro Volcanic Range*

The Nabro volcanic range, which consists of a series of basaltic, trachytic and rhyolitic edifices aligned perpendicular to the Erta ‘Ale range, represents about a fifth of the volume of magmatic products erupted in Afar during the Quaternary (Wiart and Oppenheimer, 2005). The eruption in 2011 of Nabro volcano was widely studied by the use of remote sensing techniques and has raised concerns over volcanic hazards associated with the range (Hamlyn et al., 2014; Yirgu et al., 2014). In particular it has been noted that this 2011 eruption was the largest single contributor of sulfur to the atmosphere since the eruption of Mt. Pinatubo in 1991 (Donovan et al., 2018). Further concern over volcanic hazards in the Nabro Volcanic Range come from Dubbi volcano, whose 1861 eruption (pyroclastic flows and lava flows) is the largest historical eruption in Africa (Wiart and Oppenheimer, 2000). The range consists of the following edifices from SW to NE: SSW lava field (basalt), Asavyo (also Bara ‘Ale - basalt/dark trachyte), Sork ‘Ale (basalt/dark trachyte), Mallahle (trachyte and rhyolite), Nabro (trachyte and rhyolite), Mabda (rhyolite), Dubbi (basalt and recent rhyolite), Edd lava field (basalt), and Kod Ali & Edd Islands (basalt) (Wiart et al., 2004). The volcanic range traverses different types of crust, from the highly intruded basaltic material adjacent to the Red Sea at sea level, to the Precambrian Danakil Metamorphic Block at the core of the range (Nabro Volcano) at elevations greater than 2000m. Wiart and Oppenheimer, (2005) have created a generalized stratigraphy for the volcanic range which commences with the basaltic eruptions of Bara ‘Ale and Sork ‘Ale followed by the trachytes of Mallahle and Nabro. Subsequent magmatism was dominantly pyroclastic with ignimbrites and pumice fall deposits in addition to rhyolite lava flows and obsidian domes. The most recent magmatic activity is a basaltic flow fed from fissures at the apex of the range and the 2011 eruption of trachybasalt from Nabro (Donovan et al., 2018). Wiart and Oppenheimer,

(2005) notes the coincidence of evolved magmatic activity with the presence of the Precambrian basement in the highlands area, which may promote the creation of a crystal mush zone (Donovan et al., 2018). Studies of melt inclusions from Nabro suggest mixing between magma batches stalled within extensive crystal mush zones (Donovan et al., 2018). Unlike the other rift sectors in Afar, the lava field within the Nabro Volcanic Field are not significantly dissected by the surface expression of faulting, suggesting the field is not a zone of focused magmatic and tectonic activity. However, earthquake records show a degree of transtensional activity in this region, indicating deformation of the Danakil block along this corridor (Hamlyn et al., 2014).

*Sept Freres*

Also referred to as the Sawabi Islands or Seba Islands (Barberi et al., 1974a; Varet, 2017). These are a Series of hyaloclastite cones that appear as islands within the Red Sea. The composition of the lava is alkali-olivine basalt with abundant ultramafic xenoliths present (Varet, 2017). Little further information is available on this system.

*Assab*

The Assab transverse field shows little evidence of surface faulting, but recent volcanism is present here (Varet, 2017). Civetta et al. (1975) dated recent rocks in this area to between 0.6 Ma (± 0.20) and 0.28 Ma (± 0.10 – using $^{230}$Th). However, this region is best known as a mantle xenolith locality (Ottonello et al., 1978; Ottonello, 1980; Teklay et al., 2010). Moreover, many of the xenoliths appear to have cumulate-like characteristics suggesting accumulation during the Afar plume phase of magmatic activity (Teklay et al., 2010).

*Geochemical Variation*

As a group, the transverse volcanics form typically coherent evolutionary trends that are comparable to other volcanic units in the region (Fig. 16). The slightly lower values of $CaO/Al_2O_3$ at a given value of MgO might suggest a greater role for clinopyroxene in these lavas, perhaps consistent with the less developed magmatic plumbing systems and deeper ponding depths as seen within the MER for less developed sectors of the rift (c.f. Rooney et al., 2011). It is notable that these lavas exhibit enrichments in $TiO_2$, Zr, Nb and many incompatible trace elements (Fig. 16). The chondrite normalized REE pattern shows a similar enrichment in the most incompatible REE (Fig. 17), but also a notable slope in the HREE that results in significant fractionation of Tb/Yb (Fig. 16). The primitive mantle normalized pattern of these lavas exhibits a clear Type III style (Fig. 18). Taken together the evidence points to a smaller degree of partial melting at deeper levels of a source that is compositionally similar to other axial magmas in the region. Such an interpretation is consistent with such Transverse Volcanics being located off the primary axes of extension, resulting in lower degrees of adiabatic decompression melting under a thicker lithosphere, and with the consequent evolution of a less-developed magmatic plumbing system in comparison to the axial zones.

## 4. Conclusions

### *4.1 Constraints on the origin of magmatism in Afar and Yemen*

The attenuated continental lithosphere that characterizes the Afar Depression should provide insights into the composition of sub-lithospheric reservoirs contributing to magmatism. In practice, however, complexities arise from pronounced crustal assimilation that dominates the isotopic characteristics of many of the earlier magma series (e.g., Mablas and Dalha Series). While the precise reason for such significant assimilation has yet to be established, the combined impact of increased heat flow into the crust resulting from lithospheric thinning and repeated magmatic intrusion likely plays a role. Where crustal assimilation is less dominant, three magma types can be distinguished in Afar and Yemen – Type II, III, and a newly defined Type VI. The origin of these lavas and their distribution in Afar and Yemen reveal clues as to how such magmas are generated, with broader application elsewhere in the East African Rift.

Type II lavas in Afar are spatially and temporally restricted to modern magmatism within the Erta ‘Ale range. This curious limitation, however, provides evidence as to the source of Type II magmas more broadly. Modern magmatism within the Erta ‘Ale range differs from other Quaternary zones of focused strain and magmatic intrusion in Afar in terms of significantly greater volumes of magmas erupted here. This is most clearly evident in the formation of Quaternary aged shield volcanoes in this sector of the rift. The reason for such a large flux of magmas is not immediately evident: existing data suggests that the convecting mantle beneath Afar has a broadly elevated mantle potential temperature (ca. 140°C above ambient mantle) (Rooney et al., 2012b; Ferguson et al., 2013b) and modern strain (and thus lithospheric thinning) is currently distributed to all rift sectors. Thus, the enhanced magmatic activity in Erta ‘Ale is puzzling if the source of magmatism for the Erta ‘Ale range is assumed similar to the other rift sectors. However, Type II magmas are hypothesized to be derived from the melting of easily-fusible amphibole bearing metasomes within the lithospheric mantle (Rooney, 2017). The increased magma flux at Erta ‘Ale in comparison to the other rift sectors (which do not exhibit Type II magmatism) supports this assertion. The modern breaching of the Danakil Block by the Erta ‘Ale rift sector, in contrast to the MER and Gulf of Aden which traverse thinned lithosphere, provides further support for a model wherein the lithospheric mantle of the Danakil block contains amphibole-bearing metasomes that are currently contributing to melt generation in the Erta ‘Ale rift sector. The origin of these metasomes appears recent – the isotopic characteristics of Erta ‘Ale lavas parallel that of the Afar Plume composition, confirming prior studies that have shown metasomatism associated with the Afar Plume has pervasively altered the lithosphere in this part of the East African Rift (Baker et al., 1997).

Type III lavas are, by far, the most common magma type erupted within the Afar depression. These lavas are hypothesized to represent a mixture of the Afar plume, and a hybrid depleted upper mantle – Pan-African lithosphere component (Rooney et al., 2012a; Rooney, 2017). The pervasiveness of this magma type in Afar and its persistence despite the evidence of lithospheric attenuation, is supportive of a sub-lithospheric origin. The implication of this observation is that there is widespread distribution of plume-derived material in the upper mantle beneath Afar, consistent with mantle potential temperature estimates (Rooney et al., 2012b). Moreover, the hybridization of the regional upper mantle with African lithosphere material must be a pervasive process. Type VI lavas, which are described herein from three rare occurrences, are characterized by extreme depletion in the most incompatible trace elements but display isotopic values inconsistent with a simple MORB-source. The current model for the genesis of such lavas is through melting of a depleted component 'intrinsic' to the Afar plume (Barrat et al., 2003; Daoud et al., 2010). However, further examination of these lavas is necessary to constrain the exact origin of this rare component.

### *4.2 Summary stratigraphy of magmatic events in Yemen*

There is no current evidence of any significant magmatic events in Yemen between ca. 20 Ma to 11 Ma. Magmatism in this region recommences during a time of intense basaltic volcanism that is evident throughout much of the East African Rift – termed the Mid-Miocene Resurgence. In Yemen this event is synchronous with activity around the margin of the Afar depression and consisted of basaltic plateaus and shield volcanoes. Later magmatic events in Yemen are focused dominantly from 6 Ma to present and are distinctly less volumetrically significant and more alkaline than prior phases of activity. These observations are consistent with a migration in primary magmatic activity in this region towards the evolving Gulf of Aden.

### *4.3 Summary stratigraphy of magmatic events in Afar*

*Development of the Rift Margin (ca. 20 Ma to 10 Ma).* This period is dominated by explosive silicic volcanism with lesser volumes of highly crustally contaminated Mablas Basalts. Magmatism during this phase is correlated with the development of the rift margin (Wolfenden et al., 2005; Stab et al., 2016). These observations are consistent with those from other parts of the East African rift linking periods of rift development with large volume silicic eruptions. It should be noted that this period coincides with the massive basaltic flows that comprise the Mid Miocene Resurgence elsewhere within the East African Rift. The absence of such flows along the Afar margin requires further exploration.

*Dalha Series and Rift Marginal Basins (10 to 5.6 Ma).* This period commences with silicic magmatism, but is also coincident with the eventual development of rift marginal basins and the basin-ward migration of volcanism at ca. 7 Ma. Volcanism coincident with this migration is overwhelmingly basaltic and manifests as widespread fissural activity over older tilted units (Stab et al., 2016). Basalts of the Dalha Series extend to more magneisan values and exhibit less crustal contamination in comparison to the previous Mablas Series. I terminate the Dalha Series magmas with the commencement of the deposition of the Sagantole Formation at 5.6 Ma.

*Dalhoid Series – a unit in transition (5.6 Ma to 3.9 Ma)*. The ambiguity with respect to the boundary between the Dalha and subsequent Afar Stratoid Series initially necessitated the need for the formation of the Dalhoid Series, however the correlation of a distinct pulse of magmatism and basin formation during this interval suggests a separate event. This event appears focused along the rifts margins, and further examination of lavas from this period is needed to resolve potential geochemical distinctions between the Dalha, Dalhoid, and Afar Stratoid Series.

*Afar Stratoid Series (3.9 to ca. 1 Ma).* The initiation of the lower member of the Afar Stratoid Series is defined on the basis of a cluster of dates indicating a renewed magmatic phase ca. 3.9 Ma. The lower member of the Afar Stratoid Series is roughly correlated with the deposition of the paleoanthropologically important Hadar Formation at ca. 3.8 Ma. The upper member of the Afar Stratoid Series, which is thought to commence ca. 2.6 Ma, is also synchronous with the deposition of another important sedimentary unit – the Busidima Formation, starting ca. 2.7 Ma and considered evidence of a major tectonic reorganization at this time (Quade et al., 2008; Wynn et al., 2008; Campisano, 2012). The eruption of the Afar Stratoid Series, which the most widespread and volumetrically significant magmatic unit in Afar, thus appears linked with extensional events recorded by the deposition of distinct sedimentary units.

*The Gulf Series (ca. 2.8 to 0.3 Ma).* Unlike prior units, the definition of the Gulf Series (a new umbrella term) focuses on the surface manifestation of volcanism and its relationship with the localization of strain. The earliest members of the Gulf Series are those associated with the propagation of the Tadjoura Rift into Afar at ca. 2.8 Ma. It is notable that the period from 2.6 to 2.8 Ma, which heralds the upper Afar Stratoid Series, the Gulf Series, and the Busidima Formation correlates with the propagation of the Tadjoura Rift and may explain the tectonic reorganization suggested Quade et al. (2008) and Wynn et al. (2008). Although the upper member of the Afar Stratoid Series and the Gulf Series may have erupted synchronously in different parts of Afar, the progressive migration of strain during this interval towards discrete rift sectors resulted in the eventual localization of magmatic activity within these sectors throughout Afar.

*The Axial Series (0.7 Ma to Present).* This period reflects the spatially limited expression of magmatism within the modern Afar depression. The localization of strain into zones of focused magmatism and deformation has yielded three rift sectors aligned with the Red Sea, Gulf of Aden, and Main Ethiopian Rift. These sectors are typically characterized by central silicic volcanoes and basaltic cinder cones and associated flows. Diking is an important mechanism of strain accommodation within these rift sectors (Wright et al., 2006), which exhibit some of the characteristics of nascent oceanic rifts such as an axial temporal symmetry in the age of magmatism (Bridges et al., 2012; Ferguson et al., 2013a). Non-axial volcanics are also evident in Afar during this period and are termed “Transverse Volcanics”, which erupt along pre-existing structural weaknesses reactivated by rifting.

From 20 Ma to present, magmatism within Afar has evolved from initial large-scale silicic volcanic events to basin-wide fissural basaltic flows, to modern zones of focused magmatism. This magmatic progression parallels the localization of strain within Afar during the same period. These observations require an intimate relationship between the mechanism of strain accommodation and magmatism in Afar with the implication that the current zones of focused magmatism and strain are the pre-cursors of oceanic spreading centers. However, whether these zones are the *direct* precursors to oceanic spreading centers remains very much an open question. While this synthesis necessarily terminates without answering this unresolved question, “if you look on every exit as being an entrance somewhere else” (Stoppard, 1967), future synergies with the ocean ridge community may eventually help bridge the gap between the terminal stage of rifting and the initiation of an oceanic spreading center.

**Acknowledgements**

I would like to thank all the authors I contacted who provided more details and answers to my queries on their work – there were many and I am not able to mention them all here. This work is a synthesis of all the hard work put in by the persons cited herein and the contributions from these persons should be acknowledged. Peter Purcell is thanked for providing the digital files for the rift maps used in the accompanying maps. Thanks is provided to the MSU Library and in particular Kathleen Weessies at the Map Library and the interlibrary loans group – they tried to obtain the requests I placed, and most always succeeded. Thanks goes to Raphaël Pik and Martin Stab for providing maps from Afar. I am grateful to Bernard Le Gall for providing the new

Geological Map of Djibouti and Piero Manetti for tables of Yemen geochemical data. I am indebted to the persons who read and provided feedback on this work prior to publication: Chris Campisano, Naomi Levin, Ramon Arrowsmith, Emily Zawacki, Ian Bastow. I am grateful for the formal peer review comments by Dave Ferguson and an anonymous reviewer. I am indebted to Andrew Kerr for his tireless editorial handling of this synthesis series. This work was supported by US National Science Foundation Grants: EAR 1551872 and EAR 1850606. Lastly, I acknowledge the NSF GeoPRISMS program which was part of the motivation for undertaking this synthesis, and the African Rift Valley Research Consortium meeting in Afar in January 2019 to help frame my thoughts in the broader context presented herein.

**References Cited**

Acocella, V., Abebe, B., Korme, T., and Barberi, F., 2008, Structure of Tendaho Graben and Manda Hararo Rift: implications for the evolution of the southern Red Sea propagator in Central Afar: Tectonics, v. 27.

Alene, M., Hart, W.K., Saylor, B.Z., Deino, A., Mertzman, S., Haile-Selassie, Y., and Gibert, L.B., 2017, Geochemistry of Woranso–Mille Pliocene basalts from west-central Afar, Ethiopia: Implications for mantle source characteristics and rift evolution: Lithos, v. 282, p. 187–200.

Amelung, F., Oppenheimer, C., Segall, P., and Zebker, H., 2000, Ground deformation near Gada ‘Ale Volcano, Afar, observed by radar interferometry: Geophysical Research Letters, v. 27, p. 3093–3096.

Audin, L., Quidelleur, X., Coulié, E., Courtillot, V., Gilder, S., Manighetti, I., Gillot, P. -Y., Tapponnier, P., and Kidane, T., 2004, Palaeomagnetism and K-Ar and 40Ar/39Ar ages in the Ali Sabieh area (Republic of Djibouti and Ethiopia): constraints on the mechanism of Aden ridge propagation into southeastern Afar during the last 10 Myr: Geophysical Journal International, v. 158, p. 327–345, doi:10.1111/j.1365-246X.2004.02286.x.

Audin, J., Vellutini, P.J., Coulon, C., Piguet, P., and Vincent, J., 1990, The 1928–1929 eruption of Kammourta volcano—evidence of tectono-magmatic activity in the Manda-Inakir rift and comparison with the Asal Rift, Afar depression, Republic of Djibuti: Bulletin of Volcanology, v. 52, p. 551–561.

Ayele, A., Keir, D., Ebinger, C., Wright, T.J., Stuart, G.W., Buck, W.R., Jacques, E., Ogubazghi, G., and Sholan, J., 2009, September 2005 mega-dike emplacement in the Manda-

Harraro nascent oceanic rift (Afar depression): Geophysical Research Letters, v. 36, p. L20306, doi: 10.1029/2009gl039605, doi:Artn L20306 Doi 10.1029/2009gl039605.

Baker, J.A., Menzies, M.A., Thirlwall, M.F., and Macpherson, C.G., 1997, Petrogenesis of quaternary intraplate volcanism, Sana'a, Yemen: Implications for plume-lithosphere interaction and polybaric melt hybridization: Journal of Petrology, v. 38, p. 1359–1390.

Baker, J.A., Thirlwall, M.F., and Menzies, M.A., 1996, Sr-Nd-Pb isotopic and trace element evidence for crustal contamination of plume-derived flood basalts: Oligocene flood volcanism in western Yemen: Geochimica Et Cosmochimica Acta, v. 60, p. 2559–2581.

Barberi, F., Bonatti, E., Marinelli, G., and Varet, J., 1974a, Transverse tectonics during the split of a continent: data from the Afar rift: Tectonophysics, v. 23, p. 17–29.

Barberi, F., Borsi, S., Ferrara, G., Marinelli, G., Santacroce, R., Tazieff, H., and Varet, J., 1972, Evolution of the Danakil depression (Afar, Ethiopia) in light of radiometric age determinations: The Journal of Geology, v. 80, p. 720–729.

Barberi, F., Borsi, S., Ferrara, G., Marinelli, G., and Varet, J., 1970, Relations between tectonics and magmatology in the northern Danakil Depression (Ethiopia): Philosophical Transactions for the Royal Society of London. Series A, Mathematical and Physical Sciences, p. 293–311.

Barberi, F., Ferrara, G., Santacroce, R., Treuil, M., and Varet, J., 1975a, A Transitional Basalt-Pantellerite Sequence of Fractional Crystallization, the Boina Centre (Afar Rift, Ethiopia): Journal of Petrology, v. 16, p. 22–56, doi:10.1093/petrology/16.1.22.

Barberi, F., Ferrara, G., Santacroce, R., and Varet, J., 1975b, Structural evolution of the Afar triple junction:

Barberi, F., and Santacroce, R., 1980, The Afar stratoid series and the magmatic evolution of East African rift system: Bull. Soc. Geol. Fr, v. 22, p. 891–899.

Barberi, F., Santacroce, R., and Varet, J., 1974b, Silicic peralkaline volcanic rocks of the Afar depression (Ethiopia): Bulletin Volcanologique, v. 38, p. 755–790.

Barberi, F., and Varet, J., 1978, The Afar rift junction, *in* Petrology and geochemistry of continental rifts, Springer, p. 55–69.

Barberi, F., and Varet, J., 1970, The Erta Ale volcanic range (Danakil depression, northern Afar, Ethiopia): Bulletin Volcanologique, v. 34, p. 848–917.

Barnie, T.D., Keir, D., Hamling, I., Hofmann, B., Belachew, M., Carn, S., Eastwell, D., Hammond, J.O., Ayele, A., and Oppenheimer, C., 2016, A multidisciplinary study of the final episode of the Manda Hararo dyke sequence, Ethiopia, and implications for trends in volcanism during the rifting cycle: Geological Society, London, Special Publications, v. 420, p. 149–163.

Barrat, J.A., Fourcade, S., Jahn, B.M., Cheminee, J.L., and Capdevila, R., 1998, Isotope (Sr, Nd, Pb, O) and trace-element geochemistry of volcanics from the Erta'Ale range (Ethiopia): Journal of Volcanology and Geothermal Research, v. 80, p. 85–100.

Barrat, J.A., Jahn, B.M., Fourcade, S., and Joron, J.L., 1993, Magma genesis in an ongoing rifting zone: The Tadjoura Gulf (Afar area): Geochimica et cosmochimica acta, v. 57, p. 2291–2302.

Barrat, J.A., Joron, J.L., Taylor, R.N., Fourcade, S., Nesbitt, R.W., and Jahn, B.M., 2003, Geochemistry of basalts from Manda Hararo, Ethiopia: LREE-depleted basalts in Central Afar: Lithos, v. 69, p. 1–13.

Bastow, I.D., Booth, A.D., Corti, G., Keir, D., Magee, C., Jackson, C.A.-L., Warren, J., Wilkinson, J., and Lascialfari, M., 2018, The Development of Late-Stage Continental Breakup: Seismic Reflection and Borehole Evidence from the Danakil Depression, Ethiopia: Tectonics, v. 37, p. 2848–2862.

Bastow, I.D., and Keir, D., 2011, The protracted development of the continent-ocean transition in Afar: Nature Geoscience, v. 4, p. 248–250, doi:Doi 10.1038/Ngeo1095.

Bastow, I.D., Nyblade, A.A., Stuart, G.W., Rooney, T.O., and Benoit, M.H., 2008, Rifting at the edge of the African low velocity anomaly: Geochemistry Geophysics Geosystems, p. Q12022, doi:10.1029/2008GC002107.

Bastow, I.D., Pilidou, S., Kendall, J.M., and Stuart, G.W., 2010, Melt-Induced seismic anisotropy and magma assisted rifting in Ethiopia: evidence from surface waves: Geochemistry Geophysics Geosystems, p. Q0AB05, doi:10.1029/2010GC003036, doi:10.1029/2010GC003036.

Bastow, I.D., Stuart, G.W., Kendall, J.M., and Ebinger, C.J., 2005, Upper-mantle seismic structure in a region of incipient continental breakup: northern Ethiopian rift: Geophysical Journal International, v. 162, p. 479–493.

Belachew, M., Ebinger, C., and Coté, D., 2012, Source mechanisms of dike-induced earthquakes in the Dabbahu-Manda Hararo rift segment in Afar, Ethiopia: implications for faulting above dikes: Geophysical Journal International, v. 192, p. 907–917.

Belachew, M., Ebinger, C., Coté, D., Keir, D., Rowland, J.V., Hammond, J.O., and Ayele, A., 2011, Comparison of dike intrusions in an incipient seafloor-spreading segment in Afar, Ethiopia: Seismicity perspectives: Journal of Geophysical Research: Solid Earth, v. 116.

Benoit, M.H., Nyblade, A.A., and Pasyanos, M.E., 2006, Crustal thinning between the Ethiopian and East African plateaus from modeling Rayleigh wave dispersion: Geophysical Research Letters, v. 33, p. L13301, doi: 10.1029/2006gl025687, doi:Artn L13301 Doi 10.1029/2006gl025687.

Bertrand, H., Chazot, G., Blichert-Toft, J., and Thoral, S., 2003, Implications of widespread high-mu volcanism on the Arabian Plate for Afar mantle plume and lithosphere composition: Chemical Geology, v. 198, p. 47–61.

Beutel, E., van Wijk, J., Ebinger, C., Keir, D., and Agostini, A., 2010, Formation and stability of magmatic segments in the Main Ethiopian and Afar rifts: Earth and Planetary Science Letters, v. 293, p. 225–235, doi:DOI 10.1016/j.epsl.2010.02.006.

Beydoun, Z.R., As-Saruri, M.A.L., El-Nakhal, H., Al-Ganad, I.N., Baraba, R.S., Nani, A.O., and Al-Aawah, M.H., 1998, International lexicon of stratigraphy: Volume III, Republic of Yemen, second edition: international union of geological sciences and ministry of oil and mineral resources, Republic of Yemen publication, v. 34, p. 245.

Bizouard, H., Barberi, F., and Varet, J., 1980, Mineralogy and petrology of Erta Ale and Boina volcanic series, Afar rift, Ethiopia: Journal of Petrology, v. 21, p. 401–436.

Boynton, W.V., 1984, Cosmochemistry of the rare earth elements: meteorite studies, *in* Henderson, P. ed., Rare earth element geochemistry, Amsterdam, Elsevier, p. 63–114.

Bridges, D.L., Mickus, K., Gao, S.S., Abdelsalam, M.G., and Alemu, A., 2012, Magnetic stripes of a transitional continental rift in Afar: Geology, v. 40, p. 203–206, doi:10.1130/g32697.1.

Campisano, C.J., 2012, Geological summary of the Busidima Formation (Plio-Pleistocene) at the Hadar paleoanthropological site, Afar Depression, Ethiopia: Journal of Human Evolution, v. 62, p. 338–352, doi:https://doi.org/10.1016/j.jhevol.2011.05.002.

Campisano, C.J., and Feibel, C.S., 2008a, Depositional environments and stratigraphic summary of the Pliocene Hadar formation at Hadar, Afar depression, Ethiopia: The geology of early humans in the Horn of Africa, v. 446, p. 179–201.

Campisano, C., and Feibel, C.S., 2008b, Tephrostratigraphy of the Hadar and Busidima Formations at Hadar, Afar Depression, Ethiopia, *in* Quade, J. and Wynn, J.G. eds., The Geology of Early Humans in the Horn of Africa, Special Paper 446, Boulder, Co, The Geological Society of America, p. 135–162.

Capaldi, G., Chiesa, S., Conticelli, S., and Manetti, P., 1987, Jabal an Nar: An upper miocene volcanic centre near Al Mukha (Yemen Arab Republic): Journal of Volcanology and Geothermal Research, v. 31, p. 345–351, doi:https://doi.org/10.1016/0377-0273(87)90077-1.

Capaldi, G., Manetti, P., and Piccardo, G.B., 1983, Preliminary investigations on volcanism of the Sadah region (Yemen Arabic Republic): Bulletin Volcanologique, v. 46, p. 413, doi:10.1007/bf02597774.

Casey, M., Ebinger, C., Keir, D., Gloaguen, R., and Mohamed, F., 2006, Strain accomodation in transitional rifts: Extension by magma intrusion and faulting in Ethiopian rift magmatic segments, *in* Yirgu, G., Ebinger, C., and Maguire, P. eds., The Afar Volcanic Province within the East African Rift System, London, Geological Society, London, v. 259, p. 143–164.

Chang, S.-J., and Van der Lee, S., 2011, Mantle plumes and associated flow beneath Arabia and East Africa: Earth and Planetary Science Letters, v. 302, p. 448–454.

Chernet, T., Hart, W.K., Aronson, J.L., and Walter, R.C., 1998, New age constraints on the timing of volcanism and tectonism in the northern Main Ethiopian Rift-southern Afar transition zone (Ethiopia): Journal of Volcanology and Geothermal Research, v. 80, p. 267–280.

Chessex, R., Delaloye, M., and Fontignie, D., 1980, K-Ar datations on volcanic rocks of the Republic of Djibouti: Accademia nazionale dei Lincei.

Civetta, L., de Fino, M., Gasparini, P., Ghiara, M.R., La Volpe, L., and Lirer, L., 1975, Structural Meaning of East-Central Afar Volcanism (Ethiopia, T.F.A.I.): The Journal of Geology, v. 83, p. 363–373, doi:10.1086/628098.

Cornwell, D.G., Hetényi, G., and Blanchard, T.D., 2011, Mantle transition zone variations beneath the Ethiopian Rift and Afar: Chemical heterogeneity within a hot mantle? Geophysical Research Letters, v. 38, p. doi:10.1029/2011gl047575, doi:10.1029/2011gl047575.

Cox, K.G., Charnley, N., Gill, R.C.O., and Parish, K.A., 1993, Alkali basalts from Shuqra, Yemen: Magmas generated in the crust-mantle transition zone?, *in* Pritchard, H.M., Alabaster, T., Harris, N.B.W., and Neary, C.R. eds., Magmatic process and plate tectonics, London, Journal of the Geological Society Special Publications 76, p. 443–453.

Cox, K.G., Gass, I.G., and Mallick, D.I.J., 1977, The western part of the Shuqra volcanic field, South Yemen: Lithos, v. 10, p. 185–191.

Daniels, K.A., Bastow, I.D., Keir, D., Sparks, R.S.J., and Menand, T., 2014, Thermal models of dyke intrusion during development of continent–ocean transition: Earth and Planetary Science Letters, v. 385, p. 145–153.

Daoud, M.A., Le Gall, B., Maury, R.C., Rolet, J., Huchon, P., and Guillou, H., 2011, Young rift kinematics in the Tadjoura rift, western Gulf of Aden, Republic of Djibouti: Tectonics, v. 30, doi:doi:10.1029/2009TC002614.

Daoud, M.A., Maury, R.C., Barrat, J.A., Taylor, R.N., Le Gall, B., Guillou, H., Cotten, J., and Rolet, J., 2010, A LREE-depleted component in the Afar plume: Further evidence from Quaternary Djibouti basalts: Lithos, v. 114, p. 327–336, doi:DOI 10.1016/j.lithos.2009.09.008.

De Chabalier, J.-B., and Avouac, J.-P., 1994, Kinematics of the Asal Rift (Djibouti) determined from the deformation of Fieale Volcano: Science, v. 265, p. 1677–1681.

Deino, A.L., Scott, G.R., Saylor, B., Alene, M., Angelini, J.D., and Haile-Selassie, Y., 2010, 40Ar/39Ar dating, paleomagnetism, and tephrochemistry of Pliocene strata of the hominid-bearing Woranso-Mille area, west-central Afar Rift, Ethiopia: Journal of Human Evolution, v. 58, p. 111–126.

Deniel, C., Vidal, P., Coulon, C., and Vellutini, P.J., 1994, Temporal evolution of mantle sources during continental rifting - the volcanism of Djibouti (Afar): Journal of Geophysical Research-Solid Earth, v. 99, p. 2853–2869.

Desissa, M., Johnson, N.E., Whaler, K.A., Hautot, S., Fisseha, S., and Dawes, G.J.K., 2013, A mantle magma reservoir beneath an incipient mid-ocean ridge in Afar, Ethiopia: Nature Geoscience, v. 6, p. 861, doi:10.1038/ngeo1925 https://www.nature.com/articles/ngeo1925#supplementary-information.

Dickinson, D.R., Dodson, M.H., Gass, I.G., and Rex, D.C., 1969, Correlation of initial87Sr/86Sr with Rb/Sr in some Late Tertiary volcanic rocks of South Arabia: Earth and Planetary Science Letters, v. 6, p. 84–90.

DiMaggio, E.N. et al., 2015a, Late Pliocene fossiliferous sedimentary record and the environmental context of early <em>Homo</em> from Afar, Ethiopia: Science, v. 347, p. 1355–1359.

DiMaggio, E.N., Arrowsmith, J.R., Campisano, C.J., Johnson, R., Deino, A.L., Warren, M., Fisseha, S., and Cohen, A.S., 2015b, Tephrostratigraphy and depositional environment of young (<2.94 Ma) Hadar Formation deposits at Ledi-Geraru, Afar, Ethiopia: Journal of African Earth Sciences, v. 112, p. 234–250, doi:https://doi.org/10.1016/j.jafrearsci.2015.09.018.

Donovan, A., Blundy, J., Oppenheimer, C., and Buisman, I., 2018, The 2011 eruption of Nabro volcano, Eritrea: perspectives on magmatic processes from melt inclusions: Contributions to Mineralogy and Petrology, v. 173, p. 1.

Duffield, W.A., Bullen, T.D., Clynne, M.A., Fournier, R.O., Janik, C.J., Lanphere, M.A., Lowenstern, J., Smith, J.G., Giorgis, L.W., and Kahsai, G., 1997, Geothermal potential of the Alid volcanic center, Danakil Depression, Eritrea: US Geological Survey,.

Dupont-Nivet, G., Sier, M., Campisano, C.J., Arrowsmith, J.R., DiMaggio, E., Reed, K., Lockwood, C., Franke, C., and Hüsing, S., 2008, Magnetostratigraphy of the eastern Hadar Basin (Ledi-Geraru research area, Ethiopia) and implications for hominin paleoenvironments: The Geology of Early Humans in the Horn of Africa: Geological Society of America Special Paper, v. 446, p. 67–85.

Eagles, G., Gloaguen, R., and Ebinger, C., 2002, Kinematics of the Danakil microplate: Earth and Planetary Science Letters, v. 203, p. 607–620.

Ebinger, C., Ayele, A., Keir, D., Rowland, J., Yirgu, G., Wright, T., Belachew, M., and Hamling, I., 2010, Length and Timescales of Rift Faulting and Magma Intrusion: The Afar Rifting Cycle from 2005 to Present: Annual Review of Earth and Planetary Sciences, Vol 38, v. 38, p. 439–466, doi:DOI 10.1146/annurev-earth-040809-152333.

Ebinger, C.J., and Casey, M., 2001, Continental breakup in magmatic provinces: An Ethiopian example: Geology, v. 29, p. 527–530.

Ferguson, D.J., Barnie, T.D., Pyle, D.M., Oppenheimer, C., Yirgu, G., Lewi, E., Kidane, T., Carn, S., and Hamling, I.J., 2010, Recent rift-related volcanism in Afar, Ethiopia: Earth and Planetary Science Letters, v. 292, p. 409–418, doi:doi:10.1016/j.epsl.2010.02.010.

Ferguson, D.J., Calvert, A.T., Pyle, D.M., Blundy, J.D., Yirgu, G., and Wright, T.J., 2013a, Constraining timescales of focused magmatic accretion and extension in the Afar crust using lava geochronology: Nature Communications, v. 4, p. 1416, doi:http://www.nature.com/ncomms/journal/v4/n1/suppinfo/ncomms2410_S1.html.

Ferguson, D.J., Maclennan, J., Bastow, I.D., Pyle, D.M., Jones, S.M., Keir, D., Blundy, J.D., Plank, T., and Yirgu, G., 2013b, Melting during late-stage rifting in Afar is hot and deep: Nature, v. 499, p. 70–73, doi:10.1038/nature12292 http://www.nature.com/nature/journal/v499/n7456/abs/nature12292.html#supplementary-information.

Field, L., Blundy, J., Brooker, R., Wright, T., and Yirgu, G., 2012, Magma storage conditions beneath Dabbahu Volcano (Ethiopia) constrained by petrology, seismicity and satellite geodesy: Bulletin of Volcanology, p. doi: 10.1007/s00445-012-0580-6, doi:10.1007/s00445-012-0580-6.

Field, L., Blundy, J., Calvert, A., and Yirgu, G., 2013, Magmatic history of Dabbahu, a composite volcano in the Afar Rift, Ethiopia: Geological Society of America Bulletin, v. 125, p. 128–147, doi:10.1130/b30560.1.

Furman, T., Nelson, W.R., and Elkins-Tanton, L.T., 2016, Evolution of the East African rift: Drip magmatism, lithospheric thinning and mafic volcanism: Geochimica Et Cosmochimica Acta, v. 185, p. 418–434.

Gao, S.S., Liu, K.H., and Abdelsalam, M.G., 2010, Seismic anisotropy beneath the Afar Depression and adjacent areas: Implications for mantle flow: Journal of Geophysical Research: Solid Earth, v. 115.

Gass, I., and Mallick, D., 1968, Jebel Khariz: an Upper Miocene strato-volcano of comenditic affinity on the South Arabian coast: Bulletin Volcanologique, v. 32, p. 33–88.

Grandin, R., Jacques, E., Nercessian, A., Ayele, A., Doubre, C., Socquet, A., Keir, D., Kassim, M., Lemarchand, A., and King, G.C.P., 2011, Seismicity during lateral dike propagation: Insights from new data in the recent Manda Hararo–Dabbahu rifting episode (Afar, Ethiopia): Geochemistry, Geophysics, Geosystems, v. 12.

Hagos, M., Koeberl, C., and de Vries, B. van W., 2016, The Quaternary volcanic rocks of the northern Afar Depression (northern Ethiopia): Perspectives on petrology, geochemistry, and tectonics: Journal of African Earth Sciences, v. 117, p. 29–47.

Haile-Selassie, Y., Gibert, L., Melillo, S.M., Ryan, T.M., Alene, M., Deino, A., Levin, N.E., Scott, G., and Saylor, B.Z., 2015, New species from Ethiopia further expands Middle Pliocene hominin diversity: Nature, v. 521, p. 483.

Hall, C.M., Walter, R.C., Westgate, J.A., and York, D., 1984, Geochronology, stratigraphy and geochemistry of Cindery Tuff in Pliocene hominid-bearing sediments of the Middle Awash, Ethiopia: Nature, v. 308, p. 26–31.

Hamlyn, J.E., Keir, D., Wright, T.J., Neuberg, J.W., Goitom, B., Hammond, J.O., Pagli, C., Oppenheimer, C., Kendall, J.-M., and Grandin, R., 2014, Seismicity and subsidence following the 2011 Nabro eruption, Eritrea: Insights into the plumbing system of an off-rift volcano: Journal of Geophysical Research: Solid Earth, v. 119, p. 8267–8282.

Hammond, J.O.S. et al., 2013, Mantle upwelling and initiation of rift segmentation beneath the Afar Depression: Geology, v. 41, p. 635–638, doi:10.1130/g33925.1.

Hansen, S.E., and Nyblade, A.A., 2013, The deep seismic structure of the Ethiopia/Afar hotspot and the African superplume: Geophysical Journal International, v. 194, p. 118–124.

Hayward, N.J., and Ebinger, C.J., 1996, Variations in the along-axis segmentation of the Afar Rift system: Tectonics, v. 15, p. 244–257.

Heikal, M.T.S., Lebda, E.-M.M., Orihashi, Y., and Habtoor, A., 2014, Petrogenetic evolution of basaltic lavas from Balhaf–Bir Ali Plio-Quaternary volcanic field, Arabian Sea, Republic of Yemen: Arabian Journal of Geosciences, v. 7, p. 69–86, doi:10.1007/s12517-012-0726-z.

Johanson, D.C., and Taieb, M., 1976, Plio—Pleistocene hominid discoveries in Hadar, Ethiopia: Nature, v. 260, p. 293.

Juch, D., 1978, Geologic des Athiopischen Sudost-Escarpments 39° und 42° ostlicher Lange: Clausthaler Geo. Abh., v. 29, p. 139pp.

Kappelman, J., Ketcham, R.A., Pearce, S., Todd, L., Akins, W., Colbert, M.W., Feseha, M., Maisano, J.A., and Witzel, A., 2016, Perimortem fractures in Lucy suggest mortality from fall out of tall tree: Nature, v. 537, p. 503.

Katoh, S. et al., 2016, New geological and palaeontological age constraint for the gorilla–human lineage split: Nature, v. 530, p. 215.

Kidane, T., Courtillot, V., Manighetti, I., Audin, L., Lahitte, P., Quidelleur, X., Gillot, P.-Y., Gallet, Y., Carlut, J., and Haile, T., 2003, New paleomagnetic and geochronologic results from Ethiopian Afar: Block rotations linked to rift overlap and propagation and determination of a∼ 2 Ma reference pole for stable Africa: Journal of Geophysical Research: Solid Earth, v. 108.

Kimbel, W.H., and Delezene, L.K., 2009, “Lucy” redux: A review of research on Australopithecus afarensis: American journal of physical anthropology, v. 140, p. 2–48.

Kleinsasser, L.L., Quade, J., McIntosh, W.C., Levin, N.E., Simpson, S.W., and Semaw, S., 2008, Stratigraphy and geochronology of the late Miocene Adu-Asa Formation at Gona, Ethiopia, *in* J. Quade and J. G. Wynn eds., The Geology of Early Humans in the Horn of Africa:, Boulder, CO, Geological Society of America Special Paper 446, p. 33–65.

Kunz, K., Kreuzer, H., and Müller, P., 1975, Potassium-Argon age determinations of the Trap basalt of the south-eastern part of the Afar Rift: Afar depression of Ethiopia, v. 1, p. 370–374.

Lahitte, P., Gillot, P.-Y., and Courtillot, V., 2003a, Silicic central volcanoes as precursors to rift propagation; the Afar case: Earth and Planetary Science Letters, v. 207, p. 103–116.

Lahitte, P., Gillot, P.-Y., Kidane, T., Courtillot, V., and Bekele, A., 2003b, New age constraints on the timing of volcanism in central Afar, in the presence of propagating rifts: Journal of Geophysical Research: Solid Earth, v. 108, p. 2123, doi:10.1029/2001jb001689.

Lavayssière, A., Rychert, C., Harmon, N., Keir, D., Hammond, J.O.S., Kendall, J.-M., Doubre, C., and Leroy, S., 2018, Imaging Lithospheric Discontinuities Beneath the Northern East African Rift Using S-to-P Receiver Functions: Geochemistry, Geophysics, Geosystems, v. 19, p. 4048–4062, doi:10.1029/2018GC007463.

Le Gall, B., Daoud, M.A., Maury, R., Gasse, F., Rolet, J., Jalludin, M., Caminiti, A.-M., and Moussa, N., 2015, Geological Map of the Republic of Djibouti: Centre d'Etude et de Recherche de Djibouti (CERD) and CCGM.

Le Gall, B., Daoud, M.A., Rolet, J., and Egueh, N.M., 2011, Large-scale flexuring and antithetic extensional faulting along a nascent plate boundary in the SE Afar rift: Terra Nova, v. 23, p. 416–420.

Le Gall, B., Leleu, S., Pik, R., Jourdan, F., Chazot, G., Ayale, D., Yirgu, G., Cloquet, C., and Chauvet, F., 2018, The Red Beds series in the Erta Ale segment, North Afar. Evidence for a 6 Ma-old post-rift basin prior to continental rupturing: Tectonophysics, doi:https://doi.org/10.1016/j.tecto.2018.10.002.

Lowenstern, J.B., Janik, C.J., Fournier, R.O., Tesfai, T., Duffield, W.A., Clynne, M.A., Smith, J.G., Woldegiorgis, L., Weldemariam, K., and Kahsai, G., 1999, A geochemical reconnaissance of the Alid volcaniccenter and geothermal system, Danakil depression, Eritrea: Geothermics, v. 28, p. 161–187.

Magee, C., Bastow, I.D., van Wyk de Vries, B., Jackson, C.A.-L., Hetherington, R., Hagos, M., and Hoggett, M., 2017, Structure and dynamics of surface uplift induced by incremental sill emplacement: Geology, v. 45, p. 431–434.

Maguire, P. et al., 2006, Crustal structure of the Northern Main Ethiopian Rift from the EAGLE controlled source survey; a snapshot of incipient lithospheric break-up, *in* Yirgu, G., Ebinger, C., and Maguire, P. eds., The Afar Volcanic Province within the East African Rift System, Special Publication of the Geological Society, London, v. 259, p. 269–292.

Makris, J., and Ginzburg, A., 1987, The Afar Depression - Transition between Continental Rifting and Sea-Floor Spreading: Tectonophysics, v. 141, p. 199–214.

Mallick, D.I.J., Gass, I.G., Cox, K.G., De Vries, B.V.W., and Tindle, A.G., 1990, Perim Island, a volcanic remnant in the southern entrance to the Red Sea: Geological Magazine, v. 127, p. 309–318, doi:10.1017/s0016756800014874.

Manetti, P., Capaldi, G., Chiesa, S., Civetta, L., Conticelli, S., Gasparon, M., La Volpe, L., and Orsi, G., 1991, Magmatism of the eastern Red Sea margin in the northern part of Yemen from Oligocene to present: Tectonophysics, v. 198, p. 181–202.

Manighetti, I., Tapponnier, P., Courtillot, V., Gallet, Y., Jacques, E., and Gillot, P.Y., 2001, Strain transfer between disconnected, propagating rifts in Afar: Journal of Geophysical Research-Solid Earth, v. 106, p. 13613–13665.

Manighetti, I., Tapponnier, P., Gillot, P.Y., Jacques, E., Courtillot, V., Armijo, R., Ruegg, J.C., and King, G., 1998, Propagation of rifting along the Arabia-Somalia plate boundary: Into Afar: Journal of Geophysical Research: Solid Earth, v. 103, p. 4947–4974.

Mattash, M.A., Pinarelli, L., Vaselli, O., Minissale, A., Jaimes-Viera, M.C., Al-Kadasi, M., Shawki, M.N., and Tassi, F., 2014, Geochemical evolution of southern Red Sea and Yemen flood volcanism: evidence for mantle heterogeneity: Arabian Journal of Geosciences, v. 7, p. 4831–4850.

McClusky, S., Reilinger, R., Ogubazghi, G., Amleson, A., Healeb, B., Vernant, P., Sholan, J., Fisseha, S., Asfaw, L., and Bendick, R., 2010, Kinematics of the southern Red Sea–Afar Triple Junction and implications for plate dynamics: Geophysical Research Letters, v. 37, p. DOI: 10.1029/2009GL041127.

Medynski, S. et al., 2013, Controls on magmatic cycles and development of rift topography of the Manda Hararo segment (Afar, Ethiopia): Insights from cosmogenic 3He investigation of landscape evolution: Earth and Planetary Science Letters, v. 367, p. 133–145, doi:http://dx.doi.org/10.1016/j.epsl.2013.02.006.

Menzies, M., and Murthy, V.R., 1980, Nd and Sr Isotope Geochemistry of Hydrous Mantle Nodules and Their Host Alkali Basalts - Implications for Local Heterogeneities in Metasomatically Veined Mantle: Earth and Planetary Science Letters, v. 46, p. 323–334.

Mohr, P.A., 1967, Major volcano-tectonic lineament in the Ethiopian rift system: Nature, v. 213, p. 664–665.

Montagner, J.-P., Marty, B., Stutzmann, E., Sicilia, D., Cara, M., Pik, R., Lévêque, J.-J., Roult, G., Beucler, E., and Debayle, E., 2007, Mantle upwellings and convective instabilities revealed by seismic tomography and helium isotope geochemistry beneath eastern Africa: Geophysical Research Letters, v. 34, doi:10.1029/2007gl031098.

Oppenheimer, C., and Francis, P., 1998, Implications of longeval lava lakes for geomorphological and plutonic processes at Erta'Ale volcano, Afar: Journal of Volcanology and Geothermal Research, v. 80, p. 101–111.

Orihashi, Y., Al-Jailani, A., and Nagao, K., 1998, Dispersion of the Afar plume: Implications from the Spatiotemporal Distribution of the Late Miocene to Recent Volcanics, Southwestern Arabian Peninsula: Gondwana Research, v. 1, p. 221–234, doi:10.1016/S1342-937X(05)70833-9.

Ottonello, G., 1980, Rare earth abundances and distribution in some spinel peridotite xenoliths from Assab (Ethiopia): Geochimica et Cosmochimica Acta, v. 44, p. 1885–1901.

Ottonello, G., Piccardo, G.B., Joron, J.L., and Treuil, M., 1978, Evolution of the upper mantle under the Assab Region (Ethiopia): suggestions from petrology and geochemistry of tectonitic ultramafic xenoliths and host basaltic lavas: Geologische Rundschau, v. 67, p. 547–575.

Pagli, C., Wright, T.J., Ebinger, C.J., Yun, S.-H., Cann, J.R., Barnie, T., and Ayele, A., 2012, Shallow axial magma chamber at the slow-spreading Erta Ale Ridge: Nature Geoscience, v. 5, p. 284–288.

Pik, R., Marty, B., and Hilton, D.R., 2006, How many mantle plumes in Africa? The geochemical point of view: Chemical Geology, v. 226, p. 100–114.

Pinzuti, P., Humler, E., Manighetti, I., and Gaudemer, Y., 2013, Petrological Constraints on Melt Generation Beneath the Asal Rift (Djibouti) using Quaternary basalts: Geochemistry, Geophysics, Geosystems, p. 10.1002/ggge.20187, doi:10.1002/ggge.20187.

Quade, J., Levin, N., Semaw, S., Stout, D., Renne, P., Rogers, M., and Simpson, S., 2004, Paleoenvironments of the earliest stone toolmakers, Gona, Ethiopia: Geological Society of America Bulletin, v. 116, p. 1529–1544.

Quade, J., Levin, N.E., Simpson, S.W., Butler, R., McIntosh, W.C., Semaw, S., Kleinsasser, L., Dupont-Nivet, G., Renne, P., and Dunbar, N., 2008, The geology of Gona, Afar, Ethiopia: The geology of early humans in the Horn of Africa, v. 446, p. 1–31.

Reed, C.A., Almadani, S., Gao, S.S., Elsheikh, A.A., Cherie, S., Abdelsalam, M.G., Thurmond, A.K., and Liu, K.H., 2014, Receiver function constraints on crustal seismic velocities and partial melting beneath the Red Sea rift and adjacent regions, Afar Depression: Journal of Geophysical Research: Solid Earth, v. 119, p. 2138–2152.

Renne, P.R., WoldeGabriel, G., Hart, W.K., Heiken, G., and White, T.D., 1999, Chronostratigraphy of the Miocene–Pliocene Sagantole Formation, Middle Awash Valley, Afar rift, Ethiopia: Geological Society of America Bulletin, v. 111, p. 869–885.

Roman, D.C., Campisano, C., Quade, J., DiMaggio, E., and Arrowsmith, J.R., 2008, Composite tephrostratigraphy of the Dikika, Gona, Hadar, and Ledi-Geraru project areas, northern Awash, Ethiopia, *in* Quade, J. and Wynn, J.G. eds., The Geology of Early Humans in the Horn of Africa, Special Paper 446, Boulder, Co, Geological Society of America, p. 119–134.

Rooney, T.O., 2020a, The Cenozoic Magmatism of East Africa: Part III–Rifting of the craton: Lithos, p. In Review.

Rooney, T.O., 2020b, The Cenozoic Magmatism of East Africa: Part II–Rifting of the mobile belt: Lithos, p. In Press, doi:10.1016/j.lithos.2019.105291.

Rooney, T.O., 2020c, The Cenozoic magmatism of East Africa: Part V–Magma sources and processes in the East African Rift: Lithos, p. In Press, doi:10.1016/j.lithos.2019.105296.

Rooney, T.O., 2017, The Cenozoic magmatism of East-Africa: Part I — Flood basalts and pulsed magmatism: Lithos, v. 286, p. 264–301, doi:https://doi.org/10.1016/j.lithos.2017.05.014.

Rooney, T.O., Bastow, I.D., and Keir, D., 2011, Insights into extensional processes during magma assisted rifting: evidence from aligned scoria cones and maars: Journal of Volcanology and Geothermal Research, v. 201, p. 83–96, doi:doi: 10.1016/j.jvolgeores.2010.07.019.

Rooney, T.O., Hanan, B.B., Graham, D.W., Furman, T., Blichert-Toft, J., and Schilling, J.-G., 2012a, Upper Mantle Pollution during Afar Plume–Continental Rift Interaction: Journal of Petrology, v. 53, p. 365–389, doi:10.1093/petrology/egr065.

Rooney, T.O., Herzberg, C., and Bastow, I.D., 2012b, Elevated mantle temperature beneath East Africa: Geology, v. 40, p. 27–30, doi:10.1130/g32382.1.

Rooney, T.O., Nelson, W.R., Dosso, L., Furman, T., and Hanan, B., 2014, The role of continental lithosphere metasomes in the production of HIMU-like magmatism on the northeast African and Arabian plates: Geology, v. 42, p. 419–422.

Rychert, C.A., Hammond, J.O.S., Harmon, N., Michael Kendall, J., Keir, D., Ebinger, C., Bastow, I.D., Ayele, A., Belachew, M., and Stuart, G., 2012, Volcanism in the Afar Rift sustained by decompression melting with minimal plume influence: Nature Geosci, v. advance online publication, doi:http://www.nature.com/ngeo/journal/vaop/ncurrent/abs/ngeo1455.html#supplementary-information.

Sani, F., Ghinassi, M., Papini, M., Oms, O., and Finotello, A., 2017, Evolution of the northern tip of Afar triangle: Inferences from the Quaternary succession of the Dandiero — Massawa area (Eritrea): Tectonophysics, v. 717, p. 339–357, doi:https://doi.org/10.1016/j.tecto.2017.08.026.

Saylor, B.Z., Angelini, J., Deino, A., Alene, M., Fournelle, J.H., and Haile-Selassie, Y., 2016, Tephrostratigraphy of the Waki-Mille area of the Woranso-Mille paleoanthropological research project, Afar, Ethiopia: Journal of Human Evolution, v. 93, p. 25–45, doi:10.1016/j.jhevol.2015.12.007.

Schilling, J.G., Kingsley, R.H., Hanan, B.B., and McCully, B.L., 1992, Nd-Sr-Pb isotopic variations along the Gulf of Aden - Evidence for Afar mantle plume continental lithosphere interaction: Journal of Geophysical Research-Solid Earth, v. 97, p. 10927–10966.

Sgualdo, P., Aviado, K., Beccaluva, L., Bianchini, G., Blichert-Toft, J., Bryce, J.G., Graham, D.W., Natali, C., and Siena, F., 2015, Lithospheric mantle evolution in the Afro-Arabian domain: Insights from Bir Ali mantle xenoliths (Yemen): Tectonophysics, v. 650, p. 3–17.

Shaw, J.E., Baker, J.A., Kent, A.J.R., Ibrahim, K.M., and Menzies, M.A., 2007, The geochemistry of the Arabian lithospheric mantle - a source for intraplate volcanism? Journal of Petrology, v. 48, p. 1495–1512.

Stab, M., Bellahsen, N., Pik, R., Quidelleur, X., Ayalew, D., and Leroy, S., 2016, Modes of rifting in magma-rich settings: Tectono-magmatic evolution of Central Afar: Tectonics, v. 35, p. 2–38, doi:10.1002/2015tc003893.

Stoppard, T., 1967, Rosencrantz and Guildenstern Are Dead: New York, Grove Press.

Sun, S. s-, and McDonough, W.F., 1989, Chemical and isotopic systematics of oceanic basalts: Implications for mantle composition and processes., *in* Saunders, A.D. ed., Magmatism in the ocean basins, Geological Society of London Special Publication 42, p. 313–345.

Suwa, G., Beyene, Y., Nakaya, H., Bernor, R.L., Boisserie, J.-R., Bibi, F., Ambrose, S.H., Sano, K., Katoh, S., and Asfaw, B., 2015, Newly discovered cercopithecid, equid and other mammalian fossils from the Chorora Formation, Ethiopia: Anthropological Science, p. 150206.

Teklay, M., Scherer, E., Mezger, K., and Danyushevsky, L., 2010, Geochemical characteristics and Sr–Nd–Hf isotope compositions of mantle xenoliths and host basalts from Assab, Eritrea: implications for the composition and thermal structure of the lithosphere beneath the Afar Depression: Contributions to Mineralogy and Petrology, v. 159, p. 731–751, doi:10.1007/s00410-009-0451-0.

Tesfaye, S., Harding, D.J., and Kusky, T.M., 2003, Early continental breakup boundary and migration of the Afar triple junction, Ethiopia: Geological Society of America Bulletin, v. 115, p. 1053–1067.

Thompson, D.A., Hammond, J.O.S., Kendall, J.-M., Stuart, G.W., Helffrich, G.R., Keir, D., Ayele, A., and Goitom, B., 2015, Hydrous upwelling across the mantle transition zone beneath the Afar Triple Junction: Geochemistry, Geophysics, Geosystems, v. 16, p. 834–846.

Turner, S., Reagan, M., Vigier, N., and Bourdon, B., 2012, Origins of 210Pb-226Ra disequilibria in basalts: New insights from the 1978 Asal Rift eruption: Geochemistry, Geophysics, Geosystems, v. 13.

Ukstins, I.A., Renne, P.R., Wolfenden, E., Baker, J., Ayalew, D., and Menzies, M., 2002, Matching conjugate volcanic rifted margins; 40Ar/39Ar chrono-stratigraphy of pre- and syn-rift bimodal flood volcanism in Ethiopia and Yemen: Earth and Planetary Science Letters, v. 198, p. 289–306.

Varet, J., 2017, Geology of Afar (East Africa): Springer.

Varet, J., Gasse, F., scientifique (France), C. national de la recherche, DELLE RICERCHE, C.N., coopération (France), B. d'études industrielles et de, and Géotechnip, 1975, Carte géologique de l'Afar central et méridional. Ethiopie et TFAI [Territoire français des Afars et des Issas]-Geological map of central and southern Afar: Ethiopia and FTAI [French territory of Afars and Issas]: CNRS.

Vellutini, P., 1990, The Manda—Inakir rift, republic of Djibouti: A comparison with the Asal rift and its geodynamic interpretation: Tectonophysics, v. 172, p. 141–153, doi:https://doi.org/10.1016/0040-1951(90)90065-G.

Vigier, N., Bourdon, B., Joron, J.L., and Allegre, C.J., 1999, U-decay series and trace element systematics in the 1978 eruption of Ardoukoba, Asal rift: timescale of magma crystallization: Earth and Planetary Science Letters, v. 174, p. 81–98.

Villmoare, B., Kimbel, W.H., Seyoum, C., Campisano, C.J., DiMaggio, E.N., Rowan, J., Braun, D.R., Arrowsmith, J.R., and Reed, K.E., 2015, Early Homo at 2.8 Ma from Ledi-Geraru, Afar, Ethiopia: Science, v. 347, p. 1352–1355.

Volker, F., Mcculloch, M.T., and Altherr, R., 1993, Submarine basalts from the Red-Sea - New Pb, Sr, and Nd isotopic data: Geophysical Research Letters, v. 20, p. 927–930.

Walter, R.C., and Aronson, J.L., 1982, Revisions of K/Ar ages for the Hadar hominid site, Ethiopia: Nature, v. 296, p. 122–127.

Walter, R.C., Hart, W.K., and Westgate, J.A., 1987, Petrogenesis of a basalt-rhyolite tephra from the west-central Afar, Ethiopia: Contributions to Mineralogy and Petrology, v. 95, p. 462–480, doi:10.1007/bf00402206.

White, T.D., Asfaw, B., Beyene, Y., Haile-Selassie, Y., Lovejoy, C.O., Suwa, G., and WoldeGabriel, G., 2009, Ardipithecus ramidus and the paleobiology of early hominids: Science, v. 326, p. 64–86.

Wiart, P., and Oppenheimer, C., 2005, Large magnitude silicic volcanism in north Afar: the Nabro Volcanic Range and Ma'alalta volcano: Bulletin of Volcanology, v. 67, p. 99–115.

Wiart, P., and Oppenheimer, C., 2000, Largest known historical eruption in Africa: Dubbi volcano, Eritrea, 1861: Geology, v. 28, p. 291–294.

WoldeGabriel, G., Ambrose, S.H., Barboni, D., Bonnefille, R., Bremond, L., Currie, B., DeGusta, D., Hart, W.K., Murray, A.M., and Renne, P.R., 2009, The geological, isotopic, botanical, invertebrate, and lower vertebrate surroundings of Ardipithecus ramidus: Science, v. 326, p. 65-65e5.

WoldeGabriel, G., Haile-Selassie, Y., Renne, P.R., Hart, W.K., Ambrose, S.H., Asfaw, B., Heiken, G., and White, T., 2001, Geology and palaeontology of the Late Miocene Middle Awash valley, Afar rift, Ethiopia: Nature, v. 412, p. 175–178, doi:http://www.nature.com/nature/journal/v412/n6843/suppinfo/412175a0_S1.html.

Wolfenden, E., Ebinger, C., Yirgu, G., Deino, A., and Ayalew, D., 2004, Evolution of the northern Main Ethiopian rift: birth of a triple junction: Earth and Planetary Science Letters, v. 224, p. 213–228.

Wolfenden, E., Ebinger, C., Yirgu, G., Renne, P.R., and Kelley, S.P., 2005, Evolution of a volcanic rifted margin: Southern Red Sea, Ethiopia: Geological Society of America Bulletin, v. 117, p. 846–864.

Wright, T.J., Ebinger, C., Biggs, J., Ayele, A., Yirgu, G., Keir, D., and Stork, A., 2006, Magma-maintained rift segmentation at continental rupture in the 2005 Afar dyking episode: Nature, v. 442, p. 291–294.

Wright, T.J., Sigmundsson, F., Pagli, C., Belachew, M., Hamling, I.J., Brandsdóttir, B., Keir, D., Pedersen, R., Ayele, A., and Ebinger, C., 2012, Geophysical constraints on the dynamics of spreading centres from rifting episodes on land: Nature Geoscience, v. 5, p. 242.

Wynn, J.G., Roman, D.C., Alemseged, Z., Reed, D., Geraads, D., and Munro, S., 2008, Stratigraphy, depositional environments, and basin structure of the Hadar and Busidima Formations at Dikika, Ethiopia: Geological Society of America Special paper, v. 446, p. 87–118.

Yirgu, G., Ferguson, D.J., Barnie, T.D., and Oppenheimer, C., 2014, Recent volcanic eruptions in the Afar rift, northeastern Africa, and implications for volcanic risk management in the region: Extreme natural hazards, disaster risks and societal implications. Cambridge University Press, Cambridge, p. 200–213.

Zumbo, V., Féraud, G., Vellutini, P., Piguet, P., and Vincent, J., 1995, First 40Ar39Ar dating on early pliocene to plio-pleistocene magmatic events of the Afar—Republic of Djibouti: Journal of Volcanology and Geothermal Research, v. 65, p. 281–295.

Figure Captions

Figure 1: Map showing the broad structures in Afar and adjoining regions. The white translucent areas are sectors of the Red Sea Rift and Main Ethiopian Rift. The dotted line is the Tendaho-Goba'ad discontinuity. The Arabian, Nubian and Somalian plates are labelled along with the Danakil Block (microplate). Major magmatic feature names are shown in white.

Figure 2: Map showing the distribution of magmatism in Yemen since ca. 20 Ma. Note the two-fold division into volcanics broadly coeval with the Mid-Miocene Resurgence at ca. 11 to 9.5 Ma, and the more recent volcanics from ca. 6 Ma to recent.

Figure 3: XY plots for Mid Miocene from Yemen for various elements and isotopes vs MgO (A though F). Data shown are from the volcanic centers of Al Harf, Dabab, Jabal An Nar, Jabal Kharaz, and Perim. The recent magmatic activity titled 'Pliocene to Recent' is also shown for comparison.

Figure 4: XY plots for Mid Miocene from Yemen for Sr, Nd, Pb and Hf isotopes (A though C). Data shown are from the volcanic centers of Al Harf, Dabab, Jabal An Nar, Jabal Kharaz, and Perim. The recent magmatic activity titled 'Pliocene to Recent' is also shown for comparison.

Figure 5: XY plots for Pliocene to recent rocks from Yemen for various elements and isotopes vs MgO (A though F). Data shown are from the volcanic centers of Aden, Bir Ali-Balhaf, Dhamar Rada, Little Aden, Marib, Ras Imran, Sana'a, Shuqra, and Um Birka.

Figure 6: Primitive Mantle normalized diagram (Sun and McDonough, 1989) for more mafic samples from Yemen (MgO > 5 wt. %). There is a significant lack of trace element data for units from Yemen, thus the only units that can be plotted are Bir Ali-Balhaf and Sana'a. The grey lines in the upper figure are the Sana'a data, the grey lines in the lower figure at the Bir Ali-Balhaf area. These grey lines permit direct comparison between the suites. Data in green (positive and negative U anomalies) are a subset of the Bir Ali-Balhaf samples that extend to more enriched incompatible trace element concentrations. This is more fully discussed within the text.

Figure 7: XY plots for Pliocene to recent rocks from Yemen for Sr, Nd, Pb, and Hf isotopes vs MgO (A though F). Data shown are from the volcanic centers of Aden, Bir Ali-Balhaf, Dhamar Rada, Little Aden, Marib, Ras Imran, Sana'a, Shuqra, and Um Birka.

Figure 8: Stratigraphic column correlating magmatic units defined in this contribution with established sedimentary Formations. The small italic numbers represent the approximate boundary of each unit in millions of years. The boundaries of the magmatic series are linked with those of the sedimentary Formations; future revision of those Formation boundaries would require parallel adjustment of the magmatic series. Other sedimentary units, which have not yet been assigned to Formations, may occur between and among the Formations named herein (C. Campisano, personal communication, 2020). For details of the source data and rationale for the creation of these boundaries please see detailed discussion in the main text.

Figure 9: Map show the distribution of rocks during the development of the rift margin during the Miocene. Map is derived from the work of Stab et al. (2016), the Geological Map of Afar (Varet et al., 1975), and the Geological Map of Djibouti (LeGall et al., 2015). Note that the features shown as Dahla in the vicinity of the Erta 'Ale range are mapped as the Dankil Group and include sediments and volcanics. The unit is shown here as Dahla but requires additional mapping and geochronological constraints. The Miocene undifferentiated includes material from the Early Miocene Resurgence phase through eruption of the Dahla Series. Faults shown are that of Stab et al., 2016.

Figure 10: XY plots of Afar pre-axial rocks for various elements and isotopes vs MgO (A though F). Element ratio plots also shown (G, H). Data are for the Mablas Series, Dalha Series, Dalhoid Series. Afar Stratoid Series, and the Gulf Series.

Figure 11: Chondrite normalized diagram (Boynton, 1984) of Afar pre-axial rocks for more mafic samples (MgO > 5 wt. %). Units include: the Mablas Series, Dalha Series, Dalhoid Series. Afar

Stratoid Series, and the Gulf Series. Background field is the data extremes for the dataset presented in this figure. Note that missing data have been interpolated between points and are shown as a lower weight line connecting the datapoints. The interpolation is a weighted linear average which can result in curved artifacts in log space. The background data is a field showing the data limits for all samples in the plot.

Figure 12: Primitive Mantle normalized diagram (Sun and McDonough, 1989) of Afar pre-axial rocks for more mafic samples (MgO > 5 wt. %). Units include: the Mablas Series, Dalha Series, Dalhoid Series. Afar Stratoid Series, and the Gulf Series. Background field is the data extremes for the dataset presented in this figure.

Figure 13: Isotopic variation plots of Afar pre-axial rocks for Sr, Nd and Pb isotopes. Units include. Data are for the Mablas Series, Dalha Series, Dalhoid Series. Afar Stratoid Series, and the Gulf Series.

Figure 14: Map show the distribution of rocks during the Afar Stratoid Series and Gulf Series events. Map is derived from the work of Stab et al. (2016), the Geological Map of Afar (Varet et al., 1975), and the Geological Map of Djibouti (LeGall et al., 2015).

Figure 15: Map show the distribution of rocks during the development of the Axial Phase. Map is derived from the work of Stab et al. (2016), the Geological Map of Afar (Varet et al., 1975), and the Geological Map of Djibouti (LeGall et al., 2015). Volcano names and locations are largely derived from the Smithsonian Volcano database.

Figure 16: XY plots of Afar Axial rocks for various elements and isotopes vs MgO (A though F). Element ratio plots also shown (G, H). Data are for Alid, Manda Hararo, Dabbahu, and Erta ‘Ale along with the Transverse Volcanic fields of Assab, Nabro, and Sept Freres.  Volcanics from the Manda Inakir, Asal, and Tadjoura Rifts are clustered together

Figure 17: Chondrite normalized diagram (Boynton, 1984) of Afar Axial rocks for more mafic samples (MgO > 5 wt. %). Units include: Alid, Manda Hararo, Dabbahu, and Erta ‘Ale along with the Transverse Volcanic fields of Assab, Nabro, and Sept Freres. Background field is the data extremes for the dataset presented from these regions. Volcanics from the Manda Inakir, Asal, and Tadjoura Rifts are clustered together and the background dataset for these panels reflects these units. Note that missing data have been interpolated between points and are shown as a lower weight line connecting the datapoints. The interpolation is a weighted linear average which can result in curved artifacts in log space.

Figure 18: Primitive Mantle normalized diagram (Sun and McDonough, 1989) of Afar Axial rocks for more mafic samples (MgO > 5 wt. %). Units include: Alid, Manda Hararo, Dabbahu, and Erta ‘Ale along with the Transverse Volcanic fields of Assab, Nabro, and Sept Freres. Background field is the data extremes for the dataset presented from these regions. Volcanics from the Manda Inakir, Asal, and Tadjoura Rifts are clustered together and the background dataset for these panels reflects these units.

Figure 19: Isotopic plots of Afar Axial rocks for Sr, Nd, and Pb isotopes. Data are for Alid, Manda Hararo, Dabbahu, and Erta ‘Ale along with the Transverse Volcanic fields of Assab, Nabro, and Sept Freres. Volcanics from the Manda Inakir, Asal, and Tadjoura Rifts are clustered together